MIT-3903-5
MITNE-135

FINITE ELEMENT METHODS FOR SPACE-TIME REACTOR ANALYSIS

by

Chang Mu Kang, K. F. Hansen

November, 1971

Massachusetts Institute of Technology
Department of Nuclear Engineering
Cambridge, Massachusetts 02139

AEC Research and Development Report
Contract AT(30-1)3903
U.S. Atomic Energy Commission

DISCLAIMER

MASSACHUSETTS INSTITUTE OF TECHNOLOGY

DEPARTMENT OF NUCLEAR ENGINEERING

Cambridge, Massachusetts 02139

FINITE ELEMENT METHODS FOR SPACE-TIME REACTOR ANALYSIS

by

Chang Mu Kang, K. F. Hansen

November, 1971

MIT - 3903 - 5

MITNE - 135

AEC Research and Development Report

Contract AT(30-1)3903

U. S. Atomic Energy Commission

FINITE ELEMENT METHODS FOR SPACE-TIME REACTOR ANALYSIS

by

Chang Mu Kang

Submitted to the Department of Nuclear Engineering on November 30, 1971 in partial fulfillment of the requirements for the degree of Doctor of Science.

ABSTRACT

Finite element methods are developed for the solution of the neutron diffusion equation in space, energy and time domains. Constructions of piecewise polynomial spaces in multiple variables are considered for the approximation of a general class of piecewise continuous functions such as neutron fluxes and concentrations of nuclear elements. The approximate solution in the piecewise polynomial space is determined by applying the Galerkin scheme to a weak form of the neutron diffusion equation. A piecewise polynomial method is also developed for the solution of first-order ordinary differential equations. The numerical methods are applied to neutron slowing-down problems, static neutron diffusion problems, point kinetics problems and time-dependent neutron diffusion problems. The uniqueness, stability and approximation error of the numerical methods are considered. The finite element methods yield high-order accuracy, depending on the degree of the polynomials used, and thereby permit coarse-mesh calculations. The conventional multigroup method, the Crank-Nicolson and the Padé schemes are shown to be special cases of the finite element methods. Numerical examples are presented which confirm the truncation error and demonstrate the utility of the finite element methods in reactor problems.

Thesis Supervisor: Kent F. Hansen
Title: Professor of Nuclear Engineering

TABLE OF CONTENTS

TABLE OF CONTENTS (continued)

TABLE OF CONTENTS (concluded)

LIST OF FIGURES

LIST OF FIGURES (concluded)

LIST OF TABLES

ACKNOWLEDGMENTS

The author wishes to express his sincere appreciation to Professor Kent F. Hansen, his thesis supervisor, who first stimulated his interest in piecewise polynomials and provided constant ideas and guidance, and without whose encouragement this work would have been impossible.

The author wishes to extend his thanks to Professor Allan F. Henry who kindly provided constructive advice throughout this work and reviewed the final manuscript.

Thanks are due to Professor Garrett Birkhoff of Harvard University and Professor Gilbert Strang of M. I. T. who showed their interest and gave invaluable advice. The author is particularly indebted to Professor George Fix of Harvard University who provided much assistance in this work and gave comments on proofs of theorems.

The work was performed under USAEC Contract AT(30-1)-3903. The computations were performed on the IBM 360/65 computer at the M. I. T. Information Processing Service Center.

Finally, the author would also like to thank Mrs. Mary Bosco who typed this report with skill and painstaking care.

BIOGRAPHICAL NOTE

The author, Chang Mu Kang, [redacted] He received his elementary education in Seoul and was graduated from Seoul High School in March, 1959.

In April, 1959, he enrolled at the College of Engineering, Seoul National University, where he studied in the Department of Nuclear Engineering. He received his Bachelor of Science Degree in February, 1963. After two years of military service, he worked briefly in the Atomic Energy Research Institute, Seoul, Korea, until he came to the United States in August, 1965.

He enrolled at the University of Florida in September, 1965, as a graduate student in the Department of Nuclear Engineering and received his Master of Science Degree in Nuclear Engineering in April, 1967. In February, 1968, he entered the Massachusetts Institute of Technology as a graduate student in the Department of Nuclear Engineering.

Preliminary results of this work were published in Trans. Am. Nucl. Soc. 14, 199 and 201 (1971).

The author is married to the former Kunja Leigh and has a son.

Chapter I
INTRODUCTION

1.1 Introduction

This thesis is concerned with the development of numerical methods for neutron diffusion problems using piecewise polynomials in the energy, space and time variables.

Numerical methods for the solution of neutron diffusion problems have been widely used and have been shown to be more powerful than analytical methods, due to the complexity of reactor geometries and nuclear cross sections. The most widely used method is the finite difference method. This method is quite simple but requires relatively small meshes and hence a large number of unknowns. For this reason, finite difference methods have been limited to at most two-dimensional kinetics problems or coarse mesh three-dimensional problems. Therefore, alternate methods have been developed which require a relatively small number of unknowns and which can be applied to multidimensional problems.

In the synthesis method [1] - [3], the solution is expanded in terms of a small number of functions chosen to represent various transient states of the problem. A variety of synthesis techniques have evolved for treating some or all of the spatial variables and the energy variable. The advantage of this method is that the expansion functions may be obtained based on the knowledge of a particular system. However, the selection of proper expansion functions for various systems is difficult

in general. Poor selection of expansion functions can not only misrepresent the solution but also can cause numerical instabilities. Furthermore, analytic error bounds for the approximations are not known.

Another important class of approximate methods are the so-called "nodal methods." The basic idea is to treat the reactor as a small number of disjoint regions and to couple the regions through the neutron flux or current. In the "coupled reactor theory" [4], certain types of trial functions are defined on each subregion, which vanish outside the subregion. The subregions are then coupled through neutron currents. However, the neutron currents, and thus the coupling relations, depend strongly on shapes of the trial functions. Thus, as in the synthesis method, the selection of proper trial functions is a major difficulty in this method. An alternative is to use a simple constant trial function over each region, as in the FLARE [5] approach. In this approach, the proper coupling coefficients are difficult to define.

Instead of using fixed trial functions, several authors have considered using polynomial functions defined in each subregion. Riese [6] considered polynomials quadratic in each variable. The polynomials are then coupled to neighbor polynomials so that the flux continuity condition is satisfied. In the GRCORK scheme [7], the same type of polynomials was used with the difference that the subregions are coupled by partial neutron currents. The resulting solution is thus allowed to have a discontinuity along the region interfaces. In these methods, the accuracy of the solution is not known and the solution fails to satisfy the requisite continuity conditions. However, these methods are significant, since their development was based on a concept similar to that of the finite element method which will be developed in the present thesis.

In recent years, much attention has been given to approximations of functions using polynomials which are defined only over subregions of the problem domain, rather than over the entire domain. These polynomials are called "piecewise polynomials" for evident reasons. The piecewise polynomials yield high accuracy for approximations of functions and their derivatives. Furthermore, for practical computation, the piecewise polynomials provide some convenient features which ordinary polynomials lack:

(i) The piecewise polynomials provide local approximations and are thus well suited for approximating physical behaviors in which variations occur locally. In this case, a fewer number of polynomials is required using piecewise polynomials compared to the use of polynomials defined over the entire region.

(ii) Piecewise polynomials permit flexibility in imposing certain types of continuity or jump conditions at the joints of the subregions. In addition, boundary conditions are easily imposed.

(iii) Convenient piecewise polynomial basis functions can be found such that expansion coefficients are directly related to the values of functions and their derivatives at mesh points.

(iv) Used with the Ritz-Galerkin method, the system of linear equations can be made very simple and amenable to computer solution by well-developed methods.

The Ritz-Galerkin method, using piecewise polynomials as expansion functions, is called the "finite element method" by Fix and Strang [8], [9] and others [10], [11]. Many authors have suggested the use of

piecewise polynomial spaces with the Ritz-Galerkin method (e.g., see [8] - [21]). Representative spaces are spline space and the Hermite space. The spline space consists of piecewise polynomials whose derivatives satisfy the maximal continuity conditions. Therefore, the spline space has the smallest dimensions of all the piecewise polynomial spaces. The Hermite space consists of piecewise polynomials which are less continuous than the corresponding polynomials in the spline space. For example, polynomials of degree 2m-1 have continuous derivatives of order up to 2m-2 in the spline space, and up to m-1 in the Hermite space. Thus, if there are N-1 intervals in a one-dimensional space within which the piecewise polynomials are defined, the number of dimensions is N for the spline space and mN for the Hermite space. In an n-dimensional space, the number of dimensions is N^n and $(mN)^n$ for the spline and Hermite spaces, respectively. Since the dimension of the Hermite space increases sharply in multi-dimensional geometries, the Hermite space is less desirable for multi-dimensional calculations of smooth functions. In both spaces, convenient basis functions in one variable are easily found. Furthermore, the basis functions in the multivariate space can be obtained by taking tensor products [18], [21] of the basis functions of one variable.

Problems in nuclear reactor analysis consist of many regions of different materials. Thus, physical quantities in reactors are characterized by piecewise continuous functions. For example, the scalar neutron flux is continuous everywhere but has piecewise continuous first derivatives, while the concentrations of nuclear elements are continuous only within each region.

Previous studies of piecewise polynomial spaces have been developed mainly for approximations of smooth functions which are sufficiently differentiable on the entire region. Applications of piecewise polynomials to nonsmooth or piecewise continuous functions have previously been limited only to one-dimensional problems. In [16], modifications of basis functions in the Hermite space to allow jump continuity conditions are discussed. Wakoff [21] used modified cubic spline functions for the solution of one-dimensional multigroup diffusion problems. However, the extension of these modified piecewise polynomial spaces to multidimensional spaces by taking local tensor products leads to basis functions which are incompatible with the requisite continuity conditions.

The central object of this thesis is to construct appropriate and general piecewise polynomial spaces for approximations of piecewise continuous functions of multiple variables. Coarse mesh methods are devised for the solution of diffusion problems in space, time and energy, with a minimum of computational effort. We limit our consideration to linear neutron diffusion problems. However, the methods apply to any orthogonal coordinate system (e.g., Cartesian, cylindrical, polar spherical), whose partition is generated by coordinate surfaces (e.g., r_1=const., r_2=const., r_3=const.).

In the rest of this chapter, we discuss the energy-dependent neutron diffusion equation and the finite element method. Chapter II is concerned with the construction of piecewise polynomial spaces and corresponding basis functions in multiple variables for approximation of general classes of piecewise continuous functions. The uniqueness properties

and error bounds for the Hermite interpolation in these spaces are established.

In the succeeding chapters, we consider the application of the finite element method to neutron slowing-down problems (Chap. III), static neutron diffusion problems (Chap. IV), point reactor kinetics problems (Chap. V) and time-dependent neutron diffusion problems (Chap. VI). The uniqueness, stability and approximation error of the numerical method are considered. Finally, Chapter VII contains the conclusions and recommendations for further developments.

1.2 The Energy-Dependent Neutron Diffusion Equation

In this section, we introduce the energy-dependent neutron diffusion equation and discuss proper boundary conditions. The derivation of this equation can be found in Davison [22] and elsewhere [23],[24].

Let R^n be an n-dimensional space and $\underline{r}=(r_1, r_2, \ldots, r_n)$ represent a point in R^n. Consider a reactor configuration defined by an open region Ω and its boundary $\partial\Omega$. Furthermore, assume that Ω consists of disjoint open subregions Ω_ℓ, $\ell = 1, 2, \ldots, L$, each of which is bounded by $\partial\Omega_\ell$. Let $E_{min} \leq E \leq E_{max}$ and $0 \leq t \leq T$ where E and t represent the energy and time variables, respectively, and define $\mathcal{E} \equiv [E_{min}, E_{max}]$. Then, within any region Ω_ℓ, the time-dependent neutron diffusion equation with delayed precursors can be written as

$$\frac{1}{\mathcal{V}(E)} \frac{\partial}{\partial t} \phi(\underline{r}, E, t) = \underline{\nabla} \cdot D(\underline{r}, E, t) \underline{\nabla} \phi(\underline{r}, E, t)$$

$$- \Sigma_T(\underline{r}, E, t) \phi(\underline{r}, E, t)$$

$$+ \int_{\mathcal{E}} dE' \Sigma_s(\underline{r}, E' \to E, t) \phi(\underline{r}, E', t) \qquad (1.1a)$$

$$+ \chi(E)(1-\beta) \int_{\mathcal{E}} dE' \nu\Sigma_f(\underline{r}, E', t) \phi(\underline{r}, E', t)$$

$$+ \sum_{j=1}^{J} \chi_{dj}(E) \lambda_j C_j(\underline{r}, t) + Q(\underline{r}, E, t) ,$$

$$\frac{\partial}{\partial t} C_j(\underline{r}, t) = -\lambda_j C_j(\underline{r}, t) + \beta_j \int_{\mathcal{E}} dE' \nu\Sigma_f(\underline{r}, E', t) \phi(\underline{r}, E', t) , \qquad (1.1b)$$

$$j = 1, 2, \ldots, J,$$

where

$\phi(\underline{r}, E, t)$ = neutron flux $(n/cm^2 \cdot sec)$,

$\mathcal{V}(E)$ = neutron speed (cm/sec),

$D(\underline{r}, E, t)$ = neutron diffusion coefficient (cm),

$\Sigma_T(\underline{r}, E, t)$ = total macroscopic removal cross section (cm^{-1}),

$$\Sigma_T(\underline{r}, E, t) \equiv \Sigma_a(\underline{r}, E, t) + \int_{E_{min}}^{E_{max}} \Sigma_s(\underline{r}, E \to E', t) dE' ,$$

$\Sigma_a(\underline{r}, E, t)$ = macroscopic absorption cross section (cm^{-1}),

$\Sigma_s(\underline{r}, E' \to E, t)$ = macroscopic scattering cross section from E' to E (cm^{-1}),

$\Sigma_f(\underline{r}, E, t)$ = macroscopic fission cross section (cm^{-1}),

ν = average number of neutrons produced per fission,

$\chi(E)$ = fission spectrum for prompt neutrons,

$\chi_{dj}(E)$ = spectrum of delayed neutrons for the j-th group,

λ_j = decay constant of the j-th delayed neutron precursors (sec^{-1}),

β_j = fraction of delayed neutrons for the j-th group: $\beta = \sum_{j=1}^{J} \beta_j$,

$C_j(\underline{r}, t)$ = concentration of delayed neutron precursor of the j-th group,

J = number of delayed neutron groups,

$Q(\underline{r}, t)$ = neutron source/cm^2. sec.

The nuclear constants in Eqs. (1.1a, b) are assumed to satisfy the following conditions:

(i) $0 \leq \Sigma_a, \Sigma_s, \Sigma_f < \infty, \quad 0 < \frac{1}{\nu}, \quad D < \infty$,

(ii) D, Σ_a, Σ_s and Σ_f are continuous in each Ω_ℓ, $\ell = 1, 2, \ldots, L$, and may be discontinuous on $\partial\Omega_\ell$,

(iii) $\Sigma_a(E)$, $\Sigma_s(E' \to E)$, $\chi(E)\nu\Sigma_f(E')$ are positive operators such that

$$\Sigma(E', E)\, f(E', E) = \begin{cases} \Sigma(E', E)\, f(E', E) & \text{if } f(E', E) > 0, \\ 0 & \text{if } f(E', E) \leq 0. \end{cases} \tag{1.2}$$

The condition (iii) implies that the products are nonnegative. Furthermore, when $f(E', E) = f(E')$, this condition conforms to the physical fact that the reaction rate must be nonnegative. Under the condition (iii), it can be shown easily that the integral operators in Eq. (1.1a) are positive semidefinite [25], although they are nonsymmetric.

Let the initial conditions be specified by

$$\phi(\underline{r}, E, t)\big|_{t=0} = \phi_0(\underline{r}, E), \tag{1.3a}$$

$$C_j(\underline{r}, t)\big|_{t=0} = C_{j0}(\underline{r}), \qquad 1 \leq j \leq J. \tag{1.3b}$$

Let the boundary conditions on $\partial\Omega$ be homogeneous conditions

$$\phi(\underline{r}, E, t) = 0 \quad \text{or} \quad \frac{\partial}{\partial n}\phi(\underline{r}, E, t) = 0, \tag{1.4a}$$

where $\frac{\partial}{\partial n}$ represents the outward normal derivative at $\partial\Omega$.

The diffusion approximation fails in the neighborhood of material interfaces, where the solution has transients. We assume that the

solution satisfies certain boundary conditions at the interfaces. Rigorous interface boundary conditions for the diffusion approximation based on the transport theory are discussed in Davison [22]. However, the following set of interface boundary conditions is more commonly used:

$\phi(\underline{r}, E, t)$ and $D(\underline{r}, E, t) \frac{\partial}{\partial n} \phi(\underline{r}, E, t)$ are continuous on material interfaces. (1.4b)

These conditions are frequently called flux and current continuity conditions, respectively.

The point which is formed by intersections of two or more material interfaces is a singular point. In order to generate approximations to the analytic solution to the diffusion problem, it would be necessary to include the singular solutions [18], [26], [27]. However, this is an impractical computing task, at least at present. The approach to be taken in this thesis will be to ignore the singular part of the solution. The result is that we are solving a problem slightly different from the original diffusion problem, namely we have relaxed certain boundary conditions. We call this different problem the "modified" problem, or the "weak" formulation of the problem. We show in Chapter IV that the solution is unique in the modified problem (see Lemma 4.1). We call this solution the "weak" solution to the original problem. For the weak formulation, it is possible to find error bounds and rates of convergence of approximate solutions to the weak solution.

The important question is, of course, how the weak solution compares to the solution of the original problem. Fix [18] has shown that for certain eigenvalue problems in an L-shaped membrane, inclusion of the singular solution makes a considerable improvement in the

convergence of eigenvalues. However, the effect of the singular solution on reaction rates and integral properties in reactor problems would be negligible.

We remark that this "pragmatic" approach is the same as that used in finite difference approximations to diffusion problems. As one refines the difference mesh the solution approaches a limit, which again is not the analytic solution to the continuum problem. The difficulty lies not with the numerical approximations, but rather with the application of diffusion theory to a case for which the theory is not physically valid.

1.3 Finite Element Methods

Finite element methods were originally developed by engineers for structural analysis in solid mechanics. References [28] and [29] contain extensive compilations of literature in this area. In general, the Ritz-Galerkin method used with piecewise polynomial functions is called the "finite element method" [8] - [11]. Courant [12] was the first to suggest the use of piecewise linear functions in triangular meshes in the Ritz method for two-dimensional Dirichlet problems. In recent years, finite element methods were developed as higher-order methods allowing the use of high-degree polynomials. Finite element methods have been applied to boundary and eigenvalue problems in [8] - [21] and to parabolic problems in [30] - [32].

To illustrate the finite element method, consider a problem defined by

$$T\phi(\underline{r}) = Q(\underline{r}) \qquad \underline{r} \text{ in } \Omega , \tag{1.5}$$

where T is an integro-differential operator with homogeneous boundary

conditions specified on the boundary $\partial\Omega$. $Q(\underline{r})$ represents a source term.

In order to approximate the solution to Eq. (1.5), we consider a finite dimensional trial space S_M where $\{u_i(\underline{r})\}_{i=1}^{M}$ form a basis. In particular, we choose $u_i(\underline{r})$ as polynomials of a certain degree satisfying the same boundary condition as the analytic solution. We then seek an approximate solution of the form

$$\hat{\phi}(\underline{r}) = \sum_{i=1}^{M} a_i u_i(\underline{r}) . \tag{1.6}$$

The Ritz-Galerkin procedure is a well-known method [33], [34] for solving integro-differential equations. The Galerkin method is more general than the Ritz method and can be applied to problems with non-self adjoint operators. In the Galerkin method, the expansion coefficients a_i are determined from the condition that the equation obtained by the substitution of $\hat{\phi}(\underline{r})$ for ϕ in Eq. (1.5) must be orthogonal to the elements $u_1, u_2, \ldots, u_M$. This condition leads to the system of equations

$$(T\hat{\phi}, u_i) = (Q, u_i)$$

for all $i = 1, 2, \ldots, M$, where the inner product is defined by $(u, v) = \int_\Omega uv \, dV$. This equation can be rewritten in matrix form as

$$A\,\underline{a} = \underline{q} \tag{1.7}$$

where

$$A_{ij} = (T u_j, u_i) ,$$

$$\underline{a} = \text{col}\{a_1, a_2, \ldots, a_M\} ,$$

$$\underline{q} = \text{col}\{(Q, u_1), \ldots, (Q, u_M)\} .$$

The matrix A is usually called a stiffness matrix.

The coefficient vector $\underline{a}$ is determined by inverting the stiffness matrix A. The numerical inversion of A is governed by the condition number of the matrix A. The condition number is defined by

$$\text{Cond (A)} = \|A\| \, \|A^{-1}\|$$

where $\| \|$ denotes any matrix norm. If the condition number is relatively large, then A is ill-conditioned in numerical inversion. If the condition number is relatively small, then the matrix A is well-conditioned.

In finite element methods, the condition number of A depends on the selection of the polynomial expansion functions. When the operator is positive definite and the polynomials are sufficiently linearly independent, then there will be no difficulties in inverting the stiffness matrix. For example, if we choose a set of polynomials $\{x^{\mu}\}_{\mu=1}^{M} = (x^0, x^1, \ldots, x^M)$ as expansion functions, then the stiffness matrix becomes the Hilbert matrix [35]. These polynomials are nearly linearly dependent in the range $0 \leq x \leq 1$ and thus the Hilbert matrix is very ill-conditioned and difficult to invert numerically. Therefore, in finite element methods, instead of using ordinary polynomials, we select piecewise polynomials which vanish throughout most of the whole region and finite only in a few subregions. Use of the piecewise polynomials makes the stiffness matrix sparse and relatively well-conditioned. In Chapter II, we shall consider the generation of specific piecewise polynomial basis functions for use with the Galerkin method in reactor problems.

Chapter II

PIECEWISE POLYNOMIAL SPACES

In this chapter, we will discuss certain types of piecewise polynomial spaces which are of use in the solution of diffusion problems. In a heterogeneous reactor, physical quantities are characterized by piecewise continuous functions. Therefore, we will consider the construction of appropriate piecewise polynomial spaces for problems of one independent variable, i.e., univariate spaces, and multiple independent variables, i.e., multivariate spaces. The purpose of this chapter is to provide the tool for the numerical analysis of reactor problems in succeeding chapters.

We consider piecewise polynomial spaces in multivariables which can be directly applied to the Hermite interpolation. The Hermite interpolation is characterized by the fact that the interpolating polynomial is generated by the use of function values and derivatives. In particular, the same data must be available at both ends of the interpolation interval. This means, for instance, that if one has the value of the function and its first order derivatives at one end of the interval, one must also have the value of the function and its first order derivatives at the other end. Thus, the amount of data is always an even number of values; hence the interpolating polynomials are always of odd degree. For neutron diffusion problems, the flux and current continuity conditions lead naturally to the use of Hermite interpolation.

The piecewise polynomial space, which is constructed based on the

Hermite interpolation, will be called the Hermite space. The Hermite space is particularly suited for the interpolation of the piecewise continuous function as well as the continuous function. The Hermite space can be regarded as a generalization of the smooth Hermite space [14], [16] and the spline space [16], [36].

In Sections 2.1 and 2.2 we consider the generation of basis functions in the univariate and multivariate Hermite spaces, respectively. For this we introduce the element function. The element function is defined as a piecewise polynomial function which is defined in a unit mesh element and vanishes elsewhere. By using the element functions, the interpolating polynomial can be conveniently represented in terms of Hermite data. Furthermore, basis functions in the Hermite spaces can be generated by coupling the element functions so that they satisfy the pertinent continuity conditions. This method of construction is very flexible in generating basis functions in multivariate spaces for various types of continuity conditions. As special cases, this method gives local basis functions in the cubic (smooth) Hermite space [14], [16], [19] and the bicubic (smooth) Hermite space [18], [19].

In Theorems 2.2 and 2.5 we consider the dimension count, or the number of basis functions, of Hermite spaces. In Theorems 2.1 and 2.4 we establish error estimations for interpolations in Hermite spaces. In this and succeeding chapters we develop error estimations in the L^{∞}-norm only. However, since the L^{2}-norm is always less than or equal to the L^{∞}-norm, the results in this chapter can be applied to error estimations in the L^{2}-norm.

2.1 Univariate Polynomial Space

In this section we consider the construction of univariate Hermite spaces and corresponding basis functions for the approximation of general classes of piecewise continuous functions.

Let $\Omega = [a, b]$ be a closed interval in one-dimensional space and Δ be a partition of Ω such that

$$\Delta: a = x_1 < x_2 < \ldots < x_N = b. \tag{2.1}$$

Let $\Delta_i = (x_i, x_{i+1})$, $i = 1, 2, \ldots, N-1$ be open subintervals of the partition Δ.

We define $C^t(\Omega)$ to be the class of all functions which are t times differentiable in Ω. Also we define $C_p^t(\Delta)$ to be the class of all piecewise functions $f(x)$ such that $f(x) \in C^t(\Delta_i)$* for $i = 1, 2, \ldots, N-1$ and $f^{(q)}(x_i^{\pm}) \equiv \lim_{\delta \to 0} \frac{d^q}{dx^q} f(x_i \pm \delta)$ is finite for $0 \leq q \leq t$.

Let $s_i(x)$ be a polynomial of degree $2m-1$ in the interval $[x_i, x_{i+1}]$ where $m = \frac{1}{2}, 1, 2, \ldots$. Except for the case of $m = \frac{1}{2}$, the $s_i(x)$ are odd degree polynomials. We include the piecewise constant functions ($m = \frac{1}{2}$), since these functions are commonly used for approximations in the energy domain in deriving the multigroup equations in reactor physics. Then $s_i(x)$ can be expressed as

$$s_i(x) = \sum_{\mu=0}^{2m-1} a_\mu x^\mu, \qquad x \in [x_i, x_{i+1}], \tag{2.2}$$

where the a_μ are $2m$ unknown parameters to be determined.

---

* $f(x) \in C^t(\Delta_i)$ means that $f(x)$ is an element of the class $C^t(\Delta_i)$.

We consider the interpolation of a sufficiently smooth function f(x) in $[x_i, x_{i+1}]$, using polynomials of degree 2m-1. We are especially interested in interpolation problems where the derivatives of f(x) are specified at x_i and x_{i+1} so that $s_i(x)$ satisfies

$$s_i^{(p)}(x_i) = f^{(p)}(x_i), \tag{2.3a}$$

$$s_i^{(p)}(x_{i+1}) = f^{(p)}(x_{i+1}), \qquad 0 \leq p \leq m-1, \tag{2.3b}$$

where $s_i^{(p)}(x_i) = \frac{d^p}{dx^p} s_i(x)$. s(x) for $m = \frac{1}{2}$ is assumed to satisfy Eq. (2.3a) only. This type of interpolation is called Hermite interpolation and it is known [37] that the Hermite interpolate $s_i(x)$ can be uniquely determined.

In order to facilitate Hermite interpolation in numerical calculations, we consider convenient polynomial functions, which we will call element functions. The element functions $\{u_i^{p\pm}\}$ for $m \geq 1$ are defined by

$$u_i^{p-}(x) = \begin{cases} \sum_{\mu=0}^{2m-1} a_\mu^- x^\mu, & x_{i-1} \leq x \leq x_i, \\ 0, & \text{otherwise}, \end{cases} \tag{2.4a}$$

$$u_i^{p+}(x) = \begin{cases} \sum_{\mu=0}^{2m-1} a_\mu^+ x^\mu, & x_i \leq x \leq x_{i+1}, \\ 0, & \text{otherwise}, \end{cases} \tag{2.4b}$$

such that

$$\frac{d^q}{dx^q} u_i^{p\pm}(x_j^\pm) = \delta_{ij}\,\delta_{pq}, \qquad 0 \leq p \leq m-1,$$

where $x_j^\pm \equiv x_j \pm 0$. Note that $u_i^{p+}(x)$ and $u_{i+1}^{p-}(x)$ are nonvanishing over the same interval $[x_i, x_{i+1}]$. We say they have the same support, that is, the

region where the functions are non-zero.

From the definitions of the element functions, the Hermite interpolate $s_i(x)$ of $f(x)$ can then be expressed by

$$s_i(x) = \sum_{p=0}^{m-1} \{f^{(p)}(x_i^+)\, u_i^{p+}(x) + f^{(p)}(x_{i+1}^-)\, u_{i+1}^{p-}(x)\}. \tag{2.5}$$

The element functions are convenient numerically because the expansion coefficients in Eq. (2.5) are directly related to the interpolation data.

We give some explicit examples of the element functions for low degree polynomials. (See Fig. 2.1.)

(i) $m = 1/2$

$u_i^{0\pm}(x)$ are piecewise constant functions:

$$u_i^{0+} = \begin{cases} 1 , & x_i \leq x \leq x_{i+1} , \\ 0 , & \text{otherwise} , \end{cases} \tag{2.6}$$

$$u_i^{0-} = 0 , \quad \text{all } x .$$

(ii) $m = 1$

$u_i^{0\pm}(x)$ are piecewise linear functions:

$$u_i^{0\pm}(x) = \begin{cases} \dfrac{x - x_{i-1}}{x_i - x_{i-1}} , & x_{i-1} \leq x \leq x_i , \\ 0 , & \text{otherwise} , \end{cases} \tag{2.7a}$$

$$u_i^{0+}(x) = \begin{cases} \dfrac{x_{i+1} - x}{x_{i+1} - x_i} , & x_i \geq x \geq x_{i+1} , \\ 0 , & \text{otherwise} . \end{cases} \tag{2.7b}$$

(iii) $m = 2$

$u_i^{p\pm}(x)$, $p = 0, 1$, are piecewise cubic functions:

$$u_i^{0-}(x) = \begin{cases} 3\left(\frac{x - x_{i-1}}{x_i - x_{i-1}}\right)^2 - 2\left(\frac{x - x_{i-1}}{x_i - x_{i-1}}\right)^3, & x_{i-1} \leq x \leq x_i, \\ 0, & \text{otherwise}, \end{cases} \quad (2.8a)$$

$$u_i^{0+}(x) = \begin{cases} 3\left(\frac{x_{i+1} - x}{x_{i+1} - x_i}\right)^2 - 2\left(\frac{x_{i+1} - x}{x_{i+1} - x_i}\right)^3, & x_i \leq x \leq x_{i+1}, \\ 0, & \text{otherwise}, \end{cases} \quad (2.8b)$$

$$u_i^{1-}(x) = \begin{cases} \left[-\left(\frac{x - x_{i-1}}{x_i - x_{i-1}}\right)^2 + \left(\frac{x - x_{i-1}}{x_i - x_{i-1}}\right)^3\right](x_i - x_{i-1}), & x_{i-1} \leq x \leq x_i, \\ 0, & \text{otherwise}, \end{cases} \quad (2.8c)$$

$$u_i^{1+}(x) = \begin{cases} \left[\left(\frac{x_{i+1} - x}{x_{i+1} - x_i}\right)^2 - \left(\frac{x_{i+1} - x}{x_{i+1} - x_i}\right)^3\right](x_{i+1} - x_i), & x_i \leq x \leq x_{i+1}, \\ 0, & \text{otherwise}. \end{cases} \quad (2.8d)$$

The error in the maximum norm for the Hermite interpolation is stated by well-known theorems in [16], [17]. We will use the maximum-norm which is defined by

$$\|f-g\|_{L^\infty[a,b]} = \max_{a \leq x \leq b} |f(x)-g(x)|.$$

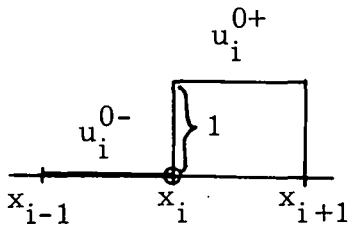

(a) m = 1/2

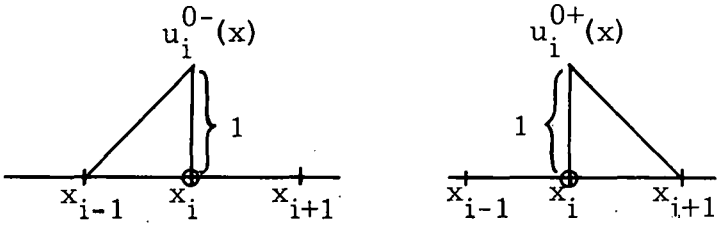

(b) m = 1

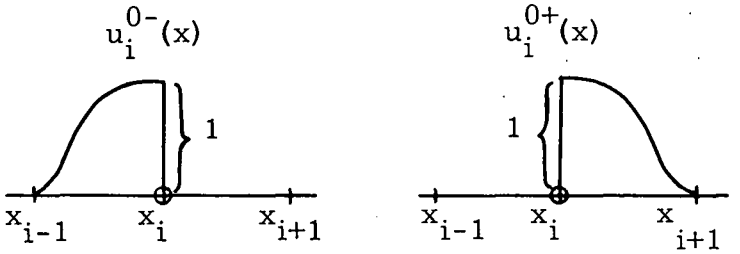

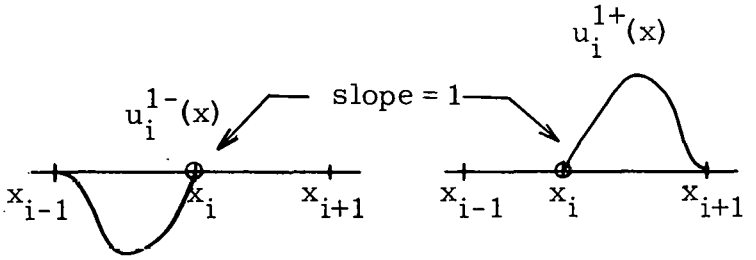

(c) m = 2

Fig. 2.1. Univariate Element Functions: $\frac{1}{2} \leq m \leq 2$

Theorem A. Assume that $f(x) \in C^t[x_i, x_{i+1}]$. Let $s_i(x)$ be a polynomial of degree 2m-1 in $[x_i, x_{i+1}]$ and be a Hermite interpolate to f(x) satisfying Eqs. (2.3a, b). Then $s_i(x)$ is unique and the interpolation error is bounded by

$$\left\| \frac{d^q}{dx^q} (f(x)-s_i(x)) \right\|_{L^\infty(\Delta_i)} \leq K \left|x_{i+1}-x_i\right|^{\mu-q}, \qquad q \leq m-1,$$

where $\mu = \min(2m, t)$ and K is a positive constant independent of $\left|x_{i+1}-x_i\right|$.

Theorem A states that the bound in the pointwise error between f(x) and s(x) for a piecewise continuous function f(x) is of order 2m. Thus, for m = 2, i.e., the cubic Hermite interpolation, the error is $O(\overline{\Delta x}^4)$. The pointwise error in the derivatives is also bounded with an appropriately lower exponent.

Now we introduce the Hermite space $H_m(\Delta)$ defined as a set of all piecewise polynomials of degree 2m-1 in each element Δ_i(i=1,2, ..., N-1) of the partition Δ. Obviously, the number of free parameters, or the dimension, of $H_m(\Delta)$ is 2m(N-1). Convenient basis functions in $H_m(\Delta)$ can be chosen from the element functions $\{u_i^{p\pm}\}$ as defined by Eq. (2.4a,b).

We consider the interpolation of a piecewise continuous function f(x) using the polynomials in the space $H_m(\Delta)$. Let the $H_m(\Delta)$-interpolate of f(x) be defined as any s(x) in the space $H_m(\Delta)$ which satisfies

$$\begin{aligned} s^{(p)}(x_1^+) &= f^{(p)}(x_1^+), \\ s^{(p)}(x_i^\pm) &= f^{(p)}(x_i^\pm), \qquad 2 \leq i \leq N-1, \\ s^{(p)}(x_N^-) &= f^{(p)}(x_N^-), \end{aligned} \tag{2.9}$$

for $0 \leq p \leq m-1$. Then, using the set of functions

$\{u_1^{p+}, u_i^{p\pm}, u_N^{p-}: 2 \leq i \leq N-1,\ 0 \leq p \leq m-1\}$ as a basis of $H_m(\Delta)$, $s(x)$ can be represented by

$$s(x) = \sum_{i=1}^{N-1} s_i(x)$$

$$= \sum_{i=1}^{N-1} \sum_{p=0}^{m-1} \{f^{(p)}(x_i^+)u_i^{p+}(x) + f^{(p)}(x_{i+1}^-)u_{i+1}^{p-}(x)\} \qquad (2.10)$$

where $s_i(x)$ represents the Hermite interpolate in the element Δ_i, defined by Eq. (2.5).

The uniqueness and the accuracy of the $H_m(\Delta)$-interpolate are stated by the following theorem.

Theorem 2.1. Assume that $f(x) \in C_p^t(\Delta)$. Let $s(x)$ be a polynomial of degree $2m-1$ satisfying Eq. (2.9). Then, $s(x)$ is uniquely determined and satisfies

$$\left\| \frac{d^q}{dx^q} (f(x)-s(x)) \right\|_{L^\infty[a,b]} \leq K \overline{\Delta x}^{\mu-q}, \qquad 1 \leq q \leq m-1,$$

where $\mu = \min(2m, t)$, $\overline{\Delta x} = \max_{1\leq i\leq N-1} |x_{i+1}-x_i|$ and K is a constant independent of $\overline{\Delta x}$.

Proof. The uniqueness of $s(x)$ results as a direct consequence of the uniquenesses of individual $s_i(x)$ for $i = 1, 2, \ldots, N-1$ from Theorem A. From the definition of the L^∞-norm,

$$\left\| \frac{d^q}{dx^q} (f(x)-s(x)) \right\|_{L^\infty[a,b]} = \max_{1\leq i\leq N-1} \left\| \frac{d^q}{dx^q} (f(x)-s(x)) \right\|_{L^\infty(\Delta_i)}$$

$$\leq \max_{1\leq i\leq N-1} K_1 |x_{i+1}-x_i|^{\mu-q}$$

$$\leq K \overline{\Delta x}^{\mu-q}$$

where $K = \max_i K_i$ and $\overline{\Delta x} = \max_i |x_{i+1} - x_i|$. This completes the proof.

Theorem 2.1 applies to piecewise continuous functions and states the same order of convergence as Theorem A. It is known that the functions in one-dimensional reactor problems such as neutron fluxes and nuclear element concentrations belong to the class C_p^∞, so that Hermite interpolation in $H_m(\Delta)$ always yields errors of $O(\overline{\Delta x}^{2m})$.

So far, we have considered only piecewise polynomials which are independent in each mesh element and not related to other polynomials in neighboring mesh elements. However, in many cases, functions to be approximated satisfy certain continuity or jump conditions for derivatives at mesh points. In such cases, it is natural to couple the piecewise polynomials satisfying the same conditions. Imposing the coupling conditions is also desirable in numerical computation because this reduces the number of unknowns, or basis functions, and thus the computational effort.

We define the set of coupling conditions $\mathcal{K}$ at each mesh point. The set $\mathcal{K}$ is defined as a collection of coupling coefficients K_i^p where

$$K_i^p = \frac{s^{(p)}(x_i^-)}{s^{(p)}(x_i^+)} \quad . \tag{2.11a}$$

The limit on the order of the derivatives, say k_i, is part of the definition of the coupling conditions $\mathcal{K}$. We can denote $\mathcal{K}$ as

$$\mathcal{K} = \left\{ K_i^p, k_i : 1 \le i \le N,\ 0 \le p \le k_i,\ -1 \le k_i \le m-1 \right\}. \tag{2.11b}$$

We limit k_i to m-1 to conform with the Hermite interpolation. We assume that p=-1 denotes that the functions are not coupled. If $K_i^p = 1$,

then $s^{(p)}(x)$ is continuous at x_i. In general, s(x) allows discontinuities in the derivatives at x_i by taking $K_i^p \neq 1$. The latter case is important for application to diffusion problems where the diffusion coefficient is different on different sides of the interpolation point. Furthermore, coupling conditions at the end points i=1,N allow us to impose periodic continuity conditions.

Associated with the coupling conditions $\mathcal{K}$, we introduce the space $H_m^{\mathcal{K}}(\Delta)$, a subspace of $H_m(\Delta)$, whose elements satisfy the coupling conditions $\mathcal{K}$ specified by Eq. (2.11). It is easy to show that the dimension of $H_m^{\mathcal{K}}(\Delta)$ is equal to the dimension of $H_m(\Delta)$ less the total number of conditions $\sum_{i=1}^{N} (k_i+1)$ in $\mathcal{K}$. This leads to the following theorem.

Theorem 2.2. Let $\mathcal{K}$ be defined by Eq. (2.11). Then the dimension of the space $H_m^{\mathcal{K}}(\Delta)$ is given by

$$\text{Dim } H_m^{\mathcal{K}}(\Delta) = 2m(N-1) - \sum_{i=1}^{N} (k_i+1).$$

The appropriate bases for the space $H_m^{\mathcal{K}}(\Delta)$ are obtained by imposing the conditions $\mathcal{K}$ on $\{u_i^{p\pm}(x)\}$ as defined by Eq. (2.11). We denote the function obtained by coupling the element functions $\{u_i^{p-}(x)\}$ and $\{u_i^{p+}(x)\}$ as $\{u_i^p(x)\}$ such that

$$u_i^p(x) = \begin{cases} \beta- \, u_i^{p-}(x), & x_{i-1} \leq x \leq x_i, \\ \beta+ \, u_i^{p+}(x), & x_i \leq x \leq x_{i+1}, \end{cases} \tag{2.12}$$

where $\beta\pm$ satisfy

$$\frac{\beta-}{\beta+} = K_i^p.$$

Then, the basis functions in the space $H_m^{\mathcal{K}}(\Delta)$ consist of $\{u_i^p(x),\ u_i^{q\pm}(x)$: $1\leq i\leq N,\ 0\leq p\leq k_i,\ k_i+1\leq q\leq m-1\}$.

We illustrate the generation of basis functions for specific coupling conditions in the examples below:

Example 2.1

In neutron diffusion problems, the coupling condition appropriate to the flux is specified by

$$\mathcal{K} = \left\{ K_i^0 = 1,\ K_i^1 = \frac{D(x_i^+)}{D(x_i^-)} :\ 2 \leq i \leq N-1 \right\} . \tag{2.13}$$

Then, the basis functions in $H_m^{\mathcal{K}}(\Delta)$ for $1 \leq m \leq 2$ can be represented by (see Fig. 2.2)

$$u_i^p(x, D) = \begin{cases} \left(\frac{\theta}{D(x_i^-)}\right)^p u_i^{p-}(x), & x_{i-1} \leq x \leq x_i , \\ \left(\frac{\theta}{D(x_i^+)}\right)^p u_i^{p+}(x), & x_i \leq x \leq x_{i+1} , \\ & p = 0, 1, \ldots, m-1 , \end{cases} \tag{2.14}$$

where θ is a normalization constant and

$$u_i^{p\pm}(x) = \begin{cases} \text{Eq. (2.7)} & m = 1 , \\ \text{Eq. (2.8)} & m = 2 . \end{cases}$$

The normalization constant θ is introduced in order to produce stiffness matrices (cf., Sec. 1.3, Chap. I) having small condition numbers. We usually choose θ such that $\frac{\theta}{D(x_i)} \approx 1$.

We note that the conditions $\mathcal{K} = \{K_i^p=1,\ k_i=m-1:\ 0\leq p\leq k_i,\ 2\leq i\leq N-1\}$ lead to the local basis functions in the smooth Hermite space [14], [16], [19]. The smooth Hermite space consists of polynomials of degree 2m-1 which have continuous derivatives of order up to m-1.

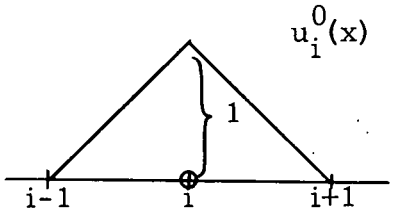

(a) Piecewise Linear Function (m=1)

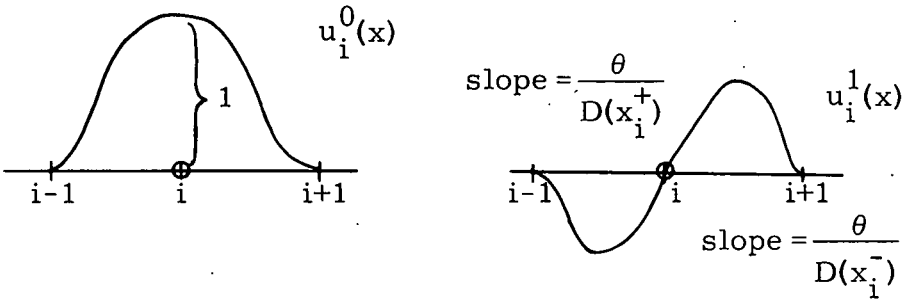

(b) Piecewise Cubic Function (m=2)

Fig. 2.2. Univariate Coupled Basis Functions: Example 2.1

Now we consider the interpolation of a piecewise continuous function f(x) in the space $H_m^{\mathcal{K}}(\Delta)$ where the coupling conditions $\mathcal{K}$ conform with the continuity conditions of f(x) at joints such that

$$\mathcal{K} = \left\{ K_i^p, k_i:\ 0 \le p \le k_i,\ i=2,3,\ldots,N-1 \right\},$$

$$K_i^p = \frac{f^{(p)}(x_i^-)}{f^{(p)}(x_i^+)}, \qquad 0 \le p \le k_i . \tag{2.15a}$$

We define the $H_m^{\mathcal{K}}(\Delta)$-interpolate of f(x) as any s(x) in the space $H_m^{\mathcal{K}}(\Delta)$ which satisfies

$$\left.\begin{aligned} s^{(p)}(x_1^+) &= f^{(p)}(x_1^+) \\ s^{(p)}(x_N^-) &= f^{(p)}(x_N^-) \end{aligned}\right\}, \qquad 0 \le p \le m-1,$$

$$s^{(p)}(x_i^+) = f^{(p)}(x_i^+), \qquad 0 \le p \le m-1,\ 2 \le i \le N-1, \tag{2.15b}$$

$$s^{(p)}(x_i^-) = f^{(p)}(x_i^-), \qquad k_i < p \le m-1,\ 2 \le i \le N-1 .$$

To facilitate representation, we assumed that $f^{(p)}(x_i^+)$ is specified in Eq. (2.15b) whenever p is not equal to -1.

If s(x) is the $H_m^{\mathcal{K}}(\Delta)$-interpolate of f(x), then s(x) can be represented by

$$\begin{aligned} s(x) = &\sum_{p=0}^{m-1} f^{(p)}(x_1^+)\, u_1^{p+}(x) + \sum_{i=2}^{N-1} \sum_{p=0}^{k_i} f^{(p)}(x_i^+)\, u_i^p(x) \\ &+ \sum_{i=2}^{N-1} \sum_{p=k_i+1}^{m-1} \left(f^{(p)}(x_i^-) u_i^{p-}(x) + f^{(p)}(x_i^+) u_i^{p+}(x) \right) \\ &+ \sum_{p=0}^{m-1} f^{(p)}(x_N^-)\, u_N^{p-}(x) . \end{aligned} \tag{2.16}$$

It can easily be shown that the interpolation data in $H_m^{\mathcal{K}}(\Delta)$ specified by Eqs. (2.15a, b) are equivalent to the set of data, Eq. (2.9) for $H_m(\Delta)$. Therefore, the uniqueness and the accuracy of the $H_m^{\mathcal{K}}(\Delta)$-interpolate can also be stated by Theorem 2.1.

2.2 Multivariate Polynomial Space

We consider a region $\Omega = \prod_{j=1}^{n} [a_j, b_j]$ in an n-dimensional space. Ω may include energy as well as space intervals. For the space domain, we assume an orthogonal coordinate system: a Cartesian, cylindrical or polar spherical coordinate system. Define π to be a partition of Ω such that

$$\begin{aligned} \pi: \quad & a_1 = r_{1,1} < r_{1,2} < \ldots < r_{1,N_1} = b_1 , \\ & \vdots \\ & a_n = r_{n,1} < r_{n,2} < \ldots < r_{n,N_n} = b_n . \end{aligned} \tag{2.17}$$

Thus the point $r_{j,k}$ is the k-th mesh point on the j-th coordinate axis. For simplicity, we will use a multiple index i to specify a given point. Thus, $i \equiv (i_1, i_2, \ldots, i_n)$. The set of all mesh points generated by π will be denoted Z_π.

The mesh elements generated by the partition π will be denoted π_ℓ, for $\ell = 1, 2, \ldots, L$, with

$$L = \prod_{j=1}^{n} (N_j - 1) .$$

Each element π_ℓ has associated with it certain mesh points, which we denote as Z_ℓ. For instance, a two-dimensional problem Z_ℓ is a set of 4 mesh points, namely the corners of the mesh element π_ℓ. (See Fig. 2.3.) Note that the set of all Z_ℓ is not Z_π due to the redundancy of all interior mesh points.

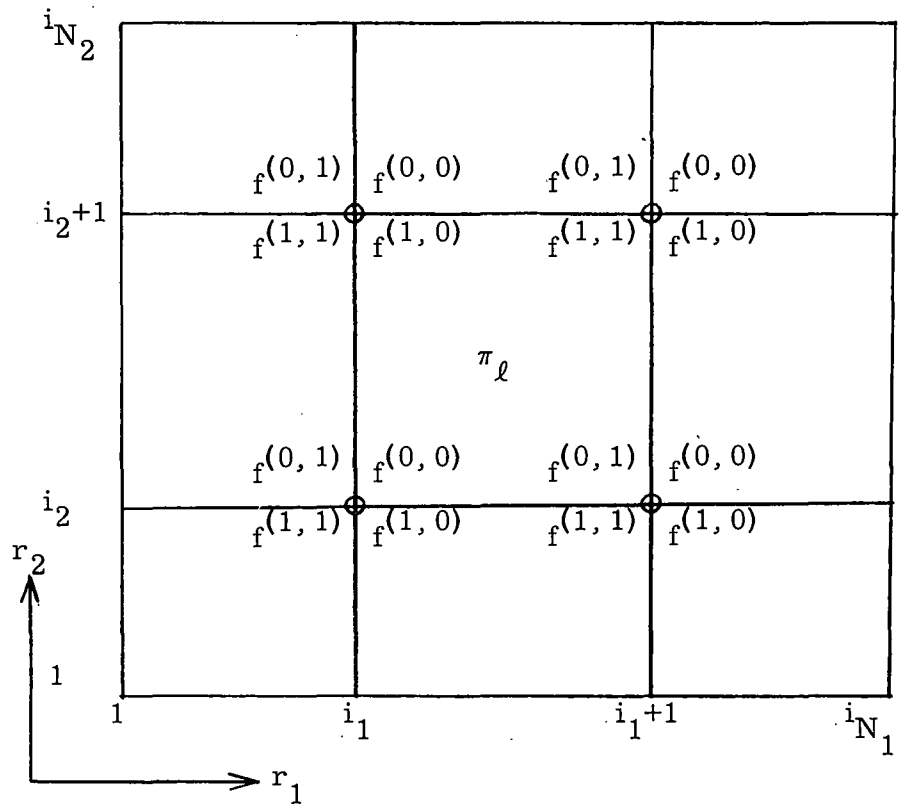

Fig. 2.3. Hermite Interpolation Data in a Rectangular Element

Let $s_\ell(\underline{r})$ be a multivariate polynomial of degree $2m_j-1$ for the j-th variable, for $j = 1, 2, \ldots, n$, in a mesh element π_ℓ. Then, $s_\ell(\underline{r})$ can be represented as

$$s_\ell(\underline{r}) = \sum_{\mu \leq 2m-1} a_\mu \underline{r}^\mu \tag{2.18}$$

where

$$\mu = (\mu_1, \mu_2, \ldots, \mu_n),$$

$$\underline{r}^\mu = r_1^{\mu_1}, r_2^{\mu_2}, \ldots, r_n^{\mu_n},$$

$$m = (m_1, m_2, \ldots, m_n),$$

$\mu \leq 2m-1$ means $\mu_j \leq 2m_j-1$ for all j.

The Hermite interpolation of $f(\underline{r})$ in π_ℓ is defined as the polynomial $s_\ell(\underline{r})$ which satisfies

$$s_\ell^{(p)}(\underline{r}_i) = f^{(p)}(\underline{r}_i) \quad \text{for} \quad i \in Z_\ell, \quad 0 \leq p \leq m-1, \tag{2.19}$$

where $p = (p_1, p_2, \ldots, p_n)$ and $s^{(p)}(\underline{r}) \equiv \dfrac{d^{p_1+p_2+\ldots+p_n}}{dr_1^{p_1} dr_2^{p_2} \ldots dr_n^{p_n}} s(\underline{r})$.

For example, consider a two-dimensional problem where $s_\ell(\underline{r})$ is to be a bicubic polynomial. Then

$$\mu = (\mu_1, \mu_2), \qquad 0 \leq \mu_1, \mu_2 \leq 3,$$

$$\underline{r}^\mu = r_1^{\mu_1} r_2^{\mu_2} .$$

Thus, we have $s_\ell(\underline{r})$ of the form

$$\begin{aligned} s_\ell(\underline{r}) = {} & a_0 + a_1 r_2 + a_2 r_2^2 + a_3 r_2^3 \\ & + b_1 r_1 + b_2 r_1^2 + b_3 r_1^3 \\ & + c_1 r_1 r_2 + c_2 r_1 r_2^2 + c_3 r_1 r_2^3 \\ & + d_1 r_1^2 r_2 + d_2 r_1^2 r_2^2 + d_3 r_1^2 r_3^3 \\ & + e_1 r_1^3 r_2 + e_2 r_1^3 r_2^2 + e_3 r_1^3 r_2^3 . \end{aligned}$$

Note that there are 16 coefficients required to specify a unique $s_\ell(\underline{r})$. For Hermite interpolation, the interpolation data required to specify $s_\ell(\underline{r})$ would be the function values at the 4 mesh points of the element π_ℓ, the first derivative in each direction at the 4 mesh points, and the 4 mixed derivatives at each mesh point, i.e., $\dfrac{\partial^2}{\partial r_1 \partial r_2}$ at each corner. Thus we have 4 values, 4 derivatives in r_1, 4 derivatives in r_2 and 4 mixed derivatives. The corresponding Hermite data are illustrated in Fig. 2.3.

In the previous section, we found that the interpolating polynomial was conveniently represented using the so-called element functions. In particular, using element functions permitted the interpolating polynomial to be represented directly in terms of the Hermite data. A similar representation is possible in the multivariate case using multivariate element functions.

In the univariate case, we have a notation which uses subscripts to identify the mesh point, superscripts to identify particular element functions, and a + or - superscript to identify the element to the left or to the right of the mesh point. We need a similar but somewhat more general notation for the multivariate case. Let $\{u_i^{p,\alpha}(\underline{r})\}$ be a set of multivariate element functions defined by

$$u_i^{p,\alpha}(\underline{r}) \equiv \prod_{j=1}^{n} u_{i_j}^{p_j,\alpha_j}(r_j), \qquad \alpha_j = (+) \text{ or } (-), \tag{2.20}$$

where $p = (p_1, p_2, \ldots, p_n)$, $\alpha = (\alpha_1, \alpha_2, \ldots, \alpha_n)$ and $u_{i_j}^{p_j,\alpha_j}(r_j)$ is a univariate element function as defined by Eq. (2.4a, b). Explicit expressions for low degree univariate element functions are given by Eqs. (2.6)-(2.8). If $[r_{j,i_j+1}, r_{j,i_j}]$, $1 \leq j \leq n$, are supports of $u_{i_j}^{p_j,\alpha_j}(r_j)$, then the support of the multivariate element function $u_i^{p,\alpha}(r)$ is specified by $\prod_{j=1}^{n} [r_{j,i_j+1}, r_{j,i_j}]$.

Using multivariate element functions, the Hermite interpolate $s_\ell(\underline{r})$ which satisfies Eq. (2.19) can be represented by

$$s_\ell(\underline{r}) = \sum_{i \in Z_\ell} \sum_{p=0}^{m-1} f^{(p)}(\underline{r}_i)\, u_i^{p,\alpha}(\underline{r}) \tag{2.21}$$

where $\alpha = (\alpha_1, \alpha_2, \ldots, \alpha_n)$ is properly chosen such that $u_i^{p,\alpha}(\underline{r})$ have support on π_ℓ.

In the study of univariate interpolation we considered certain classes of functions of one variable. In particular, we defined classes with certain differentiability properties and continuity properties. We now consider analogous multivariate classes.

Let $C^t(\Omega)$, $t = (t_1, t_2, \ldots, t_n)$ be the class of all functions defined on Ω which are t_j times differentiable for the j-th variable. Let $C_p^t(\pi)$ be the class of all functions $f(\underline{r})$ which belong to the class $C^t(\pi_\ell)$ for $\ell = 1, 2, \ldots, L$ and have finite one-sided limits on the mesh element boundaries for derivatives up to order t.

The uniqueness and the approximation error for the Hermite interpolation are stated in the following theorem.

Theorem 2.3. Assume that $f(\underline{r}) \in C^t(\pi_\ell)$. Let $s(\underline{r})$ be a multivariate polynomial of degree 2m-1 satisfying Eq. (2.19). Then, $s(\underline{r})$ is uniquely determined and satisfies

$$\left\| \frac{\partial^q}{\partial \underline{r}^q} (f(\underline{r}) - s(\underline{r})) \right\|_{L^\infty(\pi_\ell)} \leq K_1 \Delta r_1^{\mu_1 - q_1} + \ldots + K_n \Delta r_n^{\mu_n - q_n},$$

$$0 \leq q \leq m-1,$$

where

$$q = (q_1, q_2, \ldots, q_n),$$

$$\mu_j = \min(2m_j, t_j),$$

$$\Delta r_j = \left| r_{j, i_j+1} - r_{j, i_j} \right|,$$

and K_j is a constant independent of Δr_j, $j = 1, 2, \ldots, n$.

Proof. The theorem is proven in Appendix A.

Theorem 2.3 gives the pointwise error bounds in terms of exponents of varying orders depending on the degrees of the polynomials for different variables. In reactor problems, the theorem provides an estimation of the order of convergence when polynomials of different degrees for space and energy are used. In [16], [17] and [38], the error bounds were obtained only for polynomials of uniform degrees and theorems similar to Theorem 2.3 could not be found in previous works.

We now introduce the multivariate Hermite space $H_m(\pi)$, which is defined as a set of multivariate piecewise polynomials of degree $2m_j-1$ for each variable $r_j (j = 1, 2, \ldots, n)$ on elements π_ℓ, $\ell = 1, \ldots, L$ of partition π. The dimension of the space is easily shown to be $\prod_{j=1}^{n} 2m_j(N_j-1)$. In this space, the element functions $\{u_i^{p,\alpha}(\underline{r})\}^{j=1}$ defined by Eq. (2.20) can be used as a set of basis functions.

We define the $H_m(\pi)$-interpolate of a piecewise continuous function $f(\underline{r})$ as any element of $H_m(\pi)$ which satisfies

$$s^{(p)}(\underline{r}_i(\alpha)) = f^{(p)}(\underline{r}_i(\alpha)), \quad i \in Z_\pi, \quad 0 \leq p \leq m-1, \tag{2.21a}$$

where $\underline{r}_i(\alpha) = (r_{1,i_1}(\alpha_1), r_{2,i_2}(\alpha_2), \ldots, r_{n,i_n}(\alpha_n))$ and $\alpha_j = (\pm)$ for $1 \leq j \leq n$. $\underline{r}_i(\alpha)$ denotes $\underline{r}_i$ as a limiting point in a multidimensional space approached along the coordinate axes from the direction specified by α_j's.

Using the element functions $\{u_i^{p,\alpha}(\underline{r})\}$ as the basis functions of $H_m(\pi)$, the Hermite interpolate can be represented by

$$\begin{aligned} s(\underline{r}) &= \sum_{\ell=1}^{L} s_\ell(\underline{r}) \\ &= \sum_{\ell=1}^{L} \sum_{i \in Z_\ell} \sum_{p=0}^{m-1} f^{(p)}(\underline{r}_i(\alpha))\, u_i^{p,\alpha}(\underline{r}) \end{aligned} \tag{2.21b}$$

where $s_\ell(\underline{r})$ represents the Hermite interpolate in the element π_ℓ, as defined by Eq. (2.21). Thus, the convenient representation in terms of the Hermite data is possible in the multivariate case.

The uniqueness and the interpolation error bounds are stated in the following theorem.

Theorem 2.4. Assume that $f(\underline{r}) \in C_p^t(\pi)$. Let $s(\underline{r})$ be a multivariate polynomial of degree $2m-1$, $m=(m_1, m_2, \ldots, m_n)$ satisfying Eq. (2.21). Then $s(\underline{r})$ is uniquely determined and satisfies

$$\left\| \frac{\partial^q}{\partial r^q} (f(\underline{r})-s(\underline{r})) \right\|_{L^\infty(\Omega)} \leq K_1 \overline{\Delta r}_1^{\mu_1 - q_1} + \ldots + K_n \overline{\Delta r}_n^{\mu_n - q_n}, \quad 0 \leq q \leq m-1,$$

where

$$q = (q_1, q_2, \ldots, q_n),$$

$$\mu_j = \min(2m_j, t_j),$$

$$\overline{\Delta r}_j = \max_{i_j} |r_{j,i_j+1} - r_{j,i_j}|,$$

and K_j is a constant independent of $\overline{\Delta r}_j$ for $j = 1, 2, \ldots, n$.

Proof. Analogous to the univariate spaces, Theorem 2.3 holds locally for each element and can be extended to apply for the whole region. The proof is similar to that of Theorem 2.1 and will be omitted.

This theorem enables us to estimate the order of convergence for individual variables. For example, in reactor problems, if one uses step functions ($m = \frac{1}{2}$) for the energy variable and cubic functions ($m = 2$)

for the space variable, then Theorem 2.4 states that the error is given by the order $O(\Delta E) + O(\Delta r^4)$. This theorem is useful for estimating the approximation error for the solution of neutron diffusion problems in the following chapters.

Just as in the univariate space, coupling conditions can be imposed on the space $H_{rm}(\pi)$. We define the set of coupling conditions $\mathcal{K}$ by

$$\mathcal{K} = \{ K_i^{p,\alpha(j)}, k_i : 0 \leq p_i \leq k_i \leq m-1,\ 1 \leq j \leq n,\quad i \in Z_\pi \} \tag{2.22a}$$

where for any $s(\underline{r}) \in C_p^t(\pi)$,

$$\begin{aligned} K_i^{p,\alpha(j)} &\equiv K_i^{p_1\alpha_1, \ldots, p_j, \ldots, p_n\alpha_n} \\ &\equiv \frac{s^{(p)}\left(r_{1,i_1}(\alpha_1), \ldots, r_{j,i_j}(-), \ldots, r_{n,i_n}(\alpha_n)\right)}{s^{(p)}\left(r_{1,i_1}(\alpha_1), \ldots, r_{j,i_j}(+), \ldots, r_{n,i_n}(\alpha_n)\right)}, \\ \alpha_k &= + \text{ or } -, \qquad 1 \leq k \leq n. \end{aligned} \tag{2.22b}$$

As in the univariate space, we define $p_j = -1$ to mean that $s(\underline{r})$ is uncoupled at $\underline{r}_i$ in the direction of the axis of r_j.

The coupling conditions specify the ratio of derivatives approaching a mesh point in opposite directions on the coordinate axis. The conditions may apply to all derivatives of order up to m-1 and all directions, or partially to some combinations of particular derivatives and directions. When $K_i^{p,\alpha(j)} = 1$, $s^{(p)}(\underline{r})$ is continuous at $\underline{r}_i$. $K_i^{p,\alpha(j)} \neq 1$ means that $s^{(p)}(\underline{r}(\alpha))$ is bent at $\underline{r}_i$. The latter is important in applications to the diffusion problem.

Associated with the set of coupling conditions $\mathcal{K}$, we introduce the space $H_m^{\mathcal{K}}(\pi)$, a subspace of $H_m(\pi)$, whose elements satisfy the coupling

conditions $\mathcal{K}$ specified by Eq. (2.22). Similarly, as in the univariate space, it can be shown that the interpolation properties as stated by Theorem 2.4 apply to the subspaces $H_m^{\mathcal{K}}(\pi)$. The dimension of $H_m^{\mathcal{K}}(\pi)$ is easily shown to be the dimension of $H_m(\pi)$ less the total number of coupling conditions. Therefore, we obtain the following theorem.

Theorem 2.5. Let $\mathcal{K}$ be defined by Eq. (2.22). Then the dimension of the space $H_m^{\mathcal{K}}(\pi)$ is given by

$$\text{Dim } H_m^{\mathcal{K}}(\pi) = \text{Dim } H_m(\pi) - k$$

where k represents the total number of conditions specified by $\mathcal{K}$.

We now consider the generation of basis functions in the space $H_m^{\mathcal{K}}(\pi)$. The multivariate basis functions are obtained by coupling the multivariate element functions defined by Eq. (2.20) according to the coupling conditions specified by $\mathcal{K}$. Using element functions permits us to generate multivariate basis functions for various types of continuity conditions.

We take a two-dimensional space to illustrate the procedures. We shall denote $u_i^{p_1,p_2^+}(\underline{r})$ as a basis function which is obtained by coupling two element functions $u_i^{p_1^-,p_2^+}(\underline{r})$ and $u_i^{p_1^+,p_2^+}(\underline{r})$ according to the coupling condition $K_i^{p_1,p_2^+}$ such that (see Fig. 2.4)

$$u_i^{p_1,p_2^+}(\underline{r}) = \begin{cases} \beta_{II} u_i^{p_1^-,p_2^+}(\underline{r}), & \text{II} \\ \beta_I u_i^{p_1^+,p_2^+}(\underline{r}), & \text{I} \\ 0, & \text{III, IV} \end{cases} \tag{2.23a}$$

where β_I and β_{II} satisfy

$$\frac{\beta_{II}}{\beta_I} = K_i^{p_1,p_2^+} .$$

Note that $u_i^{p_1,p_2^+}(\underline{r})$ have support in regions I and II.

Similarly, we can define $u_i^{p_1,p_2^-}(\underline{r})$ by combining $u_i^{p_1^-,p_2^-}(\underline{r})$ and $u_i^{p_1^+,p_2^-}(\underline{r})$ such that

$$u_i^{p_1,p_2^-}(r) = \begin{cases} \beta_{III}\ u_i^{p_1^-,p_2^-}(\underline{r}), & \text{III} \\ \beta_{IV}\ u_i^{p_1^+,p_2^-}(\underline{r}), & \text{IV} \\ 0, & \text{I, II} \end{cases} \qquad (2.23b)$$

where β_{III} and β_{IV} satisfy

$$\frac{\beta_{III}}{\beta_{IV}} = K_i^{p_1,p_2^-} .$$

$u_i^{p_1,p_2^-}$ have support in regions III and IV. (Fig. 2.4.) $u_i^{p_1,p_2^+}(\underline{r})$ and $u_i^{p_1,p_2^-}(\underline{r})$ define partially coupled functions in the direction of the r_1-axis. We can similarly define $u_i^{p_1^-,p_2}(\underline{r})$ and $u_i^{p_1^+,p_2}(\underline{r})$ by coupling $u_i^{p_1^-,p_2^-}$ and $u_i^{p_1^-,p_2^+}$, and $u_i^{p_1^+,p_2^-}$ and $u_i^{p_1^+,p_2^+}$, respectively.

We proceed further to define $u_i^{p_1,p_2}(\underline{r})$ coupling $u_i^{p_1^\pm,p_2^\pm}(\underline{r})$ such that

$$u_i^{p_1,p_2}(\underline{r}) = \begin{cases} \beta_I\ u_i^{p_1^+,p_2^+}(\underline{r}), & \text{I} \\ \beta_{II}\ u_i^{p_1^-,p_2^+}(\underline{r}), & \text{II} \\ \beta_{III}\ u_i^{p_1^-,p_2^-}(\underline{r}), & \text{III} \\ \beta_{IV}\ u_i^{p_1^+,p_2^-}(\underline{r}), & \text{IV} \end{cases} \qquad (2.23c)$$

where β_I, β_{II}, β_{III} and β_{IV} satisfy

$$\frac{\beta_{II}}{\beta_I} = K_i^{p_1,p_2+}, \quad \frac{\beta_{III}}{\beta_{II}} = K_i^{p_1-,p_2}, \quad \frac{\beta_{III}}{\beta_{IV}} = K_i^{p_1,p_2-}$$

and

$$\frac{\beta_{IV}}{\beta_I} = k_i^{p_1+,p_2} .$$

Obviously, $u_i^{p_1,p_2}(\underline{r})$ has support in regions I, II, III and IV. We note that when all of $K_i^{p_1\pm,p_2\pm} = 1$, the coupled basis functions $u_i^{p_1,p_2}(\underline{r})$ have continuous derivatives of orders p_1 and p_2 in r_1 and r_2, respectively, and this is identical to the basis functions in the smooth Hermite space as considered in [18] and [19]. However, when $K_i^{p_1\pm,p_2\pm} \neq 1$, the generations of $u_i^{p_1,p_2}(\underline{r})$ as given by Eq. (2.23c) is more involved and in some cases, the coupling conditions can lead to $\beta = 0$ as the only acceptable constants.

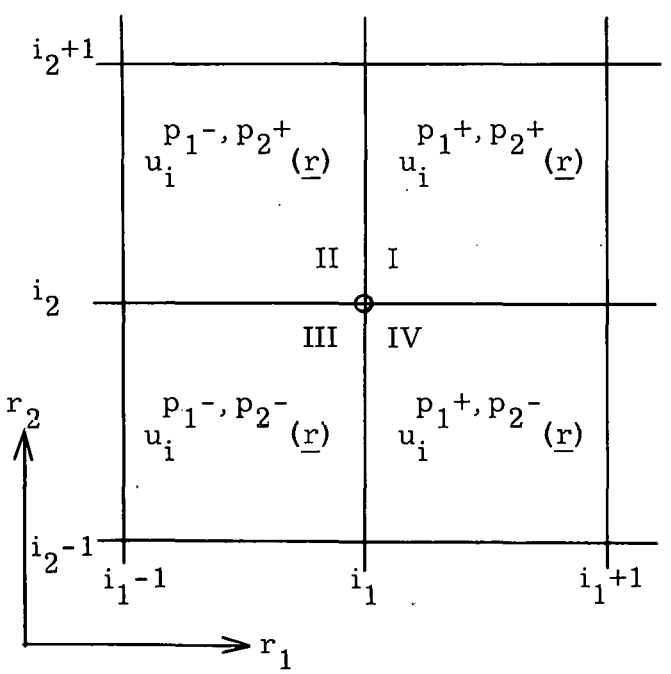

Fig. 2.4. Element Functions in a Two-Dimensional Partition

This case is discussed in detail in the following examples, in which some practical polynomial spaces in the reactor analysis are considered.

Example 2.2

Let $\Omega = [a, b]$ and $\mathcal{E} = [E_{min}, E_{max}]$ and let π be a partition of $\Omega \times \mathcal{E}$ such that $\pi = \pi_\Omega \times \pi_\mathcal{E}$ where

$$\pi_\Omega: \quad a = x_1 < x_2 < \ldots < x_N = b,$$

$$\pi_\mathcal{E}: \quad E_{min} = E_1 < E_2 < \ldots < E_{N_E} = E_{max}.$$

The diffusion coefficient D is assumed to be piecewise constant in each element of π.

In this example, we are interested in generating basis functions to approximate the neutron flux in subspaces of the Hermite space $H_m(\pi)$ where $m = (m_x, m_E)$. The neutron flux is assumed to satisfy the conditions:

$$\text{(i)} \quad \phi \in C^{t_E}(\mathcal{E}), \quad t_E \geq 2m_E,$$

$$\text{(ii)} \quad \phi \in C_p^{t_x}(\pi_\Omega), \quad t_x \geq 2m_x, \tag{2.24}$$

$$\text{(iii)} \quad \phi(x, E) \text{ and } D \frac{\partial}{\partial x} \phi(x, E) \text{ are continuous at } x = x_i, \quad 2 \leq i \leq N-1.$$

Let $\mathcal{K}$ be the set of coupling conditions defined by Eq. (2.22) and conforming to Eq. (2.24). Then, we define basis functions in the space $H_m^{\mathcal{K}}(\pi)$ for $1 \leq m_x \leq 2$ and $m_E \geq 1/2$ as follows (see Fig. 2.5)

$$u_{i,g}^{p_x,p_E}(x, D) = \begin{cases} \left(\frac{\theta}{D_I}\right)^{p_x} u_i^{p_x+}(x)\, u_g^{p_E+}(E), & \text{I} \\ \left(\frac{\theta}{D_{II}}\right)^{p_x} u_i^{p_x-}(x)\, u_g^{p_E+}(E), & \text{II} \\ \left(\frac{\theta}{D_{III}}\right)^{p_x} u_i^{p_x-}(x)\, u_g^{p_E-}(E), & \text{III} \\ \left(\frac{\theta}{D_{IV}}\right)^{p_x} u_i^{p_x+}(x)\, u_g^{p_E-}(E), & \text{IV} \end{cases} \tag{2.25}$$

where $0 \leq p_x \leq m_x-1$ and $0 \leq p_E \leq m_E-1$. θ is a normalization constant and usually is taken to be $\frac{\theta}{D} \approx 1$. $u_i^{p_x\pm}(x)$ and $u_g^{p_E\pm}(E)$ are univariate element functions and are defined by Eqs. (2.4), (2.6), (2.7) and (2.8).

The constructed basis functions for various degrees of polynomials in x and E are illustrated in Fig. 2.5. Note that the basis functions $u_{i,g}^{p_x,p_E}(x, E)$ with $m_x = 2$ and $m_E = 1$ satisfy the conditions specified by Eq. (2.24). Also note that the basis function, in which $m_E = 1/2$, leads to the conventional multigroup approximation. In this case, the basis functions are not continuous in the energy domain.

We further comment on the definition of the basis functions. In general, the diffusion coefficient is dependent on the energy and space variables. The proper basis functions, which satisfy the requisite conditions Eq. (2.24), are then defined by Eq. (2.25) by permitting D to be a function of both energy and space. However, when $\frac{\theta}{D}$ is not a constant, the resulting basis functions do not belong to the space $H_m(\pi)$ and thus Theorem 2.4 cannot be applied.

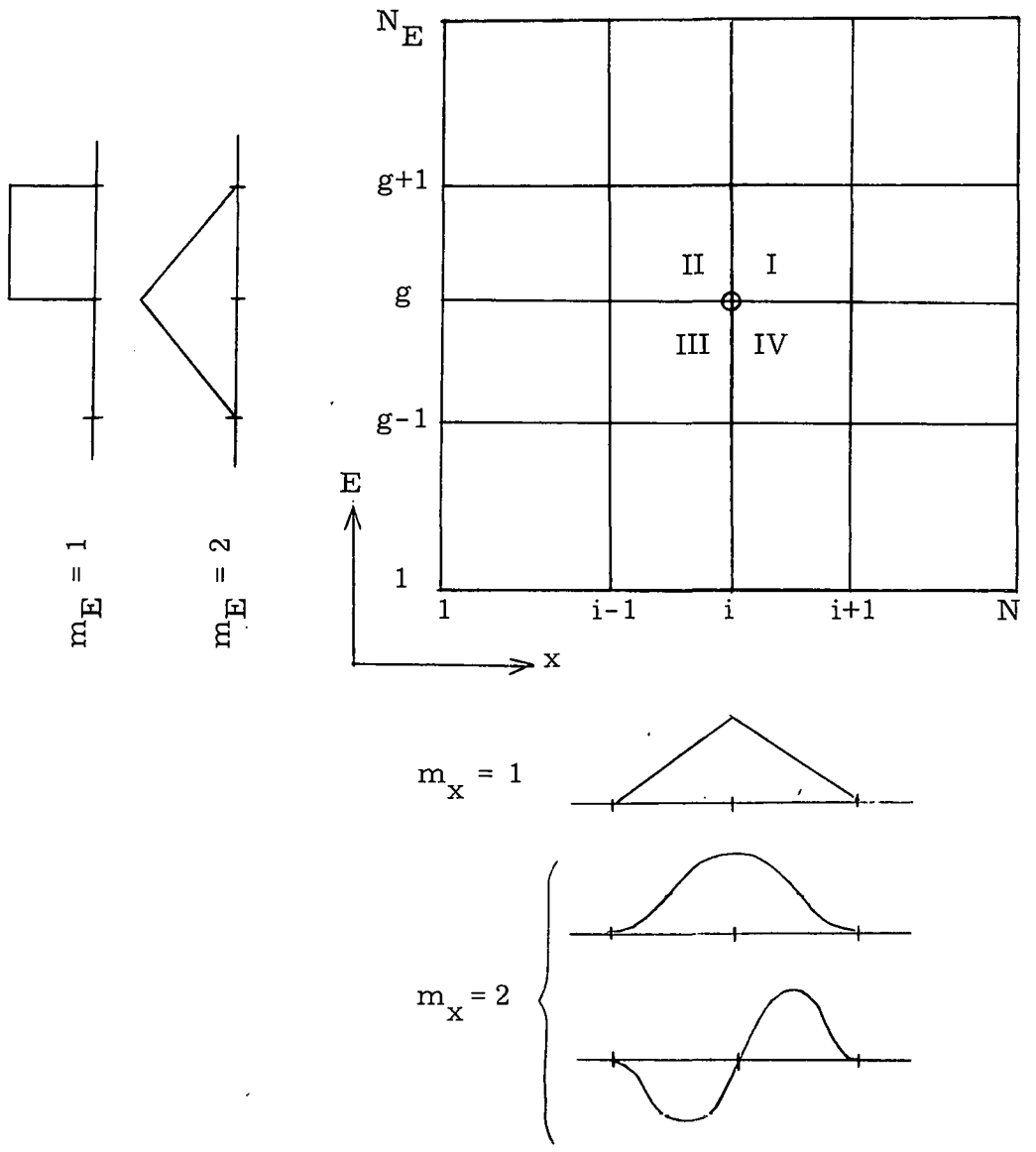

Fig. 2.5. Energy- and Space-Dependent Basis Functions: Example (2.2)

Example 2.3

Consider $\Omega = [a, b] \times [c, d]$ in a two-dimensional space and let π be the partition of Ω as defined by Eq. (2.17). Let $i = (i_x, i_y)$. We designate the mesh elements surrounding $\underline{r}_i$ as shown in Fig. 2.6. And assume that the diffusion coefficients are constant in each element.

In this example, we are interested in generating practical basis functions in two space variables for the approximation of neutron fluxes, which satisfy the conditions:

$$\begin{aligned} &\text{(i)} \qquad \phi(\underline{r}) \in C_p^t(\pi), \qquad t \geqslant 2m, \\ &\text{(ii)} \qquad \phi(\underline{r}),\ D \frac{\partial}{\partial n} \phi(\underline{r}) \text{ are continuous at element interfaces,} \end{aligned} \tag{2.26a}$$

where $\frac{\partial}{\partial n}$ denotes the derivative normal to the interface. Hence, we define $\mathcal{K}$ as the set of coupling conditions, denoted by Eq. (2.22), which conforms with the continuity conditions, Eq. (2.26a). Thus, we consider the selection of basis functions in the subspace $H_m^{\mathcal{K}}(\pi)$ for $m_x = m_y = 1$ and 2.

First, we consider the space of bilinear functions $H_{(1,1)}^{\mathcal{K}}(\pi)$. Then, there is one basis function at each mesh point which is defined by

$$u_i^{(0,0)}(x, y) = \begin{cases} u_i^{0+}(x)\, u_i^{0+}(y), & \text{I} \\ u_i^{0-}(x)\, u_i^{0+}(y), & \text{II} \\ u_i^{0-}(x)\, u_i^{0-}(y), & \text{III} \\ u_i^{0+}(x)\, u_i^{0-}(y), & \text{IV} \end{cases} \tag{2.27}$$

where $u_i^{0\pm}(x)$, $u_i^{0\pm}(y)$ are defined by Eq. (2.7). $u_i^{(0,0)}(x, y)$ is continuous; however, it does not satisfy the continuity of $D \frac{\partial}{\partial n} \phi$ in Eq. (2.26a).

Next, we consider the bicubic space, $H^{\mathcal{K}}_{(2,2)}(\pi)$. The basis functions in $H^{\mathcal{K}}_{(2,2)}(\pi)$ depend on the diffusion coefficients surrounding $\underline{r}_i$. Thus, we consider two cases separately.

Case (1). $D_I D_{III} = D_{II} D_{IV}$

This condition is satisfied for any interior mesh points or interface points except the singular points. Proper basis functions are given by (see Fig. 2.6)

$$u_i^{(0,0)}(\underline{r}) = \begin{cases} u_i^{0+}(x)\, u_i^{0+}(y), & \text{I} \\ u_i^{0-}(x)\, u_i^{0+}(y), & \text{II} \\ u_i^{0-}(x)\, u_i^{0-}(y), & \text{III} \\ u_i^{0+}(x)\, u_i^{0-}(y), & \text{IV} \end{cases} \tag{2.28a}$$

$$u_i^{(1,0)}(\underline{r}, D) = \begin{cases} \frac{\theta}{D_I}\, u_i^{1+}(x)\, u_i^{0+}(y), & \text{I} \\ \frac{\theta}{D_{II}}\, u_i^{1-}(x)\, u_i^{0+}(y), & \text{II} \\ \frac{\theta}{D_{II}}\, u_i^{1-}(x)\, u_i^{0-}(y), & \text{III} \\ \frac{\theta}{D_I}\, u_i^{1+}(x)\, u_i^{0-}(y), & \text{IV} \end{cases} \tag{2.28b}$$

or $\frac{\theta}{D_I}$ and $\frac{\theta}{D_{II}}$ may be replaced by $\frac{\theta}{D_{IV}}$ and $\frac{\theta}{D_{III}}$, respectively.

$$u_i^{(0,1)}(\underline{r}, D) = \begin{cases} \frac{\theta}{D_{II}} u_i^{0+}(x)\, u_i^{1+}(y), & \text{I} \\ \frac{\theta}{D_{II}} u_i^{0-}(x)\, u_i^{1+}(y), & \text{II} \\ \frac{\theta}{D_{III}} u_i^{0-}(x)\, u_i^{1-}(y), & \text{III} \\ \frac{\theta}{D_{III}} u_i^{1+}(x)\, u_i^{1-}(y), & \text{IV} \end{cases} \tag{2.28c}$$

or $\frac{\theta}{D_{II}}$ and $\frac{\theta}{D_{III}}$ may be replaced by $\frac{\theta}{D_I}$ and $\frac{\theta}{D_{IV}}$, respectively.

$$u_i^{(1,1)}(\underline{r}, D) = \begin{cases} \frac{\theta}{D_I} u_i^{1+}(x)\, u_i^{1+}(y), & \text{I} \\ \frac{\theta}{D_{II}} u_i^{1-}(x)\, u_i^{1+}(y), & \text{II} \\ \frac{\theta}{D_{III}} u_i^{1-}(x)\, u_i^{1-}(y), & \text{III} \\ \frac{\theta}{D_{IV}} u_i^{1+}(x)\, u_i^{1-}(y), & \text{IV} \end{cases} \tag{2.28d}$$

θ denotes a normalization constant and is generally taken such that $\frac{\theta}{D} \approx 1$. $u_i^{p\pm}(x)$, $u_i^{p\pm}(y)$, $p = 0, 1$, are univariate cubic element functions defined by Eq. (2.8). The basis functions satisfy the interface conditions Eq. (2.26a) for the neutron fluxes.

Case (2). $D_I D_{III} \neq D_{II} D_{IV}$

In this case, $\underline{r}_i$ is a singular point. When $D_I D_{III} \neq D_{II} D_{IV}$, it is easy to show that the interface condition (2.26a) permits $\phi(\underline{r})$ to have only

$$\frac{\partial}{\partial x} \phi(\underline{r}_i) = \frac{\partial}{\partial y} \phi(\underline{r}_i) = 0 .$$

Therefore, in Eq. (2.28), $u_i^{(0,1)}(\underline{r})$ and $u_i^{(1,0)}(\underline{r})$ can be suppressed and the proper basis functions in the space $H_m^{\mathcal{K}}(\pi)$ consist of two functions,

$$\begin{aligned} &u_i^{(0,0)}(\underline{r}) \ ; \quad \text{Eq. (2.28a)} , \\ &u_i^{(1,1)}(\underline{r}, D) \ ; \quad \text{Eq. (2.28d)} . \end{aligned} \tag{2.29}$$

At singular points, where $D_I D_{III} \neq D_{II} D_{IV}$, the acceptable Hermite interpolation data must include $\frac{\partial}{\partial x} \phi(\underline{r}_i) = \frac{\partial}{\partial y} \phi(\underline{r}_i) = 0$, so that the basis functions in Eq. (2.29) are adequate for the interpolation problem. The sets of basis functions defined in cases (1) and (2) are compatible with the conditions in Eq. (2.26a) and they form complete bases in $H_m^{\mathcal{K}}(\pi)$. Furthermore, Theorem 2.4 applies for interpolations of functions using the basis functions defined by Eqs. (2.28) and (2.29).

In solving neutron diffusion problems, the singular solution requires special consideration if high-order accuracy is to be obtained. However, in this thesis, no attempt is made to improve the solution with singularities for the reasons mentioned in Chapter I. As we shall see in Chapters IV and VI, we can reformulate the neutron diffusion problem to a weak form where the current continuity condition appears as a natural interface condition. In the weak form, acceptable solutions are the functions which satisfy the conditions (cf., Sec. 4.1, Chap. IV):

$$\begin{aligned} &\text{(i)} \quad \phi(\underline{r}) \text{ is continuous in } \Omega, \\ &\text{(ii)} \quad \underline{\nabla} \phi(\underline{r}) \text{ is square integrable in } \Omega. \end{aligned} \tag{2.26b}$$

The bilinear function defined by Eq. (2.27), and the bicubic functions defined by Eqs. (2.28) and (2.29) satisfy the above conditions and thus are acceptable for calculations with the weak formulation.

However, since the analytic solution at singular points are not necessarily required to satisfy $\frac{\partial}{\partial x}\phi(\underline{r}_i) = \frac{\partial}{\partial y}\phi(\underline{r}_i) = 0$, the use of the basis functions defined by Eq. (2.29) can distort the solution and can lead to poor approximations, especially for coarse mesh calculations. The condition (2.26b) relaxes the current continuity condition, and thus it would be desirable to choose basis functions at the singular point which are continuous but for which the first derivatives are unspecified. The reason for this particular choice is that we want the approximation schemes themselves to choose the optimal coupling relation.

By using the procedure described in this section, it is possible to generate various types of basis functions in subspaces of $H_{(2,2)}(\pi)$, which satisfy the condition (2.26b) and partially the current continuity condition. Below we give an example of such a set of basis functions, which has a minimum number of functions but whose first derivatives are not unnecessarily restrained.

$$u_i^{(0,0)}(\underline{r}) = \text{Eq. (2.28a)}, \tag{2.30a}$$

$$u_i^{(1-,0)}(\underline{r}) = \begin{cases} u_i^{1-}(x)\, u_i^{0+}(y), & \text{II} \\ u_i^{1-}(x)\, u_i^{0-}(y), & \text{III} \\ 0, & \text{I \& IV} \end{cases} \tag{2.30b}$$

$$u_i^{(1+,0)}(\underline{r}) = \begin{cases} u_i^{1+}(x)\, u_i^{0+}(y), & \text{I} \\ u_i^{1+}(x)\, u_i^{0-}(y), & \text{IV} \\ 0, & \text{II \& III} \end{cases} \tag{2.30c}$$

$$u_i^{(0,1-)}(\underline{r}) = \begin{cases} u_i^{0-}(x)\, u_i^{1-}(y), & \text{III} \\ u_i^{0+}(x)\, u_i^{1-}(y), & \text{IV} \\ 0, & \text{I \& II} \end{cases} \tag{2.30d}$$

$$u_i^{(0,1+)}(\underline{r}) = \begin{cases} u_i^{0+}(x)\, u_i^{1+}(y), & \text{I} \\ u_i^{0-}(x)\, u_i^{1+}(y), & \text{II} \\ 0, & \text{III \& IV} \end{cases} \tag{2.30e}$$

$$u_i^{(1,1)}(\underline{r}) = \text{Eq. (2.28d)}. \tag{2.30f}$$

These functions are also shown in Fig. 2.6.b. There are six independent basis functions according to Theorem 2.5. $u_i^{(0,0)}$ and $u_i^{(1,1)}$ satisfy both the continuity of flux and currents. The remaining functions are partially coupled basis functions, and so the interface conditions are partially satisfied by these functions. Note that the coupling between $u_i^{(1-,0)}$ and $u_i^{(1+,0)}$, and $u_i^{(0,1-)}$ and $u_i^{(0,1+)}$ are unspecified so as to be determined by a particular numerical scheme, say the Galerkin scheme. Numerical results (c.f., Sec. 4.4, Chap. IV) indicate that approximations using these sets give better convergence on flux shape and eigenvalues than those using basis functions, whose derivatives are erroneously fixed, such as the functions given by Eq. (2.29) or Set B in Example 4.4 in Chapter IV.

In this example, we have limited the diffusion coefficients to piecewise constant functions. However, they are generally dependent on the space and energy variables and the proper basis functions, which satisfy

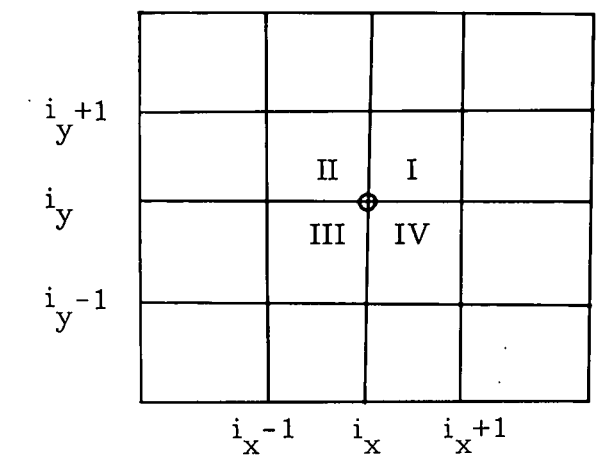

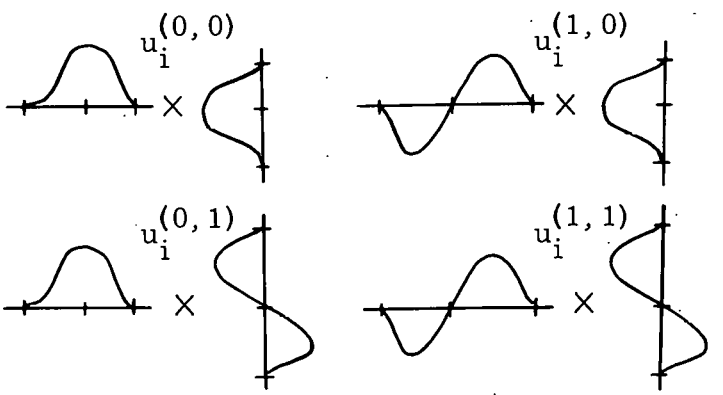

(a) Eq. (2.28)

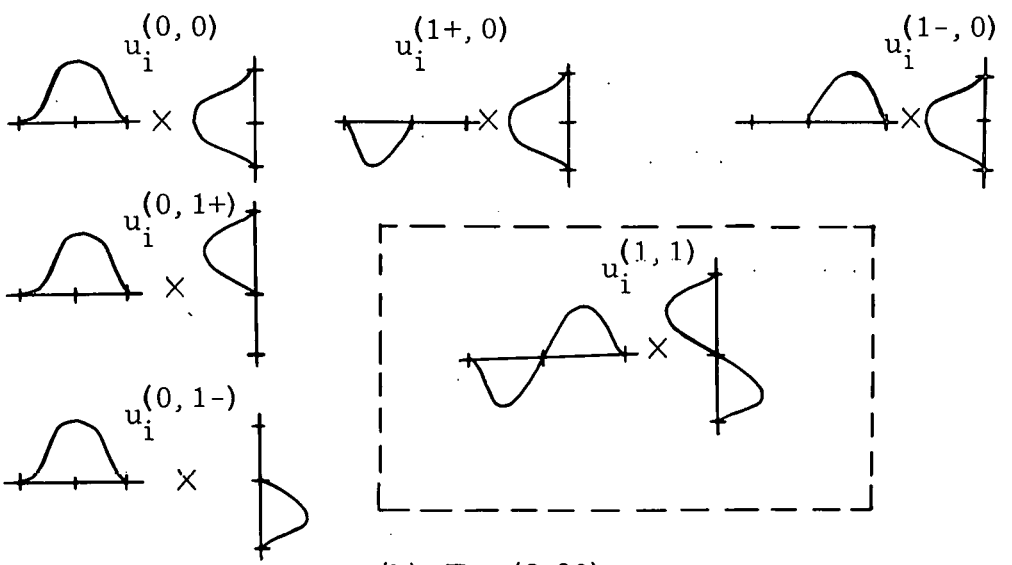

(b) Eq. (2.30)

Fig. 2.6. Bicubic Basis Functions: Example 2.3

the requisite continuity conditions Eq. (2.26a), can be obtained by using variable diffusion coefficients in Eqs. (2.28) - (2.30). However, the resulting basis functions do not belong to the Hermite space $H_m(\pi)$ (cf., Example 2.2), and thus Theorem 2.4 cannot be applied in this case.

In summary, for solving the weak form of neutron diffusion problems, we may use the set of bilinear basis functions defined by Eq. (2.27), and the set of bicubic basis functions defined by Eq. (2.28) for all mesh points except singular points and Eq. (2.30) for singular points.

Generation of basis functions on the boundary can be considered as a special case of the above considerations. These are obtained by coupling element functions whose supports are nonzero. For example, we consider a rectangular polygon as shown in Fig. 2.7. The basis functions at point A coincide with element functions in region I. The basis functions at point B are obtained by coupling two element functions in regions I and II (cf., Eqs. (2.23a, b)). Finally, the basis functions at point C are obtained by coupling three element functions defined on regions I, II and III.

We have confined our consideration to two-dimensional spaces. However, the basic procedure for generating basis functions at regular and singular points can be carried over directly and applied in three-dimensional spaces.

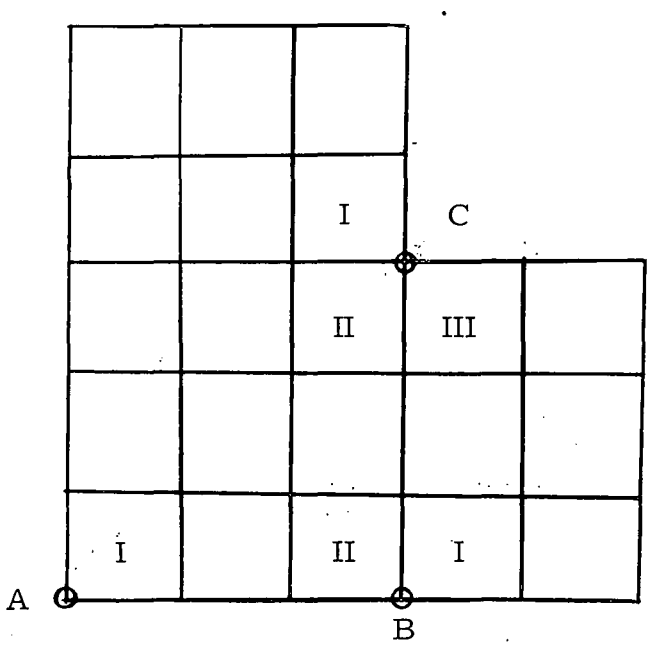

Fig. 2.7. Basis Functions on Boundary Points of a Rectangular Polygon

Chapter III

NEUTRON SLOWING-DOWN PROBLEMS

The principal application of the finite element method, in this thesis, is to few group diffusion theory problems. The few group equations are obtained from the continuous energy problem by some form of discretization of the energy variable. The customary practice in the field is to associate some spectrum with each region of the reactor and use this spectrum to generate few group cross sections, based on the conservation of reaction rates.

The spectrum used for the determination of group constants is found by solving a space-independent neutron slowing-down equation. Obviously, the truncation error in the energy variable is determined by the numerical procedure used in solving for the spectrum. To date, most spectrum codes use many energy intervals and simple step function behavior of the spectrum over each interval.

In this chapter of the thesis, we shall generalize methods of computing spectra to include the use of piecewise polynomials over energy intervals. The usual procedure will appear as a special case of the general method. A particularly important result of the application is the development of rigorous error bounds for the spectrum.

The application of the finite element method to spectrum problems will serve as a simple prototype of univariate expansions. The procedures to be discussed carry over to the spatial and temporal variables. We remark that we do not obtain specific numerical results in this

chapter, but rather use this problem as an example, which extends to the more important treatment of the space and time variables.

3.1 Basic Equation

The basic equation for the neutron slowing-down problem can be obtained from the energy-dependent diffusion equation, Eq. (1.1), neglecting the space and time dependencies. Then, the basic equation can be written as

$$\begin{aligned} T\phi(E) \equiv \Sigma_T(E)\phi(E) - \int_{\mathcal{E}} dE' \, \Sigma_s(E' \to E)\phi(E') \\ - \frac{\chi(E)}{\lambda} \int_{\mathcal{E}} dE' \, \nu \Sigma_f(E')\phi(E') \\ = Q(E) . \end{aligned} \tag{3.1}$$

Definitions for Eq. (3.1) are developed in Chapter I. If $Q(E) = 0$, then Eq. (3.1) defines an eigenvalue problem where λ is an eigenvalue.

Frequently, activation experiments are performed to investigate the neutron spectrum. In this case, the governing equation can be written as

$$\int_{\mathcal{E}} dE' \, \Sigma_k(E')\lambda(E') = A_k , \qquad k = 1, 2, \ldots, K , \tag{3.2}$$

where $\Sigma_k(E')$ is the cross section for a particular reaction and A_k is the activity measured in the experiment for the k-th element. Equation (3.2) is considered as a special case of the general equation (3.1). The methods developed in this chapter could thus also be used with Eq. (3.2).

In order to develop approximations, we need the following definitions. We define the inner product by

$$(u, v)_{\mathcal{E}} = \int_{\mathcal{E}} uv \, dE$$

and the L^2-norm by

$$\| u \|_{L^2} = (u, u)_{\mathcal{E}}^{\frac{1}{2}} .$$

If ϕ is the solution to Eq. (3.1), then ϕ satisfies

$$(T\phi, v)_{\mathcal{E}} = (Q, v)_{\mathcal{E}} \tag{3.3}$$

for all $v(E) \in L^2(\mathcal{E})$.* On the other hand, in order for Eq. (3.3) to be satisfied for all $v \in L^2(\mathcal{E})$, $T\phi = Q$ must be true. Thus, Eq. (3.1) and Eq. (3.3) are equivalent in the $L^2(\mathcal{E})$ space.

The operator T is said to be positive definite [41] if there exists a positive constant γ such that

$$(T\phi, \phi) \geq \gamma \| \phi \|^2_{L^2(\mathcal{E})} . \tag{3.4}$$

Positive definite operators are generally required to be symmetric. However, under the assumption (1.2) on cross sections, a certain class of nonsymmetric integral operators in reactor physics can also be shown to be positive definite.

Now, we show the uniqueness of the solution to Eq. (3.3) as a result of the assumption (3.4). Assume that both ϕ_1 and ϕ_2 are solutions. Then

---

* $L^2(\mathcal{E})$ is a space consisting of all functions defined on $\mathcal{E}$ which are measurable and for which $|v(E)|^2$ is integrable.

$$\left(T(\phi_1-\phi_2), v\right)_{\mathcal{E}} = 0 .$$

Putting $v = \phi_1 - \phi_2$,

$$\left(T(\phi_1-\phi_2), \phi_1-\phi_2\right)_{\mathcal{E}} = 0 .$$

From the assumption Eq. (3.4),

$$\gamma \| \phi_1-\phi_2 \|^2_{L^2} \leq \left(T(\phi_1-\phi_2), \phi_1-\phi_2\right)_{\mathcal{E}} = 0$$

and this requires that $\phi_1 = \phi_2$. This leads to the following lemma.

Lemma 3.1. If the operator T satisfies the inequality (3.4), then the solution to Eq. (3.3) is unique.

3.2 Approximation

In this section, we shall develop approximation methods for the solution of Eq. (3.3). We assume that the solution is sufficiently smooth.* We consider an expansion of the neutron flux and cross sections in terms of piecewise polynomials in energy, and then apply the Galerkin process to determine the approximate solution. Finally, we show the uniqueness of the solution and establish a theorem, Theorem 3.1, on the convergence of the approximate solutions.

---

*The neutron flux is shown to be discontinuous in some cases. For example, the neutron flux exhibits sharp discontinuities when neutrons from a monochromatic source are slowed down by scattering in media of mass greater than unity (Chap. VI, [23]).

Let $\pi(\mathcal{E})$ be a partition of $\mathcal{E} = [E_{min}, E_{max}]$ such that

$$\pi(\mathcal{E}): \quad E_{min} = E_1 < E_2 < \ldots < E_{N_E} = E_{max} .$$

Let S_G be a trial space and let $\{u_g(E)\}_{g=1}^{G}$ be a basis in S_G. In particular, we select S_G as a subspace of the Hermite space $H_m(\pi(\mathcal{E}))$ as considered in Chapter II. The basis functions in the Hermite space may be reordered in a linear fashion as $\{u_g(E)\}_{g=1}^{G}$.

Let the approximate solution $\hat{\phi}(E)$ in S_G be represented by

$$\hat{\phi}(E) = \sum_{g=1}^{G} a_g u_g(E) . \tag{3.5}$$

Cross sections are frequently given by experimentally measured numerical data. In such a case, it is desirable to represent the cross sections by continuous functions using certain interpolation schemes which give the same order of accuracy as the approximation. We may choose the Hermite interpolation (cf., Chap. II) in the trial space for $\hat{\phi}$. If Σ_g and $\Sigma_{gg'}$ are proper interpolation data, then the cross sections can be represented by

$$\Sigma(E) = \sum_{g=1}^{G} \Sigma_g u_g(E) , \tag{3.6a}$$

$$\Sigma(E' \to E) = \sum_{g=1}^{G} \sum_{g'=1}^{G} \Sigma_{gg'} u_g(E)\, u_{g'}(E') . \tag{3.6b}$$

The expansion coefficients for the approximate solution $\hat{\phi}(E)$ can be determined by applying the Galerkin method (cf., Section 1.3, Chapter I) to Eq. (3.3):

$$(T\hat{\phi}, u_g) = (Q, u_g) \qquad \text{for } g = 1, 2, \ldots, G . \tag{3.7}$$

This procedure leads to G linear algebraic equations for the coefficients a_g.

We remark that if the approximate kernels, as given by Eq. (3.6a,b), are used in the operator T, then T should be replaced by $\hat{T}$, which represents the approximate operator. Furthermore, because of the physical fact that we cannot have negative reaction rate, we assume that the condition (1.2) is applied to the approximate solution $\hat{\phi}(E)$ itself, although not to the individual components of $\hat{\phi}(E)$.

In matrix form, Eq. (3.7) can be written as

$$\underline{La} - \underline{Sa} + \frac{1}{\lambda} \underline{Fa} = \underline{q} \tag{3.8}$$

where

$$L = \begin{bmatrix} L_{11} & L_{12} & \cdots & L_{1,G'+1} & & & \\ L_{21} & L_{22} & & & & & \\ \vdots & & & & & & \\ L_{G'+1,1} & & & & & & L_{G-G',G} \\ & & & & & & \\ & & & L_{G,G-G'} & \cdots & & L_{GG} \end{bmatrix},$$

$$S = \begin{bmatrix} S_{11} & \cdots & S_{1G} \\ \vdots & & \vdots \\ S_{G1} & \cdots & S_{GG} \end{bmatrix},$$

$$F = \begin{bmatrix} F_{11} & \cdots & F_{1G} \\ \vdots & & \vdots \\ F_{G1} & \cdots & F_{GG} \end{bmatrix},$$

$$\underline{a} = \mathrm{col}\{a_1, a_2, \ldots, a_G\},$$

$$\underline{q} = \mathrm{col}\{(Q, u_1)_{\mathcal{E}}, (Q, u_2)_{\mathcal{E}}, \ldots, (Q, u_G)_{\mathcal{E}}\},$$

$$L_{gg'} = (\Sigma_T u_{g'}, u_g)_{\mathcal{E}},$$

$$S_{gg'} = \left(\int dE' \Sigma_s(E' \to E)\, u_{g'}(E'), u_g(E) \right)_{\mathcal{E}},$$

$$F_{gg'} = \left(\chi(E) \int dE' \nu\Sigma_f(E')\, u_{g'}(E'), u_g(E) \right)_{\mathcal{E}}.$$

The values of inner products for the basis functions in Hermite spaces can be found in Appendix B.

The matrix L is symmetric and positive definite and has a band structure whose band width $(2G' + 1)$ depends on the degrees of the polynomials used. For the Hermite polynomial space of degree 2m-1 (cf., Chap. II), there are m basis functions at each mesh point. In this space, the half band width G' is given by 2m-1. The matrices S and F are in general nonsymmetric and do not have band structures. We remark that for $m = 1/2$ or piecewise continuous functions, Eq. (3.8) leads to the conventional method for spectrum calculations.

If $Q = 0$, then Eq. (3.1) defines an eigenvalue problem, and the corresponding discrete equations are given by

$$-L\,a + S\,a = \frac{1}{\lambda} F\,a \tag{3.9}$$

where λ is an eigenvalue. In fact, the eigenvalues are the root of the characteristic equation

$$\det \left| -L + S - \frac{F}{\lambda} \right| = 0.$$

The solutions to Eqs. (3.8) and (3.9) can be obtained by direct or iterative methods for linear algebraic systems as discussed in [35], [39] and [40].

The uniqueness of the approximate solution to Eq. (3.7) can be shown similarly as for the analytic solution, provided that the condition (3.4) holds. We now show that the numerical stability of the approximate solution to Eq. (3.7) also results from this condition. From Eq. (3.7), it is easy to show that

$$(T\hat{\phi}, \hat{\phi})_{\mathcal{E}} = (Q, \hat{\phi})_{\mathcal{E}} .$$

From the Schwarz inequality [25]

$$|(Q, \hat{\phi})_{\mathcal{E}}| \leq \|Q\|_{L^2} \|\hat{\phi}\|_{L^2} .$$

Hence,

$$\gamma \|\hat{\phi}\|^2_{L^2} \leq (T\hat{\phi}, \hat{\phi})_{\mathcal{E}} \leq \|Q\|_{L^2} \|\hat{\phi}\|_{L^2}$$

and

$$\|\hat{\phi}\|_{L^2} \leq \frac{1}{\gamma} \|Q\|_{L^2} .$$

This shows that the solution is bounded by an upper limit which includes the source and thus leads to the following lemma.

Lemma 3.2. If the inequality (3.4) holds, then the approximate solution to Eq. (3.7) is unique and the numerical process is stable.

The approximation error for the solution is stated in the following theorem. The proof is given in Appendix A.

Theorem 3.1. Assume that the inequality (3.4) holds. Let $\phi(E)$ be the solution to Eq. (3.3) and $\phi(E) \in C^t(\mathcal{E})$. If $\hat{\phi}(E)$ is the solution to Eq. (3.7)

in the space $H_m(\pi(\mathcal{E}))$, then $\hat{\phi}(E)$ satisfies

$$\| \phi - \hat{\phi} \|_{L^\infty(\mathcal{E})} \leq K \overline{\Delta E}^{\mu}$$

where $\mu = \min(2m, t)$, $\overline{\Delta E} = \max_i |E_{i+1} - E_i|$ and K is a constant independent of $\overline{\Delta E}$.

Theorem 3.1 states that the approximate solution converges to the analytic solution as $O(\overline{\Delta E}^{2m})$ as $\overline{\Delta E} \to 0$ when $t \geq 2m$. For example, for $m = 1/2$ or piecewise continuous functions, the method yields convergence of $O(\overline{\Delta E}^{1})$.

We conclude this chapter with a remark on coarse mesh calculations using the finite element method. In general, nuclear cross sections contain fine structures due to the presence of resonance reactions. For high accuracy calculations which require taking into account for effects of the individual resonance, it is necessary to divide the energy interval into a number of small mesh intervals which are comparable to resonance widths. However, the finite element method also allows us to use relatively large mesh intervals as shown in Fig. 3.1. In this case, each mesh interval may include a number of resonances. In the Galerkin scheme, which leads to the matrix equation, Eq. (3.8), the resonance effects can be accurately included in elements of the coefficient matrices by evaluating inner products.

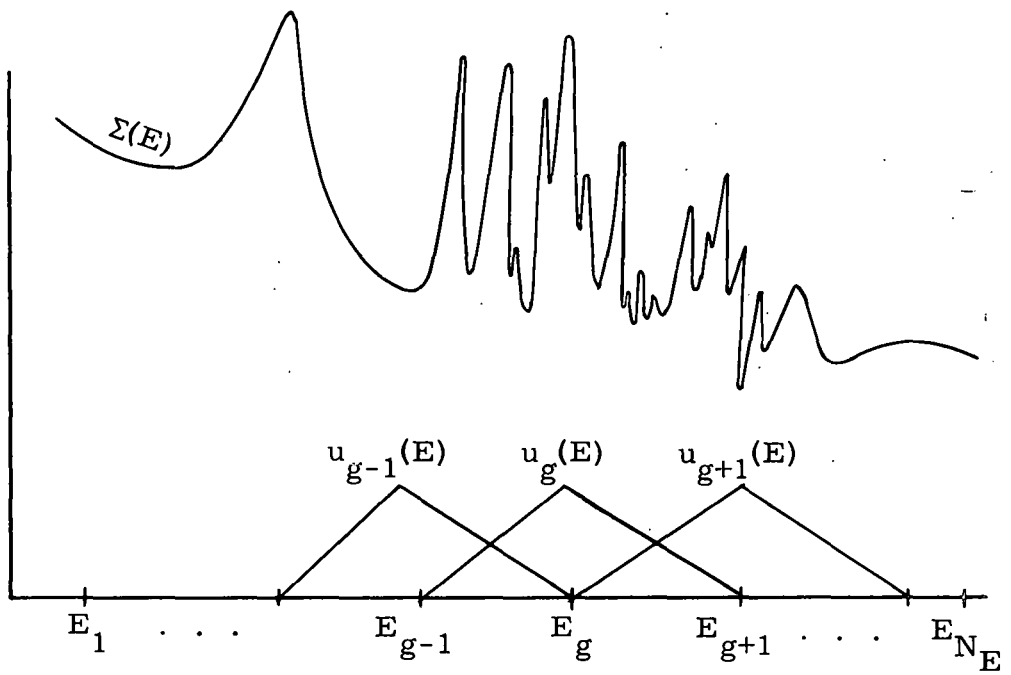

Fig. 3.1. Coarse Mesh Method for the Neutron Spectrum Calculation

Chapter IV

STATIC NEUTRON DIFFUSION PROBLEMS

In this chapter, we consider the solution of time-independent diffusion problems, using the finite element method. In Section 4.1, we shall first review the diffusion equation in the continuum, and present an alternative equivalent formulation of the problem. The alternative or "weak" formulation is more amenable to applications of the finite element method than the integro-differential formulation of the problem. We then present a few mathematical preliminaries dealing with the uniqueness of the problem solution.

The principal application of the finite element method is developed in Section 4.2, where we discuss both energy and spatial variables. The conventional multigroup method appears as a special case of the general method developed in this chapter. We present a theorem which shows the error bounds for the approximation. In Section 4.3, we discuss some numerical methods for solution of the linear systems of equations developed in Section 4.2.

In Section 4.4, we present some illustrative numerical results in one and two space dimensions which indicate the power and utility of finite element methods in reactor static problems.

4.1 Basic Equation

The time-independent neutron diffusion equation can be written from Eq. (1.1a) as

$$T\phi \equiv -\underline{\nabla}\cdot D\underline{\nabla}\phi(\underline{r},E) + \Sigma_T(\underline{r},E)\phi(\underline{r},E)$$

$$- \int_{\mathcal{E}} dE'\, \Sigma_s(\underline{r},E'\to E)\phi(\underline{r},E) - \frac{1}{\lambda}\chi(E)\int_{\mathcal{E}} dE'\, \nu\Sigma_f(\underline{r},E')\phi(\underline{r},E')$$

$$= Q(\underline{r},E) \tag{4.1a}$$

with boundary conditions

$$\phi(\underline{r},E)\big|_{\partial\Omega} = 0 \quad \text{or} \quad D\frac{\partial}{\partial n}\phi(\underline{r},E)\big|_{\partial\Omega} = 0 \tag{4.1b}$$

and

$$\phi(\underline{r},E) \text{ and } D\frac{\partial}{\partial n}\phi(\underline{r},E) \text{ continuous on the material interfaces} \tag{4.1c}$$

where $\frac{\partial}{\partial n}$ represents an outward normal derivative at the surface. Other notations are developed in Chapter I. If $Q(\underline{r},E) = 0$, then Eq. (3.1a) becomes an eigenvalue problem where λ is an eigenvalue.

The path we shall follow to generate approximate solutions to Eq. (4.1) is to expand ϕ in terms of some suitable basis functions. However, if we require the basis functions to have the same differentiability properties and continuity properties as ϕ itself, then we will have great difficulties finding the basis functions. In order to avoid these difficulties, we consider another formulation of the problem which weakens the continuity conditions and permits the use of a much broader class of expansion functions.

We will use the inner product and the L^2-norm as introduced in the last chapter. We have, for the space-energy problem

$$(u,v) \equiv \int_{\mathcal{E}} dE \int_{\Omega} dV\, uv$$

and

$$\|u\|_{L^2} \equiv (u,u)^{\frac{1}{2}}.$$

We also define a bilinear form $a(u, v)$ as

$$a(u, v) \equiv (D\underline{\nabla}u, \underline{\nabla}v) + (\Sigma_T u, v)$$

$$- \left(\int_{\mathcal{E}} dE' \, \Sigma_s(E' \to E) u(E'), v \right) - \frac{1}{\lambda} \left(\chi(E) \int_{\mathcal{E}} dE' \, \nu \Sigma_f(E') u(E'), v \right).$$

In order for the terms of $a(u, v)$ to exist, we must require that u and v be continuous and have first derivatives which are square integrable. We define $W^1(\Omega)$ as the set of all functions which satisfy the above conditions.* In view of the boundary conditions in Eq. (4.1c), we shall use a subspace of $W^1(\Omega)$, say $W_o^1(\Omega)$, whose elements satisfy the boundary conditions, Eq. (4.1b).

The weak formulation [17], [42] of the diffusion problem may be stated as a problem of finding ϕ in $W_o^1(\Omega)$ satisfying

$$a(\phi, v) = (Q, v) \tag{4.2}$$

for all v in the space $W_o^1(\Omega)$. Any $\phi(\underline{r}, E)$ which satisfies Eq. (4.2) will be called a weak solution to the diffusion problem.

We observe that any $\phi(\underline{r}, E)$ which is a solution of Eqs. (4.1a, b, c) is also a solution of Eq. (4.2). To demonstrate this, we consider integration by parts of the term

$$(D\underline{\nabla}\phi, \underline{\nabla}v) = - \sum_{\ell} \int_{\Omega_\ell} dV \, (\underline{\nabla} \cdot D \underline{\nabla}\phi, v)_{\mathcal{E}}$$

$$+ \sum_{\ell} \int_{\partial\Omega_\ell} dS \left(D \frac{\partial}{\partial \hat{n}} \phi, v \right)_{\mathcal{E}}$$

---

*The space $W^1(\Omega)$ is called a Sobolev space [41]. The norm in this space is defined by $\|u\|_{W^1(\Omega)} = \left(\int_\Omega (\nabla u^2 + u^2) \, dV \right)^{\frac{1}{2}}$ (cf., Eq. (4.13)).

where the last term on the right is the sum of the surface integrals for each subregion Ω_ℓ of Ω. Since ϕ satisfies Eqs. (4.1b, c), the summation vanishes. Thus, the equation $(T\phi, v) = (Q, v)$ leads to

$$a(\phi, v) = (Q, v) \quad \text{for any } v \text{ in } W_o^1(\underline{r}) .$$

Thus, ϕ is a solution to Eq. (4.2).

Conversely, we now show that if the weak solution is in the domain of the operator T, that is, twice differentiable in each Ω_ℓ, then it also satisfies Eqs. (4.1a, c).

Integrated by parts, the weak form Eq. (4.2) can be written

$$\sum_\ell \int_{\Omega_\ell} dV\,([T\phi - Q], v)_{\mathcal{E}} + \sum_\ell \int_{\partial\Omega_\ell} dS\left(D \frac{\partial}{\partial n} \phi, v\right)_{\mathcal{E}} = 0$$

for all $v \in W_o^1(\Omega)$. First, we choose v such that v is in $W^1(\Omega_\ell)$ and vanishes outside the region Ω_ℓ including the boundary $\partial\Omega_\ell$. Then, we obtain

$$T\phi - Q = 0 , \qquad r \in \Omega_\ell .$$

Similarly, we can show that this equation holds in all Ω_ℓ, for $\ell = 1, 2, \ldots, L$. Substituting these equations back in the original equation, we further obtain

$$\sum_\ell \int_{\partial\Omega_\ell} D \frac{\partial}{\partial n} \phi \, dS = 0 .$$

Thus, we have shown that the continuity conditions for $D \frac{\partial}{\partial n} \phi$ (current) in Eqs. (4.1a, c) are Euler equations in the variation of v in the weak form. Therefore, the weak solution satisfies Eqs. (4.1a, c). For this reason, the current continuity condition is called the "natural interface condition."

What we have done is to write the diffusion equation in a form for which the conditions on ϕ are less restrictive than the original conditions. However, If ϕ satisfies the original boundary conditions and is sufficiently differentiable, then ϕ satisfies the original statement of the problem.

In view of the less restrictive conditions on ϕ in the weak form of the problem, we should expect that the class of appropriate basis functions is much larger. ϕ is only required to be an element of the space $W_o^1(\Omega)$ and may not satisfy the current continuity condition which appears as a natural interface condition. These allow the piecewise linear function to be an acceptable function in the weak form. In fact, the weak form is very well suited for the use of piecewise polynomials as basis functions, as we develop in subsequent sections.

The bilinear form $a(\phi, \phi)$ is said to be positive definite [41] if there exists a positive constant γ such that

$$a(\phi, \phi) \geq \gamma \| \phi \|^2_{L^2} . \tag{4.3}$$

In reactor physics problems, positive definite bilinear forms are not necessarily required to be symmetric. The assumption (1.2) for the integral operator T allows also a certain class of nonsymmetric bilinear forms to be positive definite.

Analogously to Lemma 3.1, we can show the uniqueness of the weak solution.

Lemma 4.1. If the bilinear form satisfies the inequality (4.3), then the solution to Eq. (4.2) is unique.

4.2 Approximations

In this section, we shall develop approximate methods for the solution of the weak form of the neutron diffusion equation, Eq. (4.2). We consider expansions of the flux in terms of piecewise polynomials in both space and energy. We shall first give an abstract summary of the procedures to be followed, and then develop the treatment of each variable in great detail.

We denote the region of configuration space as Ω and the energy interval as $\mathcal{E} = [E_{min}, E_{max}]$. We assume our configuration space to be one of the orthogonal coordinate systems, for example, a Cartesian, cylindrical or polar coordinate system. Let $\mathcal{E}$ and Ω be partitioned into elements such that

$$\pi_{\mathcal{E}}: \quad E_{min} = E_1 < E_2 < \ldots < E_G = E_{max},$$

$$\pi_{\Omega}: \quad a_1 = r_{11} < r_{12} < \ldots < r_{1N_1} = b_1,$$
$$a_2 = r_{21} < r_{22} < \ldots < r_{2N_2} = b_2,$$
$$\vdots$$
$$a_n = r_{n1} < r_{n2} < \ldots < r_{nN_n} = b_n.$$

In particular, in partitioning Ω, we assume that the partitioning lines or surfaces coincide with the material interfaces such that the material properties in each element are continuous either because of the nature of the reactor or through the application of some homogenization procedure. This allows us to consider each subregion with uniform materials as elements of π_{Ω} and thus to use the method developed in this chapter for coarse mesh calculations.

We consider a finite dimensional trial space for the approximation of the solution. In particular, we are interested in approximating in subspaces of the Hermite space $H_m(\pi_\Omega \times \pi_{\mathcal{E}})$, whose elements satisfy the continuity conditions compatible with the interface conditions, Eq. (4.1c). The generation of basis functions in the subspace is discussed in detail in Chapter II, especially in Examples 2.1 - 2.3. We then impose boundary conditions on basis functions in $\underline{r}$ which lie on the physical boundary. For notational simplicity, we reorder the basis functions and represent them using linear indices. Let the basis functions be represented by

$$v_{ig}(\underline{r}, E) = u_i(\underline{r}, D(E))\, u_g(E), \qquad 1 \leq i \leq N, \qquad 1 \leq g \leq G,$$

where N and G are the number of basis functions in space and energy, respectively. We note that the spatial basis functions $u_i(\underline{r}, D(E))$ are functions of the diffusion coefficient, and thus functions of $\underline{r}$ and E. Since $u_i(\underline{r}, D(E))$ is separable in $\underline{r}$ and E (cf., Chap. II), we rewrite $v_{ig}(\underline{r}, E)$ as

$$v_{ig}(\underline{r}, E) = v_i(\underline{r})\, v_g(E), \qquad 1 \leq i \leq N, \qquad 1 \leq g \leq G.$$

The approximate solution, $\hat{\phi}(\underline{r}, E)$, is then represented as

$$\hat{\phi}(\underline{r}, E) = \sum_{g=1}^{G} \sum_{i=1}^{N} a_{ig}\, v_i(\underline{r})\, v_g(E). \tag{4.4}$$

The expansion coefficients can be determined by applying the Galerkin scheme to the weak form of the diffusion equation, Eq. (4.2):

$$a(\hat{\phi}, v_{ig}) = (Q, v_{ig}), \qquad 1 \leq i \leq N, \qquad 1 \leq g \leq G. \tag{4.5}$$

This procedure leads to N x G linear algebraic equations for the coefficients a_{ig}.

Our principal application of the method is to few group models, so we shall next consider the energy treatment to generate the few group equations and then turn to the spatial treatment.

4.2.1 Generalized Multigroup Equations

We consider approximations of Eqs. (4.1a, b, c) in energy. The method discussed in Chapter III is directly applicable in this section.

We define $\Phi_g(\underline{r})$ as

$$\Phi_g(\underline{r}) = \sum_{i=1}^{N} a_{ig} v_i(\underline{r}) . \tag{4.6a}$$

Equation (4.4) can then be written as

$$\hat{\phi}(\underline{r}, E) = \sum_{g=1}^{G} \Phi_g(\underline{r})\, v_g(E) .$$

We apply the Galerkin scheme to Eqs. (4.1a, b, c), such that $\hat{\phi}$ satisfies, for $g = 1, 2, \ldots, G$,

$$(T\hat{\phi}, v_g)_{\mathcal{E}} = (Q, v_g)_{\mathcal{E}} , \tag{4.7a}$$

$$(\hat{\phi}|_{\partial\Omega}, v_g)_{\mathcal{E}} = 0 , \tag{4.7b}$$

$(\hat{\phi}, v_g)_{\mathcal{E}}$ and $(D\hat{\phi}, v_g)_{\mathcal{E}}$ continuous on the material interfaces, (4.7c)

where $(u, v)_{\mathcal{E}} \equiv \int_{\mathcal{E}} uv\, dE$. Equations (4.7a, b, c) lead to the generalized multigroup equations which are given by, for $g = 1, 2, \ldots, G$,

$$- \sum_{g'=1}^{G} \underline{\nabla} \cdot D_{gg'} \underline{\nabla} \Phi_{g'}(\underline{r}) + \sum_{g'=1}^{G} \left\{ \Sigma_{Tgg'} - \Sigma_{sgg'} - \frac{\chi_g}{\lambda} \nu \Sigma_{fg'} \right\} \Phi_{g'}(\underline{r}) = Q_g(\underline{r}) \tag{4.8a}$$

with boundary conditions

$$\Phi_g(\underline{r})\big|_{\partial\Omega} = 0 , \tag{4.8b}$$

$$\Phi_g(\underline{r}), \quad \sum_{g'=1}^{G} D_{gg'} \frac{\partial}{\partial n} \Phi_{g'}(\underline{r}) \text{ continuous at material interfaces} , \tag{4.8c}$$

where

$$D_{gg'}(\underline{r}) = (D v_{g'}(E), \ v_g(E))_{\mathcal{E}} ,$$

$$\Sigma_{Tgg'}(\underline{r}) = (\Sigma_T v_{g'}(E), v_g(E))_{\mathcal{E}} ,$$

$$\Sigma_{sgg'}(\underline{r}) = \left(\int_{\mathcal{E}} dE' \, \Sigma_s(E' \to E) \, v_{g'}(E'), \, v_g(E) \right)_{\mathcal{E}} ,$$

$$\chi_g = (\chi(E), \, v_g(E))_{\mathcal{E}} ,$$

$$\Sigma_{fg'}(\underline{r}) = \int_{\mathcal{E}} dE' \, \Sigma_f(E') \, v_{g'}(E') ,$$

$$Q_g(\underline{r}) = (Q(r, E), \, v_g(E))_{\mathcal{E}} .$$

The conventional multigroup equations [22] - [24] are obtained as a special case of Eqs. (4.8 a, b, c). In this case, we specify

$$v_g(E) = \begin{cases} S(E) , & E_g \leq E \leq E_{g+1} , \\ 0 , & \text{otherwise} , \end{cases}$$

where S(E) represents an infinite medium neutron spectrum. We then obtain the conventional multigroup equation, for $g = 1, 2, \ldots, G$,

$$-\underline{\nabla}\cdot D_g \underline{\nabla}\Phi_g(\underline{r}) + \Sigma_{Tg}\Phi_g(\underline{r}) - \sum_{g'=1}^{G} \left\{ \Sigma_{sgg'}\Phi_{g'} + \frac{\chi_g}{\lambda}\nu\Sigma_{fg'}\Phi_{g'} \right\} = Q_g \qquad (4.9a)$$

with boundary conditions

$$\Phi_g(\underline{r})\big|_{\partial\Omega} = 0\,, \qquad (4.9b)$$

$$\Phi_g(\underline{r}) \text{ and } D_g \frac{\partial}{\partial n}\Phi_g(\underline{r}) \text{ continuous at material interfaces}, \qquad (4.9c)$$

where

$$D_g = \delta_{gg'} D_{gg'}\,,$$

$$\Sigma_{Tg} = \delta_{gg'}\Sigma_{Tgg'}\,.$$

Here $\delta_{gg'}$ is the Kronecker delta.

4.2.2 Spatial Approximations

In this section, we consider the approximation of the solution to the generalized multigroup equations (4.8a, b, c).

From the definition in Eq. (4.6a),

$$\Phi_g = \sum_{i=1}^{N} a_{ig}\, v_i(\underline{r})\,.$$

We apply the Galerkin scheme to the weak formulation of (4.8a) such that Φ_g satisfies

$$\sum_{g'=1}^{G} \left\{ (D_{gg'}\underline{\nabla}\Phi_{g'}, \underline{\nabla}v_i)_\Omega + \left(\left[\Sigma_{Tgg'} - \Sigma_{sgg'} - \frac{\chi_g}{\lambda}\nu\Sigma_{fg'} \right]\Phi_{g'}, v_i \right)_\Omega \right\}$$

$$= (Q_g, v_i(\underline{r}))_\Omega\,, \qquad i = 1, 2, \ldots, N\,, \qquad (4.10)$$

where $(u, v)_\Omega = \int_\Omega uv\, dV$. Rewritten in matrix form, Eq. (4.10) becomes

$$\left\{ L - S - \frac{1}{\lambda} F \right\} \underline{a} = \underline{q}\,, \qquad (4.11)$$

where

$$L = \begin{bmatrix} L_{11} & L_{12} & \cdots & L_{1,G'+1} & & \\ L_{21} & L_{22} & & & & \\ \vdots & & & & & \\ L_{G'+1,1} & & & & & L_{G-G',G} \\ & & & & & \vdots \\ & & L_{G,G-G'} & \cdots & L_{GG} & \end{bmatrix},$$

$$S = \begin{bmatrix} S_{11} & \cdots & S_{1G} \\ \vdots & & \vdots \\ S_{G1} & \cdots & S_{GG} \end{bmatrix},$$

$$F = \begin{bmatrix} F_{11} & \cdots & F_{1G} \\ \vdots & & \vdots \\ F_{G1} & \cdots & F_{GG} \end{bmatrix},$$

$$\underline{a} = \mathrm{col}\{\underline{a}_1, \underline{a}_2, \ldots, \underline{a}_G\},$$

$$\underline{q} = \mathrm{col}\{\underline{q}_1, \underline{q}_2, \ldots, \underline{q}_G\},$$

$$(L_{gg'})_{ii'} = (D_{gg'} \underline{\nabla} v_{i'}(\underline{r}), \underline{\nabla} v_i(\underline{r}))_\Omega + (\Sigma_{Tgg'} v_{i'}(\underline{r}), v_i(\underline{r}))_\Omega,$$

$$(S_{gg'})_{ii'} = (\Sigma_{sgg'} v_{i'}(\underline{r}), v_i(\underline{r}))_\Omega,$$

$$(F_{gg'})_{ii'} = \chi_g (\nu\Sigma_{fg'} v_{i'}(\underline{r}), v_i(\underline{r}))_\Omega,$$

$$\underline{a}_g = \mathrm{col}\{a_{g1}, a_{g2}, \ldots, a_{gN}\},$$

$$\underline{q}_g = \mathrm{col}\{(Q_g, v_1)_\Omega, \ldots, (Q_g, v_N)_\Omega\}.$$

The matrices L, S and F are block matrices. These matrices have the same properties as those defined in Eq. (3.8) in Chapter III, except that in this case the matrices have submatrices as their elements. The submatrices $L_{gg'}$, $S_{gg'}$, and $F_{gg'}$ are sparse matrices with band structures. The band width depends on non-zero couplings between the spatial basis functions through inner products. For example, in one-dimensional space, if there are m basis functions at each mesh point, the half band width is given by 2m-1. In two-dimensional space, if there are m^2 basis functions at each mesh point, then the resulting submatrices are block tridiagonal matrices, which have band structures with half band width $2m^2-1$.

As an example, let D and Σ_T be piecewise constant and $\{v_i(\underline{r})\}$ be piecewise linear functions in one space variable. Then the matrix L_{gg} can be represented by

$$L_{gg} = \begin{bmatrix} \left(\frac{D+}{h+} + \frac{h+\Sigma_T+}{3}\right) & \left(-\frac{D+}{h+} + \frac{h+\Sigma_T+}{6}\right) & & \bigcirc \\ \left(-\frac{D-}{h-} + \frac{\Sigma_T-h-}{6}\right) & \left(\frac{D-}{h-} + \frac{D+}{h+} + \frac{h-\Sigma_T-}{3} + \frac{h+\Sigma_T+}{3}\right) & \left(-\frac{D+}{h+} + \frac{\Sigma_T+h+}{6}\right) & \\ \bigcirc & & \left(-\frac{D-}{h-} + \frac{\Sigma_T-h-}{6}\right) & \left(\frac{D-}{h-} + \frac{h-\Sigma_T-}{3}\right) \end{bmatrix}$$

where $h\pm = |x_{i\pm1} - x_i|$. Note that the $\underline{\nabla}\cdot D\underline{\nabla}$ and Σ_T terms are related to function values at three points. It is interesting to compare with the conventional 3-point difference formula for

$$\int_{x_{i-\frac{1}{2}}}^{x_{i+\frac{1}{2}}} (-\underline{\nabla}\cdot D\,\underline{\nabla}\phi + \Sigma_T\phi)\,dx$$

$$\approx -\frac{D-}{h-}\phi_i + \left(\frac{D-}{h-} + \frac{D+}{h+} + \frac{1}{2}\Sigma_T - h- + \frac{1}{2}\Sigma_T + h+\right)\phi_i - \frac{D+}{h+}\phi_i$$

where

$$x_{i\pm\frac{1}{2}} = x_i \pm \frac{1}{2}(h\pm).$$

In this equation, the $\underline{\nabla}\cdot D\,\underline{\nabla}$ term has the same representation as in $L_{gg'}$, but the $\Sigma_T\phi$ term is represented by a single point relation. In integrating $\Sigma_T\phi$, we have assumed that ϕ is constant within $[x_{i-\frac{1}{2}}, x_{i+\frac{1}{2}}]$, and this assumption implies the use of small mesh sizes. However, in the finite element method, the assumptions for constant ϕ or Σ_T are unnecessary and the matrix elements can be determined analytically. For this reason, the finite element method allows us to use larger mesh elements than those associated with the finite difference scheme. In a two-dimensional problem, the finite element method using bilinear functions yields a 9-point formula, whereas the finite difference scheme gives a 5-point formula. The analogy for the $\underline{\nabla}\cdot D\,\underline{\nabla}$ terms between the two methods which we have seen in one-dimensional problems can no longer be established in two-dimensional problems.

If $Q(\underline{r}, E) = 0$, then Eq. (4.1a) defines an eigenvalue problem. Equation (4.11) then becomes

$$\left\{L - S\,\frac{1}{\lambda}\,F\right\}\underline{a} = 0. \tag{4.12}$$

λ is an eigenvalue which is determined by finding roots of the characteristic equation

$$\left|L - S - \frac{1}{\lambda}\,F\right| = 0.$$

We now consider the uniqueness of the approximate solution to Eq. (4.5). If the bilinear form $a(\phi, \phi)$ satisfies the inequality (4.3), then we can prove the uniqueness of the approximate solution in a manner similar to the proofs of Lemmas 3.1 and 4.1.

Lemma 4.2. If the bilinear form satisfies the inequality (4.3), then the solution to Eq. (4.5) is unique.

It is possible to provide analytic estimates of the error in the approximation to both the source problem and the eigenvalue problem. In the following theorem, the error bounds for the source problem are presented.

Theorem 4.1. Assume that the inequality (4.3) holds. Let ϕ be the solution of Eq. (4.2) and $\phi \in C_p^t(\pi_\Omega \times \pi_{\mathcal{E}})$ where $t = (t_r, t_E)$. If $\hat{\phi}$ is the solution of Eq. (4.5) in the space $H_m(\pi_\Omega \times \pi_{\mathcal{E}})$, where $m = (m_r, m_g)$, then $\hat{\phi}$ satisfies

$$\| \phi - \hat{\phi} \|_{L^\infty} \leq K_1 \overline{\Delta r}^{2\mu_r} + K_2 \overline{\Delta E}^{2\mu_E}$$

where $\mu_r = \min(2m_r, t_r)$, $\mu_E = \min(2m_E, t_E)$, $\overline{\Delta r} = \max_{\pi_\Omega} \Delta r$ and $\overline{\Delta E} = \max_{\pi_{\mathcal{E}}} \Delta E$, and K_1, K_2 are constants independent of $\overline{\Delta r}$ and $\overline{\Delta E}$, respectively.

Proof. This theorem is proven in Appendix A.

The eigenvalue problem can be represented, in the weak form of the equation, as

$$a(\phi, \phi) = b(\phi, \phi) - \frac{1}{\lambda}(F\phi, \phi) = 0$$

from Eq. (4.2). Then the eigenvalues are defined by

$$\lambda^{-1} = \frac{b(\phi, \phi)}{(F\phi, \phi)} = b(\phi, \phi),$$

$$\hat{\lambda}^{-1} = \frac{b(\hat{\phi}, \hat{\phi})}{(F\hat{\phi}, \hat{\phi})} = b(\hat{\phi}, \hat{\phi}),$$

where we normalize the eigenfunctions such that $(F\phi, \phi) = (F\hat{\phi}, \hat{\phi}) = 1$. Then

$$\begin{aligned}\lambda^{-1} - \hat{\lambda}^{-1} &= \lambda^{-1} - b(\hat{\phi}, \hat{\phi}) = \lambda^{-1}(F(\hat{\phi}, \hat{\phi}) - b(\hat{\phi}, \hat{\phi}) \\ &= \lambda^{-1}(F(\hat{\phi}-\phi+\phi), \hat{\phi}-\phi+\phi) - b(\hat{\phi}-\phi+\phi, \hat{\phi}-\phi+\phi) \\ &= \lambda^{-1}(F(\hat{\phi}-\phi, \hat{\phi}-\phi) + \lambda^{-1}(F\phi, \hat{\phi}-\phi) + \lambda^{-1}(F(\hat{\phi}-\phi), \phi) \\ &\quad + \lambda^{-1}(F\phi, \phi) - b(\hat{\phi}-\phi, \hat{\phi}-\phi) - b(\phi, \hat{\phi}-\phi) - b(\hat{\phi}-\phi, \phi) - b(\phi, \phi).\end{aligned}$$

Since $b(\phi, v) - \frac{1}{\lambda}(F\phi, v) = 0$ for all $v \in W_o^1$,

$$\begin{aligned}\lambda^{-1} - \hat{\lambda}^{-1} &= \lambda^{-1}(F(\hat{\phi}-\phi), \hat{\phi}-\phi) + \lambda^{-1}(F(\hat{\phi}-\phi), \phi) \\ &\quad - b(\hat{\phi}-\phi, \hat{\phi}-\phi) - b(\hat{\phi}-\phi, \phi).\end{aligned}$$

If T is self-adjoint, then

$$\lambda^{-1}(F(\hat{\phi}-\phi), \phi) - b(\hat{\phi}-\phi, \phi) = \lambda^{-1}(F\phi, \hat{\phi}-\phi) - b(\phi, \hat{\phi}-\phi) = 0$$

and thus

$$\lambda^{-1} - \hat{\lambda}^{-1} = \lambda^{-1}(F(\hat{\phi}-\phi), \hat{\phi}-\phi) - b(\hat{\phi}-\phi, \hat{\phi}-\phi).$$

We define the norm in the space W^1 as

$$\|u\|_{W^1} = \left\{ \int_{\mathcal{E}} \int_{\Omega} ((\nabla u)^2 + u^2)\, dV\, dE \right\}^{\frac{1}{2}},$$

then from our assumptions on cross sections in Eq. (1.1),

$$|b(u,v)| \leq K_1 \|u\|_{W^1} \|v\|_{W^1} ,$$

$$|(Fu,v)| \leq K_2 \|u\|_{L^\infty} \|v\|_{L^\infty} .$$

Thus,

$$|\lambda^{-1} - \hat{\lambda}^{-1}| \leq \begin{cases} K_1' \|\phi-\hat{\phi}\|_{W^1} + K_1'' \|\phi-\hat{\phi}\|^2_{W^1} + K_1''' \|\phi-\hat{\phi}\|_{L^\infty} + K_1'''' \|\phi-\hat{\phi}\|^2_{L^\infty} & \text{non-self-adjoint} , \\ K_2' \|\phi-\hat{\phi}\|^2_{W^1} + K_2'' \|\phi-\hat{\phi}\|^2_{L^\infty} & \text{self-adjoint} . \end{cases}$$

We consider iterative schemes to determine ϕ and λ. In these schemes, the eigenvalue problem is treated as a source problem (cf., Sec. 4.3). We assume that the iterative scheme is convergent. Then we can apply Theorem 4.1 to the converged solution. If we assume that Theorem 4.1 applies also to derivatives such that the orders of convergence are specified similarly as in Theorem 2.4, then we obtain

$$|\lambda^{-1} - \hat{\lambda}^{-1}| = \begin{cases} O\left(\overline{\Delta r}^{2m_r - 1}\right) + O\left(\overline{\Delta E}^{2m_E}\right) & \text{non-self-adjoint} , \\ O\left(\overline{\Delta r}^{4m_r - 2}\right) + O\left(\overline{\Delta E}^{4m_E}\right) & \text{self-adjoint} . \end{cases} \qquad (4.13)$$

Numerical results (Example 4.1 in Sec. 4.4) show that the order of convergence for the non-self-adjoint case can be better than the conservative limit predicted above.

4.3 Numerical Methods

We now consider appropriate numerical procedures for the solution to Eq. (4.11). The source-iterative scheme and the Cholesky method,

which are discussed in this section, are used in a computer program HERMITE-2D (Appendix D) for eigenvalue problems.

A direct method such as the Gauss elimination method is inefficient compared to iterative schemes for large systems of linear equations. We consider the source iterative scheme [43], [44], which is most commonly used in reactor physics calculations. In this method, the equation for the J-th iterative solution of Eq. (4.11) is set in the following form:

$$L_{gg}\underline{a}_g^{J+1} = \sum_{g'=1}^{G} \{-L_{gg'}(1-\delta_{gg'}) + S_{gg'} + \frac{1}{\lambda} F_{gg'}\}\underline{a}_{g'}^{J} + \underline{q}_g, \quad g = 1, 2, \ldots, G, \tag{4.14}$$

where $\delta_{gg'}$ is the Kronecker delta. $\underline{a}^0$ is an initial guess. In our case, L_{gg} is positive definite and we can use the Cholesky scheme [35], [39], which always gives a unique factorization of L_{gg} in the form

$$L_{gg} = E\,E^T \tag{4.15a}$$

where E is a lower triangle matrix. Let $L_{gg} = (\ell_{ij})$, $E = (e_{ij})$. Then we note that

$$\ell_{jj} = e_{j1}^2 + e_{j2}^2 + \ldots + e_{jj}^2,$$

$$\ell_{ij} = e_{i1}e_{j1} + e_{i2}e_{j2} + \ldots + e_{ij}e_{jj}, \quad j \leq i.$$

Therefore, e_{ij} can be determined using the algorithm,

$$e_{jj} = \left(\ell_{jj} - \sum_{k=1}^{j-1} e_{jk}^2\right)^{\frac{1}{2}},$$

$$e_{ij} = \left(\ell_{ij} - \sum_{k=1}^{j-1} e_{ik}e_{jk}\right)/e_{jj}. \tag{4.15b}$$

The matrices E and E^T possess the same band structure as L_{gg}. By using the Cholesky scheme, the numerical inversion of L_{gg} is simplified and it requires only forward and backward sweeps in inverting E and E^T, respectively.

In the eigenvalue problem defined by Eq. (4.12), only the largest eigenvalue is of interest because it corresponds to the neutron multiplication constant in the reactor physics. The largest eigenvalue of Eq. (4.12) can be determined by the power method [43], [44], [45] which will be briefly described. Suppose a^{*J+1} is the (J+1)-th iterative solution to Eq. (4.14) with $\underline{q}_g = 0$. Then, the largest eigenvalue and its eigenfunction are defined by

$$\lambda^{-1\,J+1} = \frac{\sum_g \left(\underline{a}_g^{*J+1}, \underline{a}_g^J\right)}{\sum_g \left(\underline{a}_g^{*J+1}, \underline{a}_g^{*J+1}\right)} , \tag{4.16a}$$

$$\underline{a}^{J+1} = \frac{a^{*J+1}}{\lambda^{J+1}} . \tag{4.16b}$$

Variants of the definition of λ can be found in [45]. Steps defined by Eqs. (4.14) - (4.16) are repeated until the following convergence criteria are satisfied:

$$\max_{i,g} \left| \frac{a_{ig}^{J+1} - a_{ig}^J}{a_{ig}^J} \right| \leq \epsilon_a , \tag{4.17a}$$

$$\left| \frac{\lambda^{J+1} - \lambda^J}{\lambda^J} \right| \leq \epsilon_\lambda . \tag{4.17b}$$

4.4 Numerical Results

In this section, some of the numerical results for stationary eigenvalue problems are presented in order to check the theoretical results and also to test practical aspects of the finite element method. Calculations were performed using the computer programs HERMITE-1D and HERMITE-2D (Appendix D).

In examples, the order of convergence is determined from the numerical results. For example, if $\hat{\lambda}_i$ is the approximate eigenvalue using the uniform mesh size Δr_i, then the order of convergence μ for the eigenvalue is determined from

$$\mu = \ln\left(\frac{\hat{\lambda}_1 - \hat{\lambda}}{\hat{\lambda}_2 - \hat{\lambda}}\right) \Bigg/ \ln\left(\frac{\Delta r_1}{\Delta r_2}\right) \tag{5.18}$$

where $\hat{\lambda}$ is a reference eigenvalue, which is usually the most accurate eigenvalue obtainable. The orders of convergence, which are listed in the tables of numerical examples, correspond to average values of μ's which are obtained from Eq. (5.18). We note that Eq. (5.18) is also used in determining the order of convergence in temporal approximations in Chapters V and VI.

Example 4.1. One-Dimensional Eigenvalue Problems

In this example, we consider one-dimensional eigenvalue problems previously considered by Wakoff [21]. In [21], the multigroup equations are written in the following simple forms:

$$-\frac{d}{dx}\left(\rho_i \frac{d}{dx} u_i\right) + \sigma_i u_i = \tau_{i+1} u_{i+1}, \qquad i = 1, \ldots, n-1,$$

$$-\frac{d}{dx}\left(\rho_n \frac{d}{dx} u_n\right) + \sigma_n u_n = \lambda \tau_1 u_1,$$

where u_n represents the eigenfunction in the highest energy group and $\lambda = \frac{1}{k_{eff}}$ is the eigenvalue.

We selected two examples from [21], a one-group two-region problem and a two-group two-region problem. We computed the largest eigenvalue using the cubic piecewise Hermite polynomials as defined by Eq. (2.14).

Table 4.1(a), (b) compares eigenvalues of the two examples with the results obtained by Wakoff. Eigenvalues computed by the finite difference scheme are also included for comparison.

We note that both the modified spline space and the Hermite space give convergence of order $O(\Delta x^6)$ (cf., Eq. (4.13)), whereas the finite difference scheme gives $O(\Delta x^2)$ convergence. We also note that the non-self-adjoint problem (Table (b)) has the same order of convergence as the self-adjoint problem (Table (a)).

Table 4.1. Eigenvalues on One-Dimensional Problems: Example 4.1

(a) Eigenvalues of One-Group Equation:

$$\rho_1 = \begin{cases} 2 \ [0, \frac{3}{4}) \\ 1 \ (\frac{3}{4}, 1] \end{cases} \qquad \sigma_1 = 0, \qquad \tau_1 = 0$$

Δx	Modified Cubic Spline*	Cubic Hermite	Finite Difference*
1/4	4.8100921110	4.8100919803	4.7750060178
1/8	4.8100900323	4.8100900308	4.8011066072
1/16	4.8100899964	4.8100899964	4.8078313856
1/32	4.8100899959	4.8100899959	4.8095245373
Order of convergence	5.92	5.96	2.15

*Data from G. I. Wakoff [21].

(b) Eigenvalues of Two-Group Equations

$$\rho_1 = \begin{cases} 3 \\ 2 \end{cases} \qquad \rho_2 = \begin{cases} 4 \ [0, \frac{3}{4}) \\ 3 \ (\frac{3}{4}, 1] \end{cases} \qquad \sigma_1 = \sigma_2 = 0, \qquad \tau_1 = \tau_2 = 1$$

Δx	Modified Cubic Spline	Cubic Hermite	Finite Difference
1/4	71.5395485397	71.5395459139	70.057197816
1/8	71.5395176807	71.5395176658	71.164716538
1/16	71.5395171951	71.5395171950	71.445553695
1/32	71.5395171875	71.5395171875	71.516009845
Order of convergence	6.01	5.95	2.18

Example 4.2. One-Dimensional Two-Group Two-Region Problem

We consider an eigenvalue problem for a one-dimensional two-group, two-region diffusion problem. The reactor configuration is depicted in Fig. 4.1. The multigroup parameters for Eq. (4.9a) can be found in Table C.2 in Appendix C.

For the numerical approximation using the finite element method, the linear (m=1) and cubic (m=2) Hermite basis functions as given by Eq. (2.14) were used. Calculations are also performed using the finite difference scheme.

In Table 4.2(a), comparisons are made for eigenvalues obtained by various methods. The eigenvalues converge to 0.9795 with the order $O(\Delta x^{2m-1})$ as predicted by Eq. (4.13) for the non-self-adjoint operators. The finite difference scheme gives the same order of convergence as the linear Hermite method. In Table 4.2(b), the thermal neutron fluxes at $x = 2L/3$ are compared. The neutron fluxes are seen to converge to 0.791334 with the order $O(\Delta x^{2m})$ in coincidence with Theorem 4.1. On the other hand, for the finite difference method, the order of convergence is found to be somewhat less than the expected value 2.0.

In Fig. 4.2, the thermal flux distributions computed using the cubic Hermite method and the finite difference scheme are compared. In this figure, it is seen that the flux shape converges rapidly to a limit as the mesh sizes are refined. The results obtained by finite element methods compare favorably with the finite difference result which is obtained by using smaller mesh size $\Delta x = L/24$. We also note in this figure that the finite element method using coarse meshes can accurately predict local thermal flux peak in the reflector region.

In Table 4.2(c), the integrated thermal fluxes and related errors are compared. Finally, in Table 4.2(d), comparisons are made for the

Table 4.2. One-Dimensional Two-Group, Two-Region Eigenvalue Problem: Example 4.2

(a) Eigenvalues $(1/\lambda)$

	Hermite Method		
Δx	m = 1	m = 2	Finite Difference
$L^*/3$	0.97576214	0.97899829	0.97658226
L/6	0.97792715	0.97946629	0.97646699
L/12	0.97897935	0.97952296	0.97803760
L/24	0.97937656	—	0.97905549
Order of convergence	1.59	3.84	1.40

*L = 60 cm.

(b) Thermal Flux at $x = 2L/3^*$

	Hermite Method		
Δx	m = 1	m = 2	Finite Difference
L/3	0.65557645	0.81027209	0.80887720
L/6	0.82029106	0.79471040	0.81289463
L/12	0.79589912	0.79139325	0.80204605
L/24	0.79255659	—	0.79473074
Order of convergence	2.30	4.1†	1.31

*Normalized to $\phi_2(L) = 1.0$.

†Reference flux $\phi_2 = 0.7913344$ for $m = 2$, $\Delta x = L/60$.

Table 4.2 (Concluded)

(c) Integrated Thermal Flux $\int_0^L \phi_2(x)\,dx$

	Hermite Method		
Δx	m = 1	m = 2	Finite Difference
L/3	(19.5%)* 30.978644	(1.32%) 37.969594	(28.4%) 49.415513
L/6	(3.15%) 37.263231	(0.011%) 38.482219	(17.3%) 45.121380
L/12	(0.52%) 38.680668	(0.003%) 38.479082	(4.4%) 36.772008
L/24	(0.14%) 38.533171	—	(3.8%) 39.952596

*Relative errors based on the reference data $\int_0^L \phi_2\,dx = .38477937 \times 10^2$ for m = 2, $\Delta x = L/15$.

(d) Computation Time (sec)

	Hermite Method		
Δx	m = 1	m = 2	Finite Difference
L/3	—	2.89	—
L/6	2.81	3.74	2.81
L/12	5.72	9.25	5.81
L/24	10.80	—	11.02

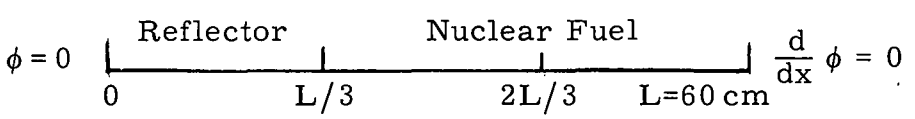

Fig. 4.1. Reactor Configuration for Example 4.2

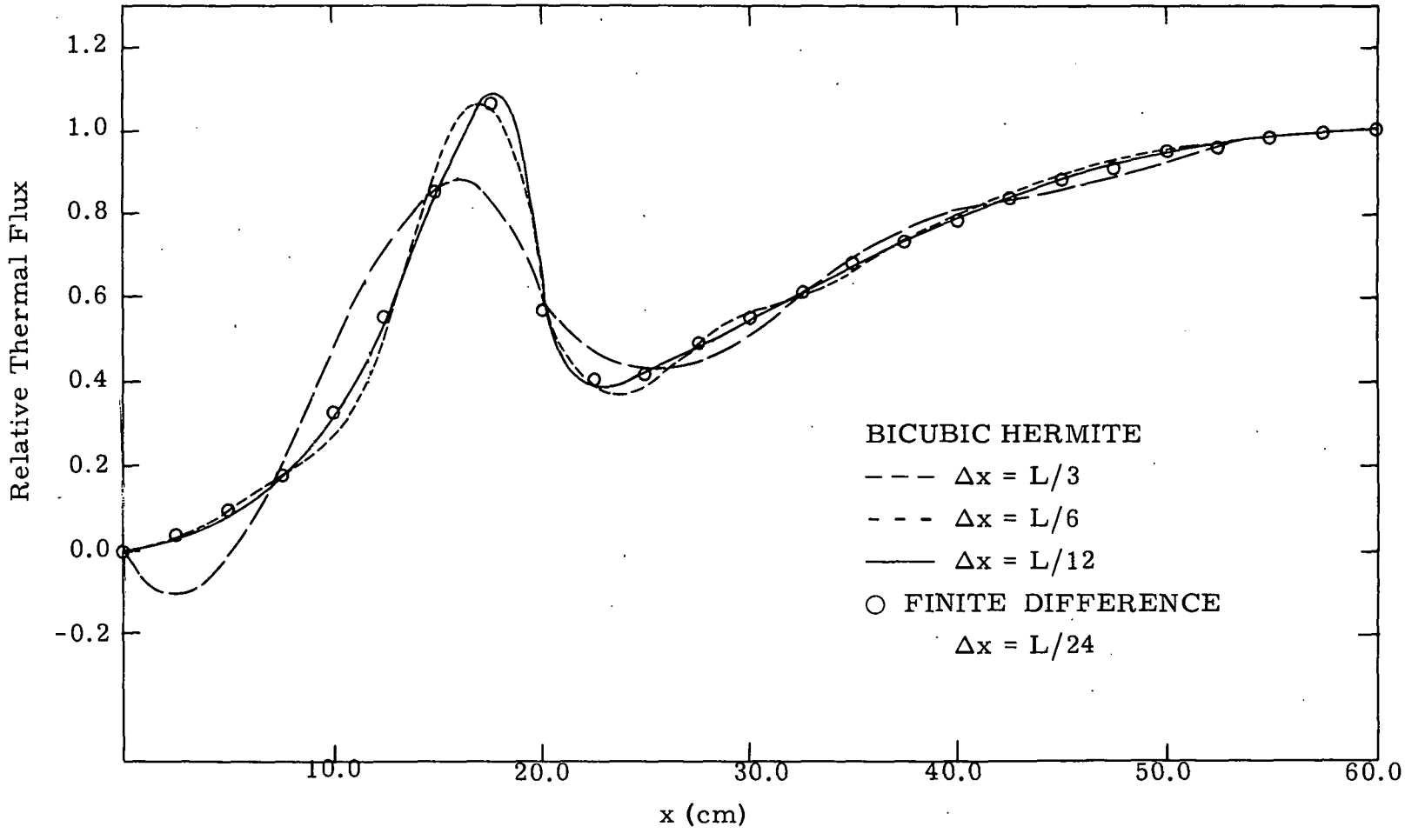

Fig. 4.2. Thermal Neutron Fluxes: Example 4.2

computation time required for the eigenfunctions to satisfy a convergence criterion of $\epsilon_a = 10^{-10}$ (cf., Eq. (4.17a)).

Comparing numerical results in the tables, it is seen that the finite element method using linear functions is somewhat more accurate than the finite difference scheme. Also, in this example it is demonstrated that the finite element method in cubic Hermite space is highly accurate and, in fact, that this method can be used as coarse mesh method to reduce computation time as compared with other methods. For example, the finite element method in the cubic Hermite space for $\Delta x = L/3$ yields about the same accuracy for the eigenvalue and the integrated flux as the finite difference scheme using $\Delta x = L/24$. Furthermore, it is shown in Table (d) that the finite element method requires less than 1/3 of the computation time of the finite difference scheme.

Example 4.3. Two-Dimensional, One-Group Model Problem

In this example, we consider an eigenvalue problem for a two-dimensional neutron diffusion equation. The configuration of interest consists of uniform nuclear fuel (Fig. 4.3). The one-group nuclear data are given in Table C.2 of Appendix C.

Table 4.3 lists eigenvalues for different meshes obtained by the finite element method using piecewise cubic Hermite polynomials and the finite difference scheme. In the finite element method, the basis functions defined by Eq. (2.28) were used. In this result, we obtain $O(\Delta r^6)$ convergence for the finite element method and $O(\Delta r^2)$ for the finite difference scheme. Also we note that the finite element method for $\Delta x = L/2$ yields more accurate eigenvalues than the finite difference scheme which uses $\Delta r = L/6$.

Table 4.3. Eigenvalues $1/\lambda$ of a Two-Dimensional, One-Group Model Problem: Example 4.3

	Cubic Hermite	Finite Difference
L/2	0.9230904055	0.92280573
L/4	0.9230903703	0.92301801
L/6	0.9230903697	0.92305812
Order of convergence	5.89	2.65

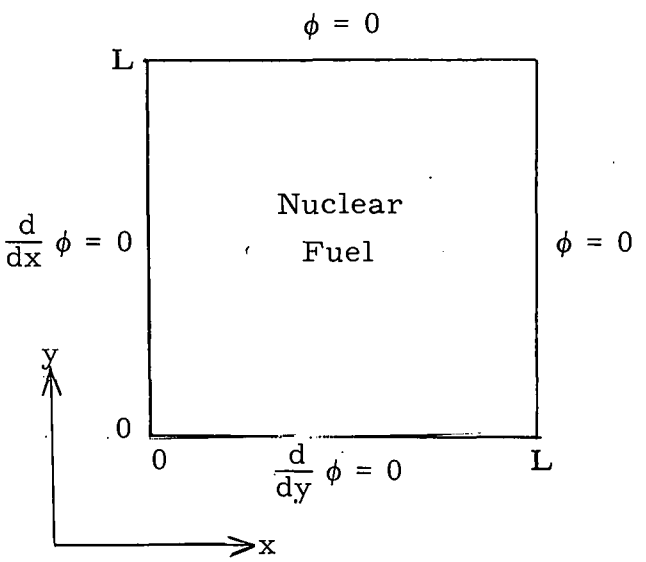

L = 40 cm

Fig. 4.3. Reactor Configuration for Example 4.3

Example 4.4. Two-Dimensional, Two-Group Problem

In this example, we consider an eigenvalue problem of two-group neutron diffusion equations. The system consists of a fuel region inside and a reflector outside (Fig. 4.4). The nuclear parameters of the materials are given in Table C.2 in Appendix C.

For this calculation, we use the bicubic basis functions defined by Eq. (2.28). At the singular point, we consider three different types of bicubic functions:

Set A: Two basis functions which satisfy ϕ and $D \frac{\partial}{\partial n} \phi$ continuity at the corner. These are given by Eq. (2.29).

Set B: Four basis functions which are continuous. These are given by Eq. (2.28) with $\frac{\theta}{D} = 1$ for $u^{(1, 0)}$ and $u^{(0, 1)}$.

Set C: Six basis functions which are continuous. These are given by Eq. (2.30).

Table 4.4 summarizes the eigenvalues obtained by the finite difference method and the finite element method using linear and cubic polynomials. We note that methods using cubic polynomials for $\Delta x = L/2$ yield accuracy comparable to that of the finite difference scheme for $\Delta x = L/20$. Furthermore, we notice that, although set A has low-order convergence, it gives quite accurate eigenvalues for large Δx. Eigenvalues for sets B and C converge in the order of $O(\Delta x^3)$. All of the eigenvalues are seen to converge to the value $1/\lambda = 1.114$.

In Fig. 4.5, thermal fluxes for the Sets A, B and C are compared. Figure 4.5(a) shows that at $y = 0$, where the singular functions vanish, the fluxes have similar shapes and all converge to the finite difference results for $\Delta x = L/20$. Figure 4.5(b) shows that at $y = 20$ cm, flux shapes for Set A are rather distorted and have slow convergence. On

the other hand, the flux using sets B and C functions converges rapidly. By comparison, we notice that set A basis functions approximate poorly the flux for coarse mesh calculations, and that set C functions give better approximations than the other sets.

Table 4.4. Eigenvalues $1/\lambda$ of Two-Dimensional, Two-Group, Two-Region Problem: Example 4.4

Δx	Hermite Method				Finite Difference
		m = 2			
	m = 1	A	B	C	
L/2	1.0802150	1.1157980	1.1081760	1.1082321	1.0783013
L/4	1.0962251	1.1153879	1.1134294	1.1134916	1.0797120
L/6	1.1040456	1.1149521	1.1140668	1.1140943	1.0895577
L/20	—	—	—	—	1.1105031
	Order of convergence				
	1.4	0.95	3.2	3.2	0.8

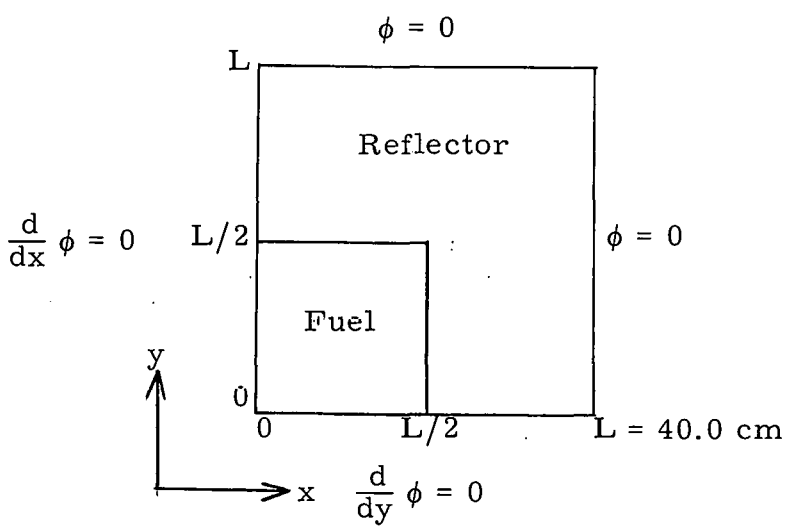

Fig. 4.4. Reactor Configuration for Example 4.4

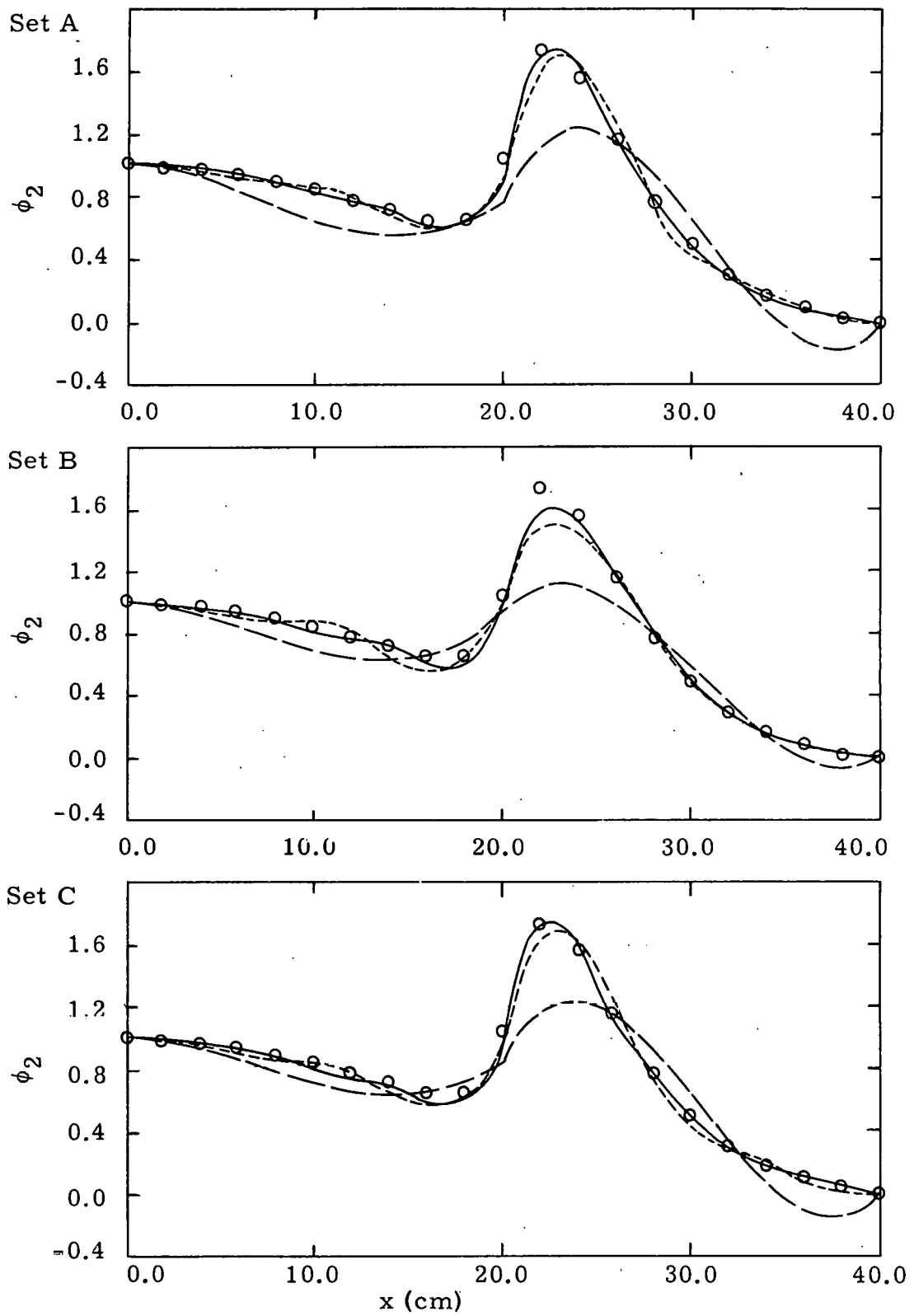

(a) y = 0.0 cm

Fig. 4.5. Thermal Neutron Fluxes: Example 4.4

KEY: Bicubic Hermite, – – – $\Delta x = L/2$, - - - $\Delta x = L/3$, —— $\Delta x = L/6$; ○ Finite Difference $\Delta x = L/20$.

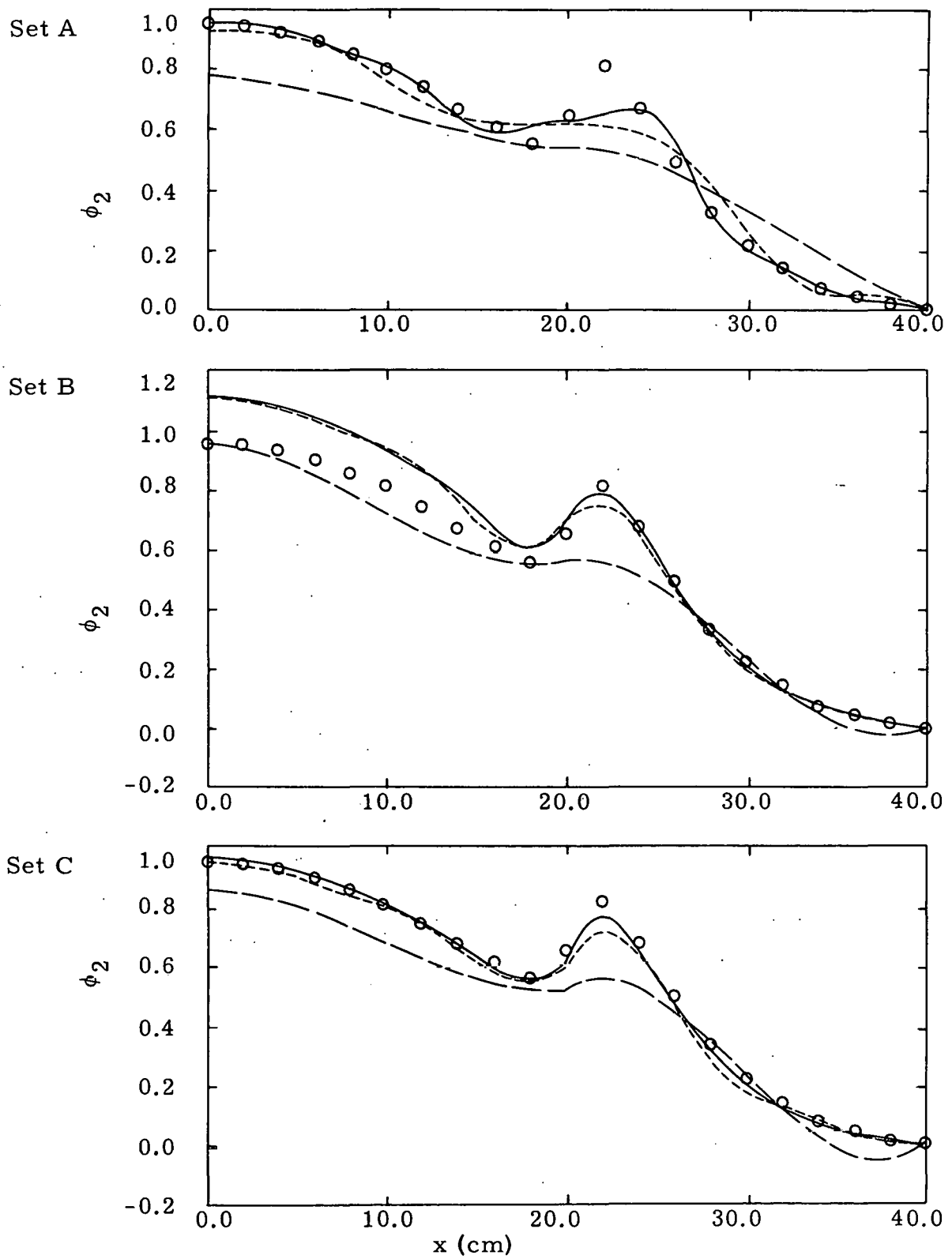

Fig. 4.5(b) y = 20.0 cm

Chapter V

POINT KINETICS PROBLEMS

In this chapter, we develop the application of univariate piecewise approximations to problems in space-independent kinetics, that is, point kinetics problems. We first develop a general procedure for the solution of a system of first-order ordinary differential equations using piecewise polynomials in Section 5.1. We term this procedure the Hermite method, as it is based upon Hermite interpolation. The Hermite method results in a single-step algorithm and, for equations with variable coefficient A(t), yields a truncation error of order $2m$ for interpolation polynomials of degree $2m-1$. It is shown that certain classic methods, i.e., the Crank-Nicolson method and the Padé (m, m) rational approximations for exponential functions [40], [46] appear as special cases of the Hermite method.

We then apply the method to the point kinetics equations in Section 5.2. Especially, we present an alternative form of the kinetics equations which avoid the numerical operations of matrix inversion necessary to carry out the forward time step in the direct approach. Finally, numerical results are presented in Section 5.3 which confirm the accuracy of the error analysis.

A number of authors considered the use of piecewise polynomials for initial value problems (e.g., see [47] - [50]); however, these studies have been limited either to the use of discontinuous polynomials [47], [48] or to problems with constant coefficients [49], [50]. Nassif [51] extended

the Hermite method for polynomials of arbitrary degrees, and his study asserts the analogy between the Hermite method and the Padé (m, m) approximations for the general m.

5.1 The Hermite Method

In this section we shall develop the application of piecewise polynomials to systems of coupled ordinary differential equations. We consider a system of the first-order ordinary differential equations

$$\frac{d}{dt}\underline{\phi}(t) = A(t)\,\underline{\phi}(t), \qquad 0 \leq t \leq T, \tag{5.1a}$$

$$\underline{\phi}(0) = \underline{\phi}_0, \tag{5.1b}$$

where $\underline{\phi}(t) = \text{col}\{\phi_1(t), \phi_2(t), \ldots, \phi_N(t)\}$ and A(t) is an $N \times N$ matrix. A(t) may be discontinuous in t. In reactor kinetics problems, the point kinetics equations and the semidiscrete neutron diffusion equations can be represented in the form of Eq. (5.1a).

We divide the interval $[0, T]$ into a partition π_t such that

$$\pi_t: \; 0 = t_1 < t_2 < \ldots < t_{N_t} = T.$$

If A(t) is discontinuous at some points in $[0, T]$, then we assume that the partition includes such points as mesh points.

We limit our consideration to a particular subinterval $[t_i, t_{i+1}]$. Assume that $\underline{\phi}(t_i)$ is given as the initial condition or as a result of previous computation, and $\underline{\phi}(t_{i+1})$ is to be determined. However, when A(t) is discontinuous at $t = t_i$ (or t_{i+1}), $\underline{\phi}(t_i)$ (or $\underline{\phi}(t_{i+1})$) is to be interpreted as the one-sided limit, $\underline{\phi}(t_i^+)$ (or $\underline{\phi}(t_{i+1}^-)$).

Let $\{u_j^{p\pm}(t)\}_{p=0}^{m-1}$ $(j = i, i+1)$ be the element functions of degree $2m-1$ as defined by Eq. (2.4) in Chapter II. And let the approximation solution to $\underline{\phi}(t)$ be represented by

$$\hat{\underline{\phi}}(t) = \sum_{p=0}^{m-1} \{\hat{\underline{\phi}}_i^{(p)} u_i^{p+}(t) + \hat{\underline{\phi}}_{i+1}^{(p)} u_{i+1}^{p-}(t)\} \tag{5.2}$$

where

$$\hat{\underline{\phi}}_j^{(p)} \equiv \frac{d^p}{dt^p} \hat{\underline{\phi}}(t)\Big|_{t_j}, \qquad j = i, i+1 .$$

In order to determine $\hat{\underline{\phi}}(t)$, we assume that $\hat{\underline{\phi}}(t)$ satisfies

$$\int_{t_i}^{t_{i+1}} d\hat{\underline{\phi}}(t) = \int_{t_i}^{t_{i+1}} A(t)\, \hat{\underline{\phi}}(t)\, dt . \tag{5.3}$$

Integrating explicitly,

$$\hat{\underline{\phi}}_{i+1} - \hat{\underline{\phi}}_i = \int_{t_i}^{t_{i+1}} A(t) \sum_{p=0}^{m-1} \{\hat{\underline{\phi}}_i^{(p)} u_i^{p+}(t) + \hat{\underline{\phi}}_{i+1}^{(p)} u_{i+1}^{p-}(t)\}\, dt$$

$$= \sum_{p=0}^{m-1} \{\mathcal{A}_i^{(p+)} \hat{\underline{\phi}}_i^{(p)} + \mathcal{A}_{i+1}^{(p-)} \hat{\underline{\phi}}_{i+1}^{(p)}\} \tag{5.4a}$$

where

$$\mathcal{A}_i^{(p+)} = \int_{t_i}^{t_{i+1}} A(t)\, u_i^{p+}(t)\, dt ,$$

$$\mathcal{A}_{i+1}^{(p-)} = \int_{t_i}^{t_{i+1}} A(t)\, u_{i+1}^{p-}(t)\, dt . \tag{5.4b}$$

Furthermore, we assume that

$$\frac{d}{dt} \hat{\underline{\phi}}_j = A(t_i) \hat{\underline{\phi}}_j , \qquad j = i, i+1 . \tag{5.5a}$$

Then we can define $A_i^{\{p\}}$ such that

$$\begin{aligned}\hat{\underline{\phi}}_i^{(p)} &= \frac{d^{p-1}}{dt^{p-1}} A(t)\, \hat{\underline{\phi}}(t)\Big|_{t_i} \\ &= \frac{d^{p-2}}{dt^{p-2}} \left\{ \left(\frac{d}{dt} A(t) \right) \hat{\underline{\phi}} + A^2 \hat{\underline{\phi}} \right\} \Big|_{t_i} \\ &\vdots \\ &\equiv A_i^{\{p\}} \hat{\underline{\phi}}_i . \end{aligned} \tag{5.5b}$$

Similarly,

$$\hat{\underline{\phi}}_{i+1}^{(p)} = A_{i+1}^{\{p\}} \hat{\underline{\phi}}_{i+1} . \tag{5.5c}$$

We note that if A is independent of t, then $A_i^{\{p\}} = A_i^p$, $A_{i+1}^{\{p\}} = A_{i+1}^p$. In general, for variable A(t), Eq. (5.4a) can be written as

$$\left\{ I - \sum_{p=0}^{m-1} \mathcal{A}_{i+1}^{(p-)} A_{i+1}^{\{p\}} \right\} \hat{\underline{\phi}}_{i+1} = \left\{ I + \sum_{p=0}^{m-1} \mathcal{A}_i^{(p+)} A_i^{\{p\}} \right\} \hat{\underline{\phi}}_i \tag{5.6a}$$

where I is the unit matrix. Eq. (5.6a) is a single-step equation. If $\hat{\underline{\phi}}_{i+1}$ is determined by solving Eq. (5.6a), then its derivatives $\hat{\underline{\phi}}_{i+1}^{(p)}$ can be found from Eq. (5.5c). These are substituted into Eq. (5.2a) to construct $\hat{\underline{\phi}}(t)$ in the interval $[t_i, t_{i+1}]$. This method will be called the Hermite method because the method is based on the Hermite interpolation. (Cf., Chap. II.) The error bound for the approximation in the Hermite method is stated in the following theorem.

Theorem 5.1

Let $\underline{\phi}(t)$ be the solution to Eq. (5.1) where A(t) is Lipschitz continuous, i.e., there exists a positive constant σ such that

$$[]A(t)\,(\underline{f}(t)-\underline{g}(t))[]_\infty \leq \sigma\,[]\underline{f}(t)-\underline{g}(t)[]_\infty .$$

Let $\hat{\underline{\phi}}(t)$ be the solution of Eq. (5.6) in the space $H_m(\pi_t)$. Assume that there exists a constant τ such that $[]\sum_{p=0}^{m-1} \mathcal{A}_{i+1}^{p-} A_{i+1}^{p}[]_\infty \leq 1$ if $|t_{i+1}-t_i| < \tau$ for $1 \leq i \leq N_t-1$. If $\underline{\phi} \in C_p^t(\pi_t)$ and $\Delta t = \max_{1\leq i\leq N_t} |t_{i+1}-t_i| < \tau$, then $\hat{\underline{\phi}}$ satisfies

$$\max_{[0,T]} []\frac{d^q}{dt^q}(\underline{\phi}(t) - \hat{\underline{\phi}}(t))[]_\infty \leq K\,\Delta t^{\mu-q}$$

where $\mu = \min(2m, t)$ and K is a constant independent of Δt.

Proof. The theorem is proven in Appendix A.

As a special case, when A(t) is constant, the Hermite method leads to the Padé approximation for $e^{A\Delta t}$ [39], [44]. For example,

(i) m = 1 (linear function)

$$\left\{I - \frac{\Delta t}{2} A\right\} \hat{\underline{\phi}}_{i+1} = \left\{I + \frac{\Delta t}{2} A\right\} \hat{\underline{\phi}}_i \qquad (5.6b)$$

(ii) m = 2 (cubic function)

$$\left\{I - \frac{\Delta t}{2} A + \frac{\Delta t^2}{12} A^2\right\} \hat{\underline{\phi}}_{i+1} = \left\{I + \frac{\Delta t}{2} A + \frac{\Delta t^2}{12} A^2\right\} \hat{\underline{\phi}}_i . \qquad (5.6c)$$

Equations (5.6b) and (5.6c) correspond to the (1.1) and (2.2) elements in the Padé table, respectively. Equation (5.6b) is also known as the Crank-Nicolson formula.

The solution for $\hat{\underline{\phi}}_{i+1}$ in Eqs. (5.6a, b, c) requires inversion of the coefficient matrices. For matrices of large order, iterative schemes

are often more effective than direct methods. In this case, the initial value of $\hat{\underline{\phi}}_{i+1}$ needs to be estimated or extrapolated from previous values. Below, we give some low-order extrapolation formulae [49], which can be used with the one-step method:

$$\hat{\underline{\phi}}_{i+1} = 2\hat{\underline{\phi}}_i - \hat{\underline{\phi}}_{i-1} , \tag{5.7a}$$

$$\hat{\underline{\phi}}_{i+1} = 2\hat{\underline{\phi}}_i - \hat{\underline{\phi}}_{i-1} - \Delta t_{i-1}(\hat{\underline{\phi}}'_{i-1} - \hat{\underline{\phi}}'_i) . \tag{5.7b}$$

The advantage of the Hermite method is that the method can accurately account for the variable A(t) within each mesh element. Consequently, the Hermite method allows the use of relatively large mesh elements compared to the Padé approximation and other collocation schemes. Another important feature of the Hermite method is that the method permits A(t) to be discontinuous. In reactor kinetics problems, A(t) can represent the reactor controls such as the control movement or the coolant flow rate, which change discontinuously in time. Then the Hermite method can be a powerful method for studying the response to such discontinuous controls.

5.2 Point Kinetics Equations

In this section, we consider the solution of the point kinetics equation applying the Hermite method developed in the preceding section. In particular, we consider two versions of the point kinetics equations: equations with precursors in the differential forms and the time-integrated point kinetics equation in which the precursors are eliminated by integration.

5.2.1. Point Kinetics Equations with Precursors

The point kinetics equation with precursors can be written as [52], [53]

$$\frac{d}{dt}\underline{\phi}(t) = A(t)\,\underline{\phi}(t)\,, \tag{5.8a}$$

$$\underline{\phi}(0) = \underline{\phi}_o\,, \tag{5.8b}$$

where

$$\underline{\phi}(t) = \mathrm{col}\{n(t), C_1(t), \ldots, C_J(t)\}\,,$$

$$A(t) = \begin{bmatrix} \frac{\rho(t)-\beta}{\Lambda} & \lambda_1 \cdots \lambda_J \\ \frac{\beta_1}{\Lambda} & -\lambda_1 \\ \vdots & \ddots \\ \frac{\beta_J}{\Lambda} & -\lambda_J \end{bmatrix}.$$

$n(t)$ is the neutron concentration, $\rho(t)$ is the reactivity and Λ is the generation time. Other definitions can be found in Section 1.1.

The approximate solution can be found by applying the Hermite method described in Section 5.1. For example, we consider the linear variation of the reactivity of the form

$$\rho(t) = \rho_o + \rho_\Delta t\,.$$

Let

$$\hat{\underline{\phi}}(t) = \sum_{p=0}^{m-1} \left\{ \hat{\underline{\phi}}_i^{(p)}\, u_i^{p+}(t) + \hat{\underline{\phi}}_{i+1}^{(p)}\, u_{i+1}^{p-}(t) \right. \tag{5.9}$$

Then, the Hermite method yields the following one-step equation,

$$B_{i+1}\hat{\underline{\phi}}_{i+1} = B_i\hat{\underline{\phi}}_i \,, \tag{5.10a}$$

(i) $m = 1$ (linear function)

$$B_i = I + \frac{\Delta t}{2} A_{i+1} - \frac{\Delta t^2}{3} A_\Delta \,,$$

$$B_{i+1} = I - \frac{\Delta t}{2} A_i - \frac{\Delta t^2}{3} A_\Delta \,, \tag{5.10b}$$

(ii) $m = 2$ (cubic function)

$$B_i = I + \frac{\Delta t}{2} A_{i+1} - \frac{7\Delta t^2}{20} A_\Delta + \left\{ \frac{\Delta t^2}{12} A_{i+1} - \frac{\Delta t^3}{20} A_\Delta \right\} A_i \,,$$

$$B_{i+1} = I - \frac{\Delta t}{2} A_i - \frac{7}{20} \Delta t^2 A_\Delta + \left\{ \frac{\Delta t^2}{12} A_i + \frac{\Delta t^3}{20} A_\Delta \right\} A_{i+1} \,, \tag{5.10c}$$

where

$$A_i = A(t_i)$$

and

$$A_\Delta = \begin{bmatrix} \frac{\rho_\Delta}{\Lambda} & \vdots & \\ \cdots & \cdots & \\ & \bigcirc & \end{bmatrix} .$$

Comparing with the Padé (m, m) approximations, we note that Eqs. (5.10b, c) contain some additional terms in Δt^2 and Δt^3. In fact, these are the correction terms which account for the linear variation of the reactivity $\rho(t)$.

5.2.2. Time-Integrated Point Kinetics Equation

The time integrated point kinetics equation is obtained by integrating the precursors and eliminating them from Eq. (5.8a). The result can be written as

$$\frac{d}{dt} n(t) = \frac{\rho(t) - \beta}{\Lambda} n(t) + \sum_{j=0}^{J} \lambda_j \left\{ C_{jo} e^{-\lambda_j t} + \frac{\beta_j}{\Lambda} \int_0^t n(s) e^{-\lambda_j (t-s)} ds \right\}, \tag{5.11a}$$

$$n(0) = n_o . \tag{5.11b}$$

Let

$$\hat{n}(t) = \sum_{p=0}^{m-1} \left\{ \hat{n}_i^{(p)} u_i^{p+}(t) + \hat{n}_{i+1}^{(p)} u_{i+1}^{p-}(t) \right\} . \tag{5.12}$$

Then we require that $\hat{n}(t)$ satisfies

$$\hat{n}_{i+1} - \hat{n}_i = \int_{t_i}^{t_{i+1}} \frac{\rho(t) - \beta}{\Lambda} \hat{n}(t)\, dt + \sum_{j=1}^{J} \int_{t_i}^{t_{i+1}} \lambda_j \left\{ C_{jo} e^{-\lambda_j t} + \frac{\beta_j}{\Lambda} \int_0^t \hat{n}(s) e^{-\lambda_j (t-s)} ds \right\} dt . \tag{5.13}$$

Proceeding as in Section 5.1, we obtain a single-step equation from Eq. (5.13).

For example, we consider a simple case of approximation using linear functions (m=1) and a ramp reactivity

$$\rho(t) = \rho_o + \rho_\Delta t .$$

Then Eq. (5.13) becomes

$$B_{i+1} \hat{n}_{i+1} = B_i \hat{n}_i + \sum_{j=1}^{J} \left(e^{-\lambda_j t_i} - e^{-\lambda_j t_{i+1}} \right) S_{j,i} \tag{5.14}$$

where

$$B_{i+1} = 1 - \frac{\rho_i - \beta}{\Lambda}\frac{\Delta t_i}{2} - \frac{\rho_\Delta}{\Lambda}\frac{\Delta t_i^2}{3} + \sum_{j=1}^{J}\frac{\beta_j}{\Lambda\Delta t_i}\alpha_{j,i+1} ,$$

$$B_i = 1 + \frac{\rho_i - \beta}{\Lambda}\frac{\Delta t_i}{2} + \frac{\rho_\Delta}{\Lambda}\frac{\Delta t_i^2}{6} + \sum_{j=1}^{J}\frac{\beta_j}{\Lambda\Delta t_i}\alpha_{j,i} ,$$

$$\rho_i = \rho_o + \rho_\Delta t_i, \qquad \Delta t_i = t_{i+1} - t_i ,$$

$$\alpha_{j,i+1} = -\frac{\Delta t_i}{\lambda_j}\left(\frac{\lambda_j\Delta t_i}{2} - 1\right) + \frac{1}{\lambda_j^2}\left(e^{-\lambda_j\Delta t_i} - 1\right) ,$$

$$\alpha_{j,i} = \frac{\Delta t_i}{\lambda_j}\left(\frac{\lambda_j\Delta t_i}{2} + 1\right) + \left(\frac{\Delta t_i}{\lambda_j} + \frac{1}{\lambda_j^2}\right)\left(e^{-\lambda_j\Delta t_i} - 1\right).$$

$S_{j,k+1}$ can be determined recursively from

$$S_{j,1} = C_{jo} ,$$

$$S_{j,k+1} = S_{j,k} + \frac{\beta_j\hat{n}_k}{\Lambda\Delta t_k}\left\{\frac{e^{\lambda_j t_{k+1}}}{\lambda_j^2} - \left(\frac{\Delta t_k}{\lambda_j} + \frac{1}{\lambda_j^2}\right)e^{\lambda_j t_k}\right\}$$

$$+ \frac{\beta_j\hat{n}_{k+1}}{\Lambda\Delta t_k}\left\{\left(\frac{\Delta t_k}{\lambda_j} - \frac{1}{\lambda_j^2}\right)e^{\lambda_j t_{k+1}} + \frac{1}{\lambda_j^2}e^{\lambda_j t_k}\right\} .$$

$\hat{n}_{i+1}$ is a scalar and can be determined from Eq. (5.14) by dividing by the scalar B_{i+1}.

5.3 Numerical Results

The computer program, HERMITE-OD, was prepared for calculations in the numerical examples in this section. HERMITE-OD solves the point kinetics equations by the Crank-Nicolson scheme (Eq. 5.6b)

and the Hermite method using piecewise linear or cubic polynomials (Eqs. (5.10a, b, c) and (5.14)).

Example 5.1

Consider a point kinetics problem defined by

$$\rho(t) = \frac{\beta}{2} t$$

with six delayed neutrons (Table C.1) and the following constants

$$\Lambda = 5 \times 10^{-5} \text{ sec},$$

$$n(0) = 1.0,$$

$$0 \leq t \leq 2 \text{ sec}.$$

Table 5.1(a) compares n(t) computed by the Hermite method using polynomials of various degrees and the Crank-Nicolson method. In the latter, a constant reactivity in each time interval is assumed such that

$$\rho(t) = \rho(t_i), \qquad t_i \leq t \leq t_{i+1}.$$

Convergence of order $O(\Delta t^{2m})$ is observed for Hermite methods using polynomial of degree 2m-1. This coincides with the statement in Theorem 5.1. However, the Crank-Nicolson scheme shows only $O(\Delta t^{1})$ convergence. This example demonstrates that the Hermite method retains high-order convergence for variable coefficients (reactivity), in contrast to the Crank-Nicolson scheme and other collocation schemes.

We remark at this point that results by the Crank-Nicolson scheme can be improved by using the average of $\rho(t)$ in the interval $[t_i, t_{i+1}]$ instead of values at mesh points. Thus, let

$$\rho(t) = \bar{\rho} = \frac{\rho(t_i) + \rho(t_{i+1})}{2}, \qquad t_i \leq t \leq t_{i+1}.$$

Table 5.1. Point Kinetics Problem, $\Lambda = 5 \times 10^{-4}$ sec: Example 5.1

(a) n(t)

t	Δt	Crank-Nicolson	Hermite Method		
			m = 1	m = 2	m = 1 (time-integ.)
1.0	0.5	1.5316543	1.9144400	1.9465955	1.9046032
	0.1	1.8513059	1.9482021	1.9499962	1.9476481
	0.05	1.9002958	1.9495497	1.9499987	1.9494094
	0.01	1.9400027	1.9499808	1.9499987	1.9499751
	0.005	1.9540000	1.9499942	1.9499987	1.9499928
	Order of convergence	0.95	1.92	4.48	2.08
2.0	0.5	5.4308838	11.145270	10.943181	10.925652
	0.1	9.7275836	11.243498	11.227962	11.219269
	0.05	10.450756	11.232274	11.228356	11.226118
	0.01	11.068160	11.228529	11.228372	11.228282
	0.005	11.147961	11.228411	11.228372	11.228349
	Order of convergence	0.95	1.97	4.36	2.09

(b) n(t) by the Crank-Nicolson scheme using $\bar{\rho}$

Δt	t = 1.0	t = 2.0
0.5	1.8818173	10.013090
0.1	1.9467323	11.189778
0.05	1.9491803	11.218824
0.01	1.9499660	11.227991
0.005	1.9499905	11.228276
Order of convergence	1.93	1.86

Results of the Crank-Nicolson scheme using $\bar{\rho}$ are shown in Table 5.1(b). The table shows that use of $\bar{\rho}$ improves the solution as well as the order of convergence.

Example 5.2

This example is basically the same as Example 5.1 except that $\Lambda = 10^{-7}$ sec. The neutron density in this example increases rapidly and reaches a magnitude of 10^5 two seconds after the insertion of ramp reactivity, $\rho(t) = \frac{\beta}{2} t$. This example is to test Hermite methods for numerical stability when applied to the fast system.

Table 5.2 compares n(t) obtained by the Hermite methods and the Crank-Nicolson method. For time step sizes, $5 \times 10^{-3} \leq \Delta t \leq 5 \times 10^{-1}$ in this example, uniform convergence is not observed. Also, this table compares relative errors of n(t) for $\Delta t = 0.01$ sec. We observe in this table that, for large Δt, the Hermite method as applied to the time-integrated kinetics equation gives more stable and accurate solution when compared to the kinetics equation with precursors.

Table 5.2. n(t) of a Point Kinetics Problem, $\Lambda = 10^{-7}$ sec: Example 5.2

t	Δt	Crank-Nicolson	Hermite Method		
			m = 1	m = 2	m = 1 (time-integ.)
1.0	0.5	1.7398362	2.1903963	2.1453451	2.1770162
	0.1	2.1617929	2.2835253	2.2761511	2.2823753
	0.05	2.2242740	2.2870330	2.2873140	2.2867310
	0.01	(0.613%)* 2.2741454	(2.01×10^{-3}%) 2.2881595	(2.53×10^{-4}%) 2.2881994	(6.90×10^{-4}%) 2.2881894
	0.005	2.2806399	2.2881928	2.2882052	2.2881461
	Order of convergence	0.947	1.93	3.75	1.90
2.0	0.5	0.98040854×10^{1}	0.62508242×10^{2}	0.13191022×10^{5}	0.10859238×10^{3}
	0.1	0.15045759×10^{3}	0.11526595×10^{4}	0.63665597×10^{4}	0.26780006×10^{4}
	0.05	0.51885734×10^{3}	0.39038912×10^{4}	0.67090612×10^{4}	0.80757093×10^{4}
	0.01	(68.3%) 0.65411931×10^{4}	(2.75%) 0.21227155×10^{5}	(10.92%) 0.18399171×10^{5}	(0.81%) 0.20823698×10^{5}
	0.005	0.11790377×10^{5}	0.21803225×10^{5}	0.20657232×10^{5}	0.20264628×10^{5}

* Relative error in % based on $n(1.0) = .22882052 \times 10^{1}$, $n(2.0) = .20657232 \times 10^{5}$.

Chapter VI

TIME-DEPENDENT NEUTRON DIFFUSION PROBLEMS

In this chapter, we consider the approximate solution of the time-dependent neutron diffusion equations. The equations are first developed in the weak formulation, as presented initially in Chapter IV. We include the dealyed neutrons explicitly in the formulation in order to avoid the computation of delayed neutron precursors. We show that time-dependent solutions are unique for the case of no delayed neutrons.

In Section 6.2, we derive the discrete equations in space, energy and time applying the methods developed in Chapters III, IV and V and show that the resulting approximate solution converges to the analytic solution, again for the case of no delayed neutrons. We present a theorem which shows the error bound for the approximation error. We conclude this chapter with some numerical examples and results in Section 6.3.

6.1 Basic Equations

The time-dependent diffusion equation is defined in Eq. (1.1) in Chapter I. In particular, we are interested in the time-dependent neutron diffusion equation, in which the delayed neutron precursors are eliminated by integration. For $0 \leq t \leq T$,

$$\frac{1}{\mathscr{V}(E)}\frac{\partial}{\partial t}\phi(\underline{r},E,t) = T\phi(\underline{r},E,t) + Q(\underline{r},E,t)$$

$$= \left\{\underline{\nabla}\cdot D(\underline{r},E,t)\,\underline{\nabla} - \Sigma_T(\underline{r},E,t)\right\}\phi(\underline{r},E,t)$$

$$+ \int_{\mathscr{E}} dE'\left\{\Sigma_s(\underline{r},E'\to E,t)+(1-\beta)\chi(E)\nu\Sigma_f(\underline{r},E',t)\right\}\phi(\underline{r},E',t)$$

$$+ \sum_{j=1}^{J}\left\{\chi_{dj}(E)\lambda_j C_{jo}e^{-\lambda_j t}\right.$$

$$\left. + \lambda_j\beta_j\chi_d(E)\int_0^t e^{-\lambda_j(t-s)}\int_{\mathscr{E}} dE'\,\nu\Sigma_f(\underline{r},E',s)\phi(\underline{r},E',s)\,ds\right\}$$

$$+ Q(\underline{r},E,t)\,, \tag{6.1a}$$

$$\phi(\underline{r},E,t)\Big|_{t=0} = \phi_o(\underline{r},E)\,, \tag{6.1b}$$

$$\phi(\underline{r},E,t)\Big|_{\partial\Omega} = 0\,, \tag{6.1c}$$

and

$$\phi(\underline{r},E,t),\quad D\frac{\partial}{\partial n}\phi(\underline{r},E,t) \text{ continuous on the material interfaces.} \tag{6.1d}$$

Definitions are developed in Chapter I.

We define the inner products and L^2-norm by

$$(u,v) = \int_{\mathscr{E}}\int_{\Omega} u,v\,dV\,dE\,,$$

$$\|u\|_{L^2} = (u,v)^{\frac{1}{2}}\,,$$

and the bilinear form

$$a(u,v) = (D\underline{\nabla}u,\underline{\nabla}v) + (\Sigma_T u,v)$$

$$- \left\{\left(\int_{\mathscr{E}}\Sigma_s(E'\to E)u(E')\,dE',v\right)\right\} - (1-\beta)\left\{\left(\chi(E)\int_{\mathscr{E}}\nu\Sigma_f(E')u(E')dE',v\right)\right\}.$$

In this chapter, we make an assumption that there exists $\gamma > 0$ such that

$$a(\phi,\phi) \geq \gamma\|\phi\|^2_{L^2}\,. \tag{6.2}$$

We consider the problem of finding a $\phi(\underline{r}, E, t)$ from the weak formulation of Eq. (6.1) such that

$$\left(\frac{1}{\mathscr{V}} \frac{\partial}{\partial t} \phi, v\right) + a(\phi, \mathscr{V}) = (Q_d, v), \tag{6.3a}$$

$$(\phi(\underline{r}, E, t), v)\big|_{t=0} = (\phi_o, v), \tag{6.3b}$$

for all $v \in W_o^1(\Omega)$ (cf., Sec. 4.1, Chap. IV),

where

$$Q_d = Q + \sum_{j=1}^{J} \left\{ \chi_d(E) \lambda_j C_{jo} e^{-\lambda_j t} + \lambda_j \beta_j \chi_d(E) \int_0^t ds\, e^{-\lambda_j (t-s)} \int_{\mathscr{E}} dE'\, \nu\Sigma_f(\underline{r}, E', s) \phi(\underline{r}, E's) \right\} .$$

To show the uniqueness of the solution to Eqs. (6.3a, b) when $\beta = 0$ (no delayed neutrons), we proceed as follows. Since $(D\underline{\nabla}\phi, \underline{\nabla}\phi)$, $(\Sigma_T \phi, \phi) > 0$,

$$-a(\phi, \phi) \leq \left(\int_{\mathscr{E}} \{\Sigma_s(E' \to E) + \chi(E) \nu\Sigma_f(E')\} \phi(E')\, dE', \phi(E) \right)$$

$$\leq K' \left(\int_{\mathscr{E}} \phi(E)\, dE \right)^2$$

where K' is a positive constant. Applying the Schwarz inequality, we obtain

$$-a(\phi, \phi) \leq K'' \int_{\mathscr{E}} \phi^2\, dE$$

$$= K'' \| \phi \|^2_{L^2} .$$

Using the simple inequality, $ab \leq \frac{1}{2} a^2 + \frac{1}{2} b^2$,

$$(Q, \phi) \leq \frac{1}{2} \| Q \|^2_{L^2} + \frac{1}{2} \| \phi \|^2_{L^2} .$$

Also,

$$\left(\frac{1}{\mathscr{V}}\frac{\partial}{\partial t}\phi, \phi\right) = \frac{1}{2}\frac{\partial}{\partial t}\left(\frac{1}{\mathscr{V}}\phi, \phi\right)$$

$$\geq \frac{1}{2\mathscr{V}_{max}}\frac{d}{dt}\|\phi\|^2_{L^2} .$$

Thus, Eq. (6.3a) with $v = \phi$ leads to the following differential inequality,

$$\frac{1}{2\mathscr{V}_{max}}\frac{d}{dt}\|\phi\|^2_{L^2} \leq K''\|\phi\|^2_{L^2} + \frac{1}{2}\|\phi\|^2_{L^2} + \frac{1}{2}\|Q\|^2_{L^2}$$

or

$$\frac{d}{dt}\|\phi\|^2_{L^2} \leq K_1\|\phi\|^2_{L^2} + K_2\|Q\|^2_{L^2} .$$

Solving the differential inequality leads to the following lemma:

Lemma 6.1. Let $\phi(\underline{r}, E, t)$ be the solution of Eq. (6.3) with $\beta = 0$. Then $\phi(\underline{r}, E, t)$ satisfies

$$\|\phi\|^2_{L^2} \leq e^{K_1 t}\|\phi_o\|^2_{L^2} + K_2\int_0^t e^{K_1(t-s)}\|Q\|^2_{L^2} ds . \qquad (6.4)$$

We remark that the inequality (6.4) shows that the time-dependent solution is bounded by the initial condition and the source term in the L^2-norm. It further follows that the weak formulation of Eq. (6.1) has only a trivial solution if $\phi_o = Q = 0$. Thus, Lemma 6.1 implies the uniqueness of the solution to Eq. (6.3).

When $\beta \neq 0$, some fission neutrons are emitted not immediately but with some time delays. In this case, the solution depends on the past history of the neutron flux as well as the initial condition and the source term. We will not attempt to prove this but conjecture that the solution to Eq. (6.3) with $\beta \neq 0$ exists uniquely.

6.2 Approximations

6.2.1 Semidiscretization

In this section, we derive the discrete equations in energy and space applying methods developed in Chapters III and IV.

Let π_Ω and $\pi_{\mathcal{E}}$ be the partitions of the region Ω and the energy interval $\mathcal{E}$ such that

$$\pi_\Omega: \; a_1 = r_{1,1} < r_{1,2} < \ldots < r_{1,N_1} = b_1,$$
$$\vdots$$
$$a_n = r_{n,1} < r_{n,2} < \ldots < r_{n,N_n} = b_n,$$

$$\pi_{\mathcal{E}}: \; E_{min} = E_1 < E_2 < \ldots < E_{N_E} = E_{max}.$$

Selections of proper polynomial basis functions were discussed in Chapters II and IV. Let $\{v_{ig} = v_i(\underline{r})\, v_g(E): 1 \leq i \leq N, \; 1 \leq g \leq G\}$ form a basis in the space $H_m(\pi_\Omega \times \pi_{\mathcal{E}})$ where $m = (m_r, m_E)$ and the approximate solution be represented by

$$\hat{\phi}(\underline{r}, E, t) = \sum_{g=1}^{G} \sum_{i=1}^{N} a_{ig}(t)\, v_i(\underline{r})\, v_g(E). \tag{6.5}$$

The expansion coefficients of $\hat{\phi}$ can be determined by applying the Galerkin scheme to the weak form of Eq. (6.1) such that $\hat{\phi}$ satisfies

$$\left(\frac{1}{\mathscr{V}} \frac{\partial}{\partial t} \hat{\phi}, v\right) + a(\hat{\phi}, v) = (Q_d, v), \tag{6.6}$$
$$(\hat{\phi}, v)\Big|_{t=0} = (\hat{\phi}, v),$$

where $v = v_{ig}(\underline{r}, E)$ for all i and g.

In a manner analogous to the derivation of the inequality (6.4) for the analytic solution, choosing $v = \hat{\phi}$ and $\beta = 0$ in Eq. (6.6), we obtain the following lemma:

Lemma 6.2. Let $\hat{\phi}(\underline{r}, E, t)$ be the solution to Eq. (6.6) with $\beta = 0$. Then $\hat{\phi}(\underline{r}, E, t)$ satisfies

$$\|\hat{\phi}\|^2_{L^2} \leq e^{K_1 t} \|\hat{\phi}_o\|^2_{L^2} + K_2 \int_0^t e^{K_1(t-s)} \|Q\|^2_{L^2} \, ds \, . \tag{6.7}$$

The inequality (6.7) implies that the approximate solution is unique and the Galerkin scheme is numerically stable.

Following the procedure of Chapter IV, we apply the Galerkin approximations in steps, for the energy variable first and then for the space variables.

Let

$$\Phi_g(\underline{r}, t) = \sum_{i=1}^{N} a_{ig}(t) \, v_i(\underline{r}) \, ;$$

then from Eq. (6.5),

$$\hat{\phi}(\underline{r}, E, t) = \sum_{g=1}^{G} \Phi_g(\underline{r}, t) \, v_g(E) \, .$$

Apply the Galerkin scheme to Eq. (6.1) for the energy variable such that, for $g = 1, 2, \ldots, G$,

$$\left(\frac{1}{\mathscr{V}} \frac{\partial}{\partial t} \hat{\phi}, v_g\right)_{\mathscr{E}} = (T\hat{\phi}, v_g)_{\mathscr{E}} + (Q, v_g)_{\mathscr{E}} \, , \tag{6.8a}$$

$$(\hat{\phi}(\underline{r}, E, 0), v_g)_{\mathscr{E}} = (\phi_o(\underline{r}, E), v_g)_{\mathscr{E}} \, , \tag{6.8b}$$

$$(\hat{\phi}(\underline{r}, E, t), v_g)_{\mathcal{E}} \Big|_{\partial\Omega} = 0 , \tag{6.8c}$$

$$(\hat{\phi}, v_g)_{\mathcal{E}} \left(D \frac{\partial}{\partial n} \hat{\phi}, v_g \right)_{\mathcal{E}} \text{ continuous on the material interfaces} , \tag{6.8d}$$

where

$$(u, v)_{\mathcal{E}} = \int_{\mathcal{E}} uv \, dE .$$

Equation (6.8) then leads to the generalized time-dependent multigroup equations, for $g = 1, 2, \ldots, G$,

$$\sum_{g'=1}^{G} \frac{1}{\mathscr{V}_{gg'}} \frac{\partial}{\partial t} \Phi_{g'} = \sum_{g'=1}^{G} \left\{ \underline{\nabla} \cdot D_{gg'} \underline{\nabla} - \Sigma_{Tgg'} + \Sigma_{sgg'} + \chi_g (1-\beta) \nu \Sigma_{fg'} \right\} \Phi_{g'}$$

$$+ \sum_{j=1}^{J} \left\{ \chi_{djg} \lambda_j C_{jo} e^{-\lambda_j t} + \lambda_j \beta_j \chi_{dg} \int_0^t e^{-\lambda_j (t-s)} \sum_{g'=1}^{G} \nu \Sigma_{fg'} \Phi_{g'} ds \right\}$$

$$+ Q_g \tag{6.9a}$$

with conditions

$$\sum_{g'=1}^{G} M_{gg'} \Phi_{g'}(0) = \Phi_{og}(\underline{r}) , \tag{6.9b}$$

$$\Phi_g(\underline{r}, t) \Big|_{\partial\Omega} = 0 , \tag{6.9c}$$

$$\Phi_g(\underline{r}, t), \sum_{g'=1}^{G} D_{gg'} \frac{\partial}{\partial n} \Phi_{g'}(\underline{r}, t) \text{ continuous at material interface} , \tag{6.9d}$$

where

$$\frac{1}{\mathscr{V}_{gg'}} = \left(\frac{1}{\mathscr{V}(E)} v_{g'}, v_g \right)_{\mathcal{E}} ,$$

$$\chi_{djg} = \int \chi_{dj}(E) \, v_g(E) \, dE ,$$

$$M_{gg'} = (v_{g'}, v_g)_{\mathcal{E}} ,$$

$$\phi_{og} = (\phi_o, v_g)_{\mathcal{E}} .$$

The remaining parameters are defined in Section 4.2.1. The conventional time-dependent multigroup equations can be obtained from Eq. (6.9) as a special case (cf., Sec. 4.2.1).

Now we apply the Galerkin scheme to the weak formulation of Eq. (6.9a) for the space variable such that, for i = 1, 2, . . . , N,

$$\sum_{g'=1}^{G} \frac{1}{\mathscr{V}_{gg'}} \left(\frac{\partial}{\partial t}\Phi_{g'}, v_i\right)_\Omega = \sum_{g'=1}^{G} \left\{ (D_{gg'}\underline{\nabla}\Phi_{g'}, \underline{\nabla} v_i)_\Omega \right.$$

$$\left. + \left([-\Sigma_{Tgg'} + \Sigma_{sgg'} + \chi_g(1-\beta)\nu\Sigma_{fg'}]\Phi_{g'}, v_i \right)_\Omega \right\}$$

$$+ \sum_{j=1}^{J} \left\{ \chi_{djg}\lambda_j e^{-\lambda_j t}(C_{jo}(\underline{r}), v_i)_\Omega + \lambda_j\beta_j\chi_{dg}\int_0^t e^{-\lambda_j(t-s)} \sum_{g'=1}^{G} (\nu\Sigma_{fg'}\Phi_{g'}, v_i)_\Omega ds \right\}$$

$$+ (q_g, v_i)_\Omega \qquad (6.10)$$

where

$$(u, v)_\Omega = \int_\Omega (u, v)\, dV .$$

Substituting for $\Phi_g = \sum_{i=1}^{N} a_{ig}(t)\, v_i(\underline{r})$, Eq. (6.10) can be written in matrix form as

$$V \frac{\partial}{\partial t}\underline{a}(t) = \{-L + S + (1-\beta)F\}\underline{a}(t)$$

$$+ \sum_{j=1}^{J} \left\{ \lambda_j \underline{C}_{jo} e^{-\lambda_j t} + \lambda_j\beta_j \int_0^t e^{-\lambda_j(t-s)} F_d \underline{a}(s)\, ds \right\}$$

$$+ \underline{q}(t) , \qquad (6.11a)$$

$$M\,\underline{a}(0) = \underline{\phi}_o , \qquad (6.11b)$$

where

$$V = \begin{bmatrix} V_{11} & \cdots & V_{1,G'+1} & & \\ \vdots & & \vdots & & \\ V_{G'+1,1} & \cdots & & & V_{G-G',G} \\ & & & & \vdots \\ & & V_{G,G-G'} & \cdots & V_{GG} \end{bmatrix}$$

$$M = \begin{bmatrix} M_{11} & \cdots & M_{1G'} & & \\ \vdots & & \vdots & & \\ M_{G'+1,1} & \cdots & & & M_{G-G',G} \\ & & & & \vdots \\ & & M_{G,G-G'} & \cdots & M_{GG} \end{bmatrix}$$

$$F_d = \begin{bmatrix} F_{11} & \cdots & \cdots & \cdots & F_{1G} \\ \vdots & & & & \vdots \\ \vdots & & & & \vdots \\ F_{G1} & \cdots & \cdots & \cdots & F_{GG} \end{bmatrix}$$

$$\underline{C}_{jo} = \text{col}\{\underline{C}_{j1}, \underline{C}_{j2}, \ldots, \underline{C}_{jG}\},$$

$$\underline{\phi}_o = \mathrm{col}\{\underline{\phi}_{o1} \cdots \underline{\phi}_{oG}\} ,$$

$$(V_{gg'})_{ii'} = \frac{1}{\mathscr{V}_{gg'}} (v_{i'}(\underline{r}), v_i(\underline{r}))_\Omega ,$$

$$(F_{dgg'})_{ii'} = \chi_{dg}(\nu\Sigma_{fg'} v_{i'}(\underline{r}), v_i(\underline{r}))_\Omega ,$$

$$(C_{jg})_{ii'} = \delta_{i'i} \chi_{djg}(C_{jo}(\underline{r}), v_i(\underline{r}))_\Omega ,$$

$$(M_{gg'})_{ii'} = M_{gg'}(v_{i'}(\underline{r}), v_i(\underline{r}))_\Omega ,$$

$$\underline{\phi}_{og} = \mathrm{col}\{(\phi_{og}, v_1(\underline{r}))_\Omega \cdots (\phi_{og}, v_N(\underline{r}))_\Omega\} .$$

Other matrices are defined in the same way as in Section 4.2.2. The properties of the matrices are discussed in Section 4.2.2.

The error bound for the approximate solution is stated in the following theorem.

Theorem 6.1. Assume that the inequality (6.2) holds. Let $\phi(\underline{r}, E, t)$ be the solution of Eq. (6.3) and $\phi(\underline{r}, E, t) \in C_p^t(\pi_\Omega \times \pi_\mathscr{E})$ where $t=(t_r, t_E)$. If $\hat{\phi}(\underline{r}, E, t)$ is the solution to the semidiscrete equation (6.6) in the space $H_m(\pi_\Omega \times \pi_\mathscr{E})$, then

$$\| \phi(\underline{r}, E, t) - \hat{\phi}(\underline{r}, E, t) \|_{L^\infty(\Omega \times \mathscr{E})} \leq K_1 \overline{\Delta r}^{\mu_r} + K_2 \overline{\Delta E}^{\mu_E}$$

where $\mu_r = \min(2m_r, t_r)$, $\mu_E = \min(2m_E, t_E)$ and $\overline{\Delta r} = \max_{\pi_\Omega} \Delta r$, $\overline{\Delta E} = \max_{\pi_\mathscr{E}} \Delta E$ and K_1 and K_2 are positive constants independent of $\overline{\Delta r}$ and $\overline{\Delta E}$, respectively.

6.2.2. Temporal Approximation

In this section, we consider the application of the method developed in Chapter V to the semidiscrete equation, Eq. (6.11), for approximations in time.

The semidiscrete equation, Eq. (6.11), can be rewritten as

$$V \frac{\partial}{\partial t} \underline{a}(t) = \left\{ -L(t) + S + (1-\beta)F \right\} \underline{a}(t) + \sum_{j=1}^{J} \left\{ \lambda_j C_{jo} e^{-\lambda_j t} + \lambda_j \beta_j \int_0^t e^{-\lambda_j (t-s)} F_d \underline{a}(s)\, ds \right\} .$$

For simplicity, we assume that only L(t) is a function of t and it is given by

$$L(t) = L_o + f(t)\, L .$$

Let $\hat{\underline{a}}(t)$ be an approximation of $\underline{a}(t)$ such that for $t_k \leq t \leq t_{k+1}$

$$\hat{\underline{a}}(t) = \sum_{p=0}^{m_t-1} \left\{ \underline{a}_k^{(p)} u_k^{p+}(t) + \underline{a}_{k+1}^{(p)} u_{k+1}^{p-}(t) \right\} \tag{6.12}$$

where $\left\{ u_k^{p\pm}(t) \right\}_{p=0}^{m_t-1}$ are the univariate element functions of degree $2m_t-1$ as defined in Section 2.1, Chapter II. By combining Eqs. (6.5) and (6.12), the approximate solution in $\underline{r}$, E and t can be represented by

$$\begin{aligned} \hat{\phi}(\underline{r}, E, t) &= \sum_{g=1}^{G} \sum_{i=1}^{N} \hat{a}_{ig}(t)\, v_i(\underline{r})\, v_g(E) \\ &= \sum_{g=1}^{G} \sum_{i=1}^{N} \sum_{p=0}^{m_t-1} \left\{ a_{igk}^{(p)} u_k^{p+}(t) + a_{ig(k+1)}^{(p)} u_{k+1}^{p-}(t) \right\} v_i(\underline{r})\, v_g(E) . \end{aligned} \tag{6.13}$$

Applying the Hermite method in Chapter IV, we obtain the following single step equation:

$$B_{k+1}\hat{\underline{a}}_{k+1} = B_k\hat{\underline{a}}_k + \sum_{j=1}^{J}\left(e^{-\lambda_j t_k} - e^{-\lambda_j t_{k+1}}\right)\underline{\mathscr{l}}_{jk} . \tag{6.14}$$

In particular, when m = 1 (linear function), the matrices are defined by

$$B_{k+1} = V - \frac{\Delta t_k}{2}\{-L_k+S+(1-\beta)F\} - \sum_{j=1}^{J}\gamma_{kj}\lambda_j\beta_j F_d + \mathfrak{L}_{k+1} ,$$

$$B_k = V + \frac{\Delta t_k}{2}\{-L_k+S+(1-\beta)F\} + \sum_{j=1}^{J}\alpha_{kj}\lambda_j\beta_j F_d + \mathfrak{L}_k ,$$

$$\underline{\mathscr{l}}_{j1} = \frac{\beta_j}{\lambda_j} F_d\,\underline{a}(0) = \frac{\beta_j}{\lambda_j} F_d M^{-1}\underline{\phi}_o ,$$

$$\underline{\mathscr{l}}_{j,\ell+1} = S_{j,\ell} + \lambda_j\beta_j F_d\{\mu_{\ell j}\hat{\underline{a}}_\ell + \epsilon_{\ell j}\hat{\underline{a}}_{\ell+1}\} ,$$

$$L_k = L(t_k) ,$$

$$\Delta t_k = t_{k+1} - t_k ,$$

$$\alpha_{kj} = \frac{\beta_j}{\Delta t_k}\left\{t_{k+1}\Delta t_k - \frac{1}{\lambda_j}\left[\frac{\lambda_j}{2}\left(t_{k+1}^2 - t_k^2\right) - \Delta t_k\right] + \left(e^{-\lambda_j\Delta t_k} - 1\right)\left(\frac{\Delta t_k}{\lambda_j} - \frac{1}{\lambda_j^2}\right)\right\} ,$$

$$\gamma_{kj} = \frac{\beta_j}{\Delta t_k}\left\{\frac{1}{\lambda_j}\left[\frac{\lambda_j(t_{k+1}^2 - t_k^2)}{2} - \Delta t_k\right] - t_k\Delta t_k - \left(e^{-\lambda_j\Delta t_k} - 1\right)\frac{1}{\lambda_j^2}\right\} ,$$

$$\mu_{kj} = \frac{\beta_j}{\Delta t_k}\left\{\frac{1}{\lambda_j^2} e^{-\lambda_j t_{k+1}} - \left(\frac{\Delta t_k}{\lambda_j} + \frac{1}{\lambda_j^2}\right) e^{\lambda_j t_k}\right\} ,$$

$$\epsilon_{kj} = \frac{\beta_j}{\Delta t_k}\left\{\left(\frac{\Delta t_k}{\lambda_j} - \frac{1}{\lambda_j^2}\right) e^{\lambda_j t_{k+1}} + \frac{1}{\lambda_j^2} e^{\lambda_j t_k}\right\} .$$

$\mathfrak{L}_k$ and $\mathfrak{L}_{k+1}$ depend on the functional form of L(t) in Eq. (6.13). For example, we consider two special cases:

(i) $L(t) = L_o + L_\Delta t$ (linear)

$$\mathfrak{L}_k = -\frac{\Delta t_k^2}{6} L_\Delta ,$$

$$\mathfrak{L}_{k+1} = \frac{\Delta t_k^2}{3} L_\Delta ,$$

(ii) $L(t) = L_o + L_\Delta \sin \omega t$ (oscillatory)

$$\mathfrak{L}_k = -\frac{1}{\omega^2 \Delta t_k} [\omega \Delta t_k \cos \omega t_k - \sin \omega t_{k+1} + \sin \omega t_k] L_\Delta ,$$

$$\mathfrak{L}_{k+1} = \frac{1}{\omega^2 \Delta t_k} [-\omega \Delta t_k \cos \omega t_{k+1} + \sin \omega t_{k+1} - \sin \omega t_k] L_\Delta .$$

The solution to Eq. (6.14) can be determined using general iterative schemes [35], [39], [40] which are applied to the finite difference scheme. The source iterative scheme which can be applied to the multigroup system, and Cholesky factorization scheme for the inversion of positive definite matrices, can also be applied to solve Eq. (6.14). For fast convergence of the iterations, accurate prediction is required. The extrapolation formula given by Eqs. (5.7a, b) can be used for this purpose.

6.3 Numerical Results

We consider the problem of solving the conventional time-dependent multigroup diffusion equation by the methods described in previous sections. Computer program HERMITE-2D (cf., Appendix D) basically solves Eq. (6.14) using the iterative schemes discussed in Section 4.3, Chapter IV.

Example 6.1. Uniform Linear Perturbation

Consider a one-group, two-dimensional problem with six groups of delayed neutron precursors. The configuration is a rectangular region which consists of a uniform nuclear fuel (Fig. 6.1). The thermal group nuclear data can be found in Table C.2 in Appendix C. The critical fission cross section is found to be 0.20493483.

Perturbation is induced by changing the thermal absorption cross section uniformly in the form

$$\Sigma_a(t) = (\Sigma_a)_{crit}\{1 - 0.01\ t\}.$$

For computational purposes, the rectangular region was divided into coarse meshes as shown in Fig. 6.1. Then, the bicubic basis functions as given by Eq. (2.28) were placed on the mesh elements. The total number of basis functions needed in this calculation is 18. The neutron fluxes were computed using HERMITE-2D. Table 6.1 compares the neutron flux at points A and B (cf., Fig. 6.1) for various Δt. The results shown demonstrate that the order of convergence is $O(\Delta t^2)$. This coincides with the prediction of Theorem 5.1 with $m = 1$.

Example 6.2. Local Sinusoidal Perturbation (1)

We consider a two-group, two-dimensional problem without delayed neutrons. The system is a rectangular region which consists of a uniform fuel (Fig. 6.2). The nuclear data are given in Table C.2 in Appendix C and the critical thermal fission cross section for the configuration is found to be 0.25104786.

Table 6.1. Uniform Linear Perturbation: Example 6.1

Δt	$\phi_A(t)$		$\phi_B(t)$	
	t = 0.1	t = 0.5	t = 0.1	t = 0.5
0.1	0.11357615×10^1	0.30271246×10^1	0.56788075	0.15135623×10^1
0.05	0.11484423×10^1	0.30811922×10^1	0.57422114	0.15405961×10^1
0.01	0.11467662×10^1	0.30987733×10^1	0.57338308	0.15493866×10^1
0.005	0.11468028×10^1	0.30993405×10^1	0.57340140	0.15496702×10^1
Order of convergence	2.4	1.9	2.4	2.0

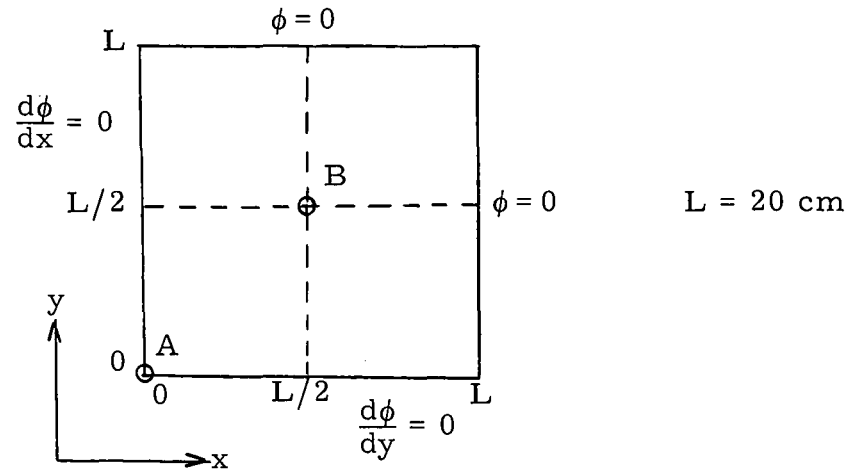

Fig. 6.1. Reactor Configuration for Example 6.1

The system is perturbed locally in R_2 (cf., Fig. 6.2) from the critical state by changing the thermal cross section sinusoidally in the form

$$\Sigma_{a2}(t) = (\Sigma_{a2})_{crit}\left\{1 + 0.2 \sin \frac{2\pi}{T} t\right\}, \qquad T = 10^{-3} \text{ sec.}$$

To apply the finite element method, the system is divided into coarse meshes as shown in Fig. 6.2. Bicubic basis functions, as given by Eq. (2.30) and Eq. (2.28), are then placed at the boundary points and internal points, respectively. A total of 18 basis functions are used.

Neutron fluxes are approximated using HERMITE-2D. In Table 6.2, thermal neutron fluxes at points A and B are compared for various time steps. We note that the solution converges to the order $O(\Delta t^2)$ as predicted by Theorem 5.1. This example demonstrates that large time steps can be used with the Hermite method. For example, the relative error for the flux is less than 5% when $\Delta t = T/4$ and less than 2% when $\Delta t = T/8$. If the finite difference scheme is used, then sine functions need to be approximated by a series of step functions, and this requires the use of many small time steps. However, as discussed in Chapter V, the Hermite method can treat perturbation analytically and for this reason the Hermite method allows use of large time steps while retaining high accuracy.

In Fig. 6.3 (a) - (c), the thermal fluxes constructed by the finite element method are plotted in three-dimensional and contour plots. In order to interpolate the flux distribution within mesh elements, mesh increments of $\Delta x = \Delta y = 0.5$ cm and 1.0 cm are used for the three-dimensional and the contour plots, respectively. In these plots, it is

demonstrated that the finite element method can approximate the local perturbation of the flux using very coarse meshes. If the finite difference scheme is used in this calculation, much smaller mesh elements will be required for an accurate approximation.

Table 6.2. Local Sinusoidal Perturbation: Example 6.2

(a) Thermal Flux at Point A

Δt	t = T/4	t = T/2	t = 3T/4	t = T
T/4	(2.1%)* 0.96849	(3.7%) 0.87589	(3.1%) 0.86531	(4.9%) 1.0188
T/8	(1.1%) 0.95864	(0.8%) 0.85150	(1.2%) 0.88171	(1.2%) 1.0585
T/16	0.94971	0.84559	0.89122	1.0678
T/20	0.94805	0.84462	0.89323	1.0714
Order of convergence	1.83	2.5	1.9	1.9

*Relative errors with respect to thermal fluxes determined for $\Delta t = T/20$.

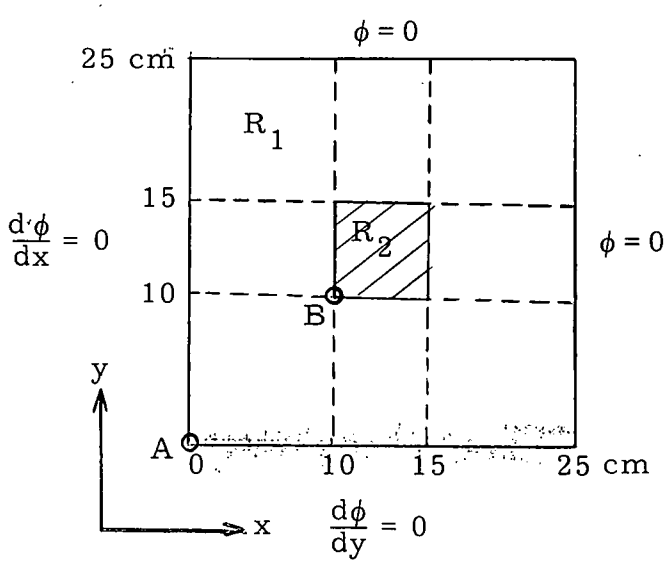

Fig. 6.2. Reactor Configuration for Example 6.2

Table 6.2 (concluded)

(b) Thermal Flux at Point B

Δt	t = T/4	t = T/2	t = 3T/4	t = T
T/4	(7.3%)* .59227	(5.0%) .50374	(3.4%) .64698	(3.7%) .76635
T/8	(0.4%) .55401	(0.9%) .52536	(2.1%) .66985	(1.2%) .74763
T/16	.55329	.52973	.68189	.73980
T/20	.55176	.53046	.68423	.73843
Order of convergence	2.4	2.6	2.0	2.2

*Relative errors with respect to thermal fluxes determined for $\Delta t = T/20$.

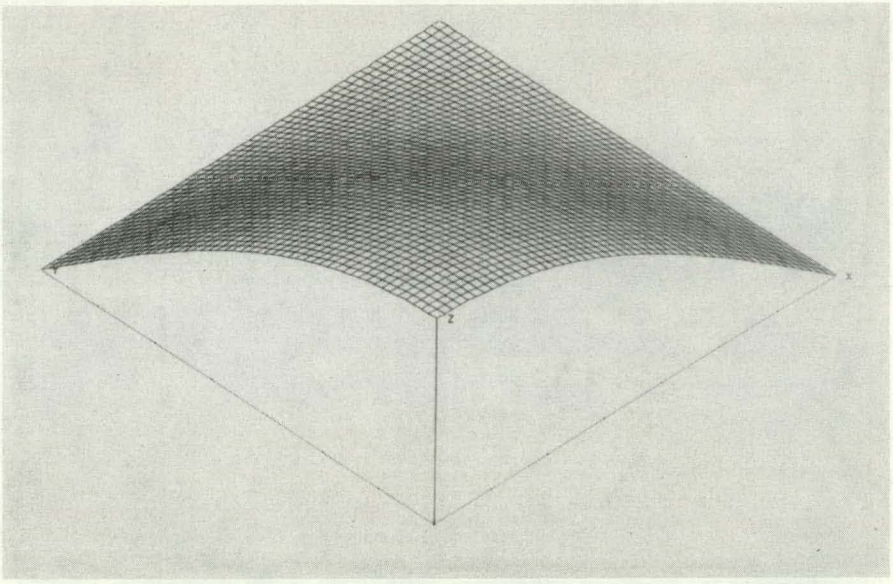

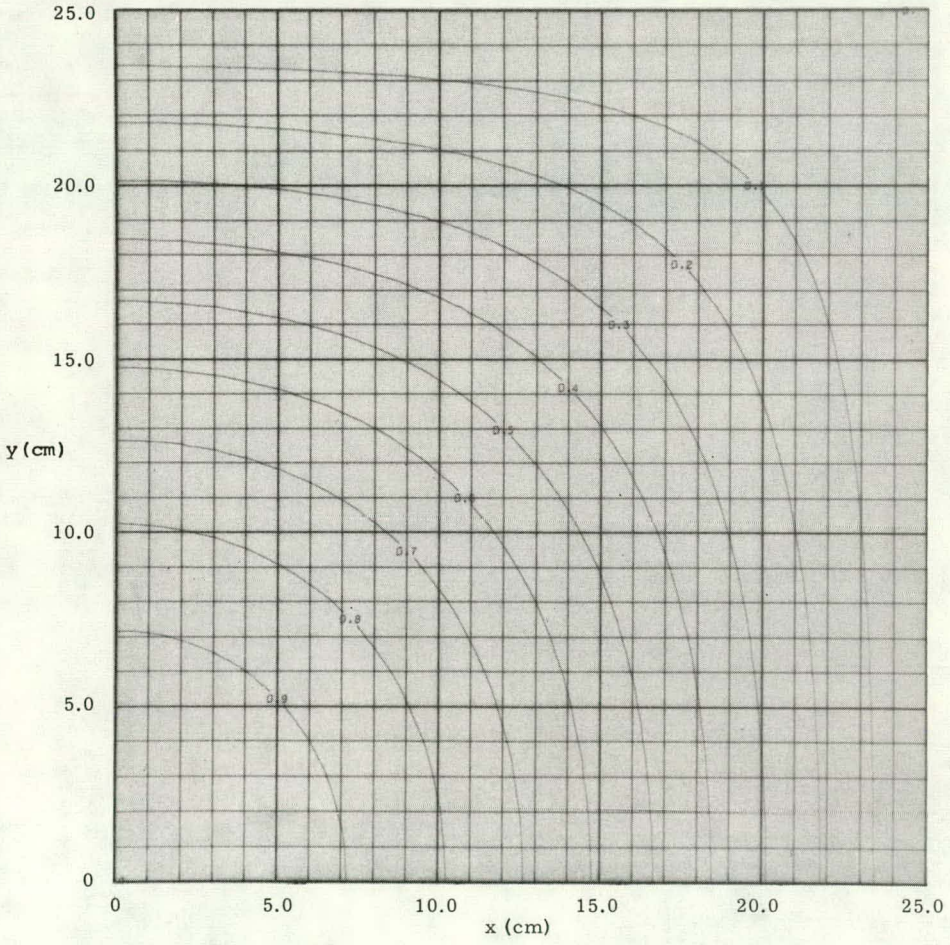

Fig. 6.3. Thermal Neutron Fluxes: Example 6.2. (a) t = 0.0

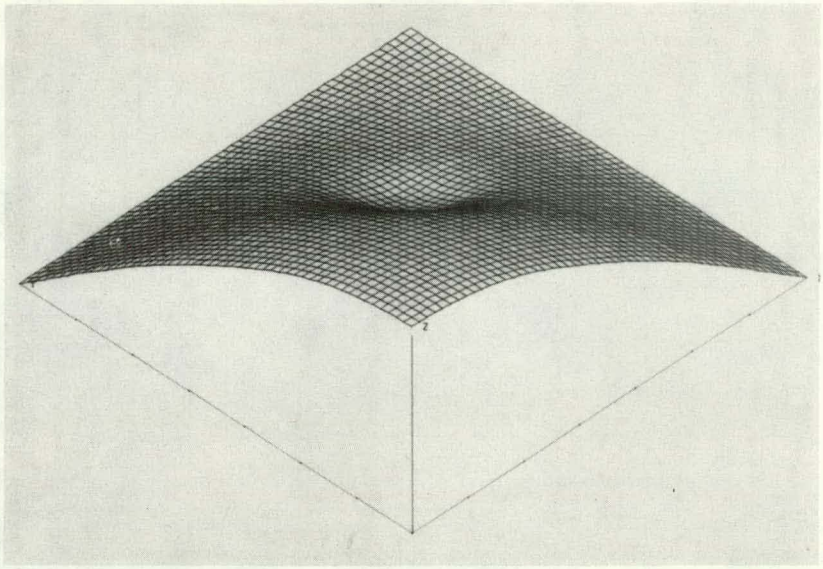

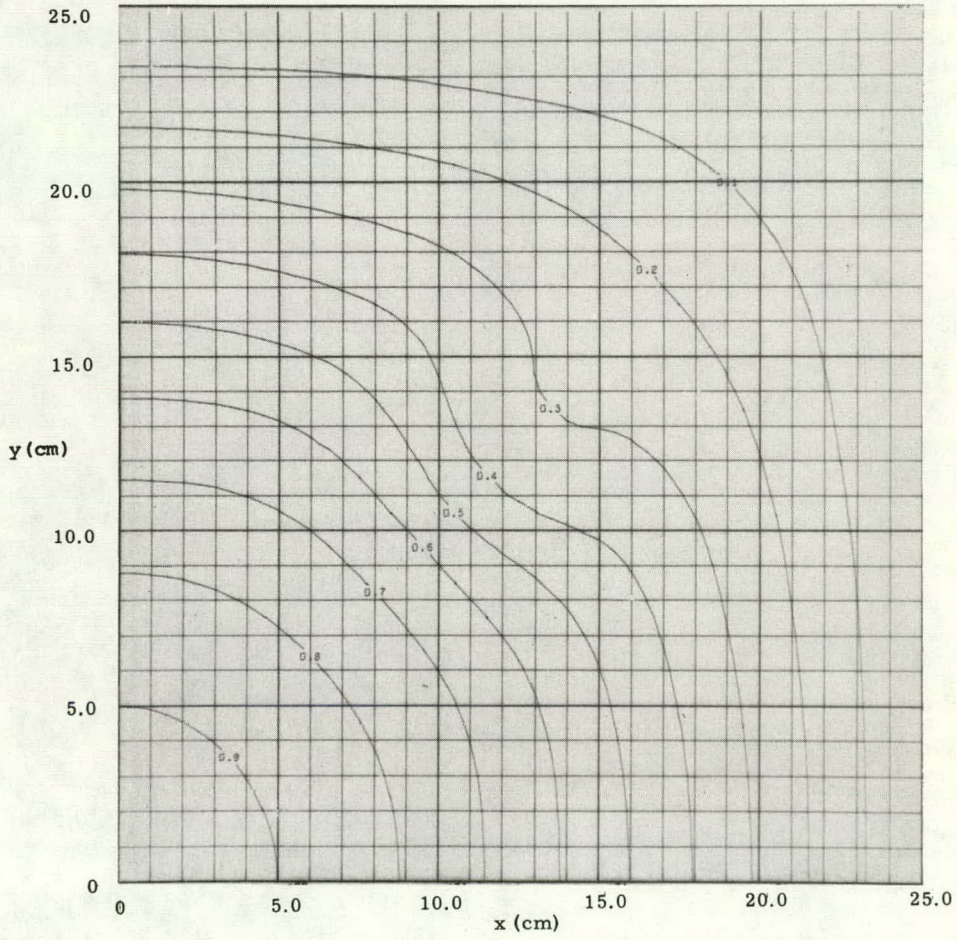
25.0
20.0
15.0
10.0
5.0
0
y (cm)
0
5.0
10.0
15.0
20.0
25.0
x (cm)
0.1
0.2
0.3
0.4
0.5
0.6
0.7
0.8
0.9

Fig. 6.3(b) $t = T/4$

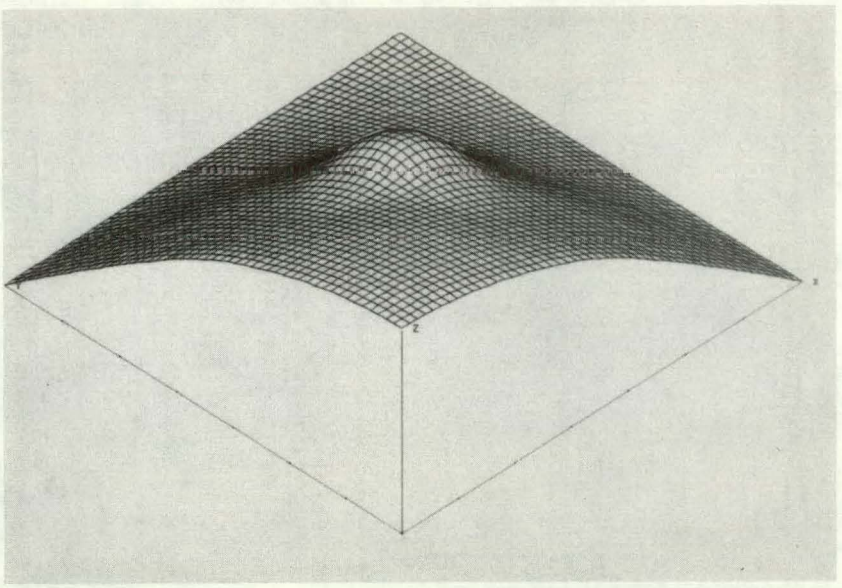

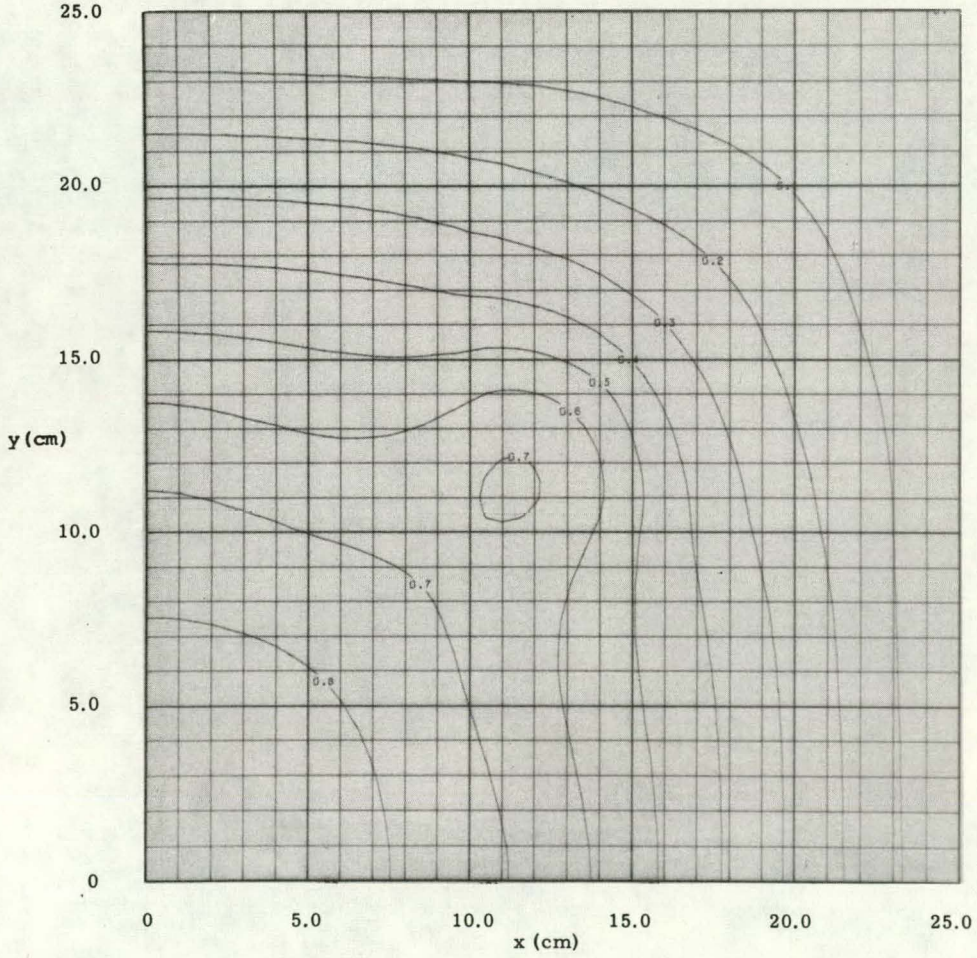
25.0
20.0
15.0
10.0
5.0
0
y (cm)
0
5.0
10.0
15.0
20.0
25.0
x (cm)
0.2
0.3
0.5
0.6
0.7
0.7
0.8

Fig. 6.3(c) $t = 3T/4$

Example 6.3. Local Sinusoidal Perturbation (2)

A symmetric perturbation was considered in Example 6.2. In this example, we consider asymmetric perturbations which are induced by two sinusoidal variations of cross sections in two subregions. The reactor consists of a uniform fuel (Fig. 6.4), whose two-group cross sections are given in Appendix C. There are six delayed groups in this example. The thermal absorption cross section in subregions R_2 and R_3 are assumed to vary from the critical values in the form

$$\Sigma_{a2}(\underline{r}, t) = \begin{cases} (\Sigma_{a2})_{crit} \left\{1 - 0.1 \sin \frac{2\pi}{T} t\right\}, & \underline{r} \in R_2, \\ (\Sigma_{a2})_{crit} \left\{1 + 0.1 \sin \frac{2\pi}{T} t\right\}, & \underline{r} \in R_3, \end{cases}$$

$$T = 10^{-3} \text{ sec.}$$

Two-group calculations were performed using HERMITE-2D. The reactor geometry was divided into 16 equal mesh elements as shown in Fig. 6.4. A total of 82 bicubic functions, defined by Eqs. (2.28) and (2.30), were then placed on the partition. For the time integration, the time step size $\Delta t = T/8$ was used. The critical thermal fission cross section was found to be 0.23766006.

Table 6.3 lists the computed thermal neutron fluxes at space points A, B and C for the first period of the perturbation. It is to be noted that the neutron flux after each period is not the same as the initial flux distribution due to the presence of local neutron diffusion. The thermal neutron fluxes are interpolated in each mesh element using mesh increments $\Delta x = \Delta y = 0.5$ cm and are also plotted in Fig. 6.5(a), (b), and (c) at $t = 0.0$, $T/4$ and $3T/4$, respectively. As in the previous example, the

figures demonstrate that the finite element method not only yields continuous approximations but also allows the use of coarse meshes in approximating local variations. The finite difference calculation using the same number of unknowns as the finite element calculation will require $9 \times 9 = 81$ mesh points on the space region. However, by using neutron fluxes at the 81 mesh points, it will be rather difficult to represent the locally peaked neutron flux distribution by a smooth surface. In fact, the flux distribution in Fig. 6.5 required the use of 60×60 interpolation points. Generally speaking, the finite difference scheme is expected to require finer mesh elements compared to the finite element method in representing the overall flux distribution.

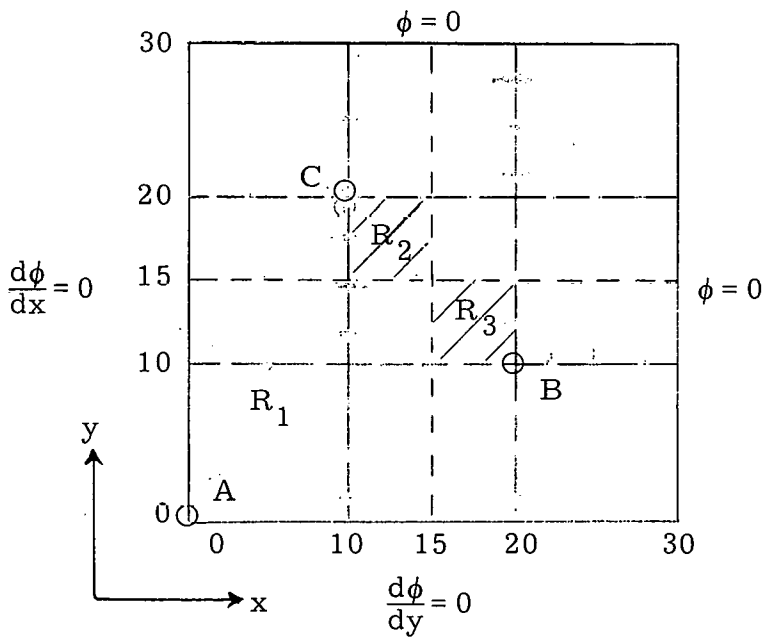

Fig. 6.4. Reactor Configuration for Example 6.3

Table 6.3. Thermal Neutron Fluxes: Example 6.3

t	$\phi_A(t)$	$\phi_B(t)$	$\phi_C(t)$
0.0	1.0000	0.43294	0.43294
T/8	1.0000	0.42492	0.44152
T/4	1.0016	0.40329	0.47167
3T/8	1.0061	0.40691	0.47747
T/2	1.0111	0.42380	0.45635
5T/8	1.0133	0.45048	0.42714
3T/4	1.0150	0.47743	0.40981
7T/8	1.0195	0.48352	0.41223
T	1.0245	0.46295	0.37714

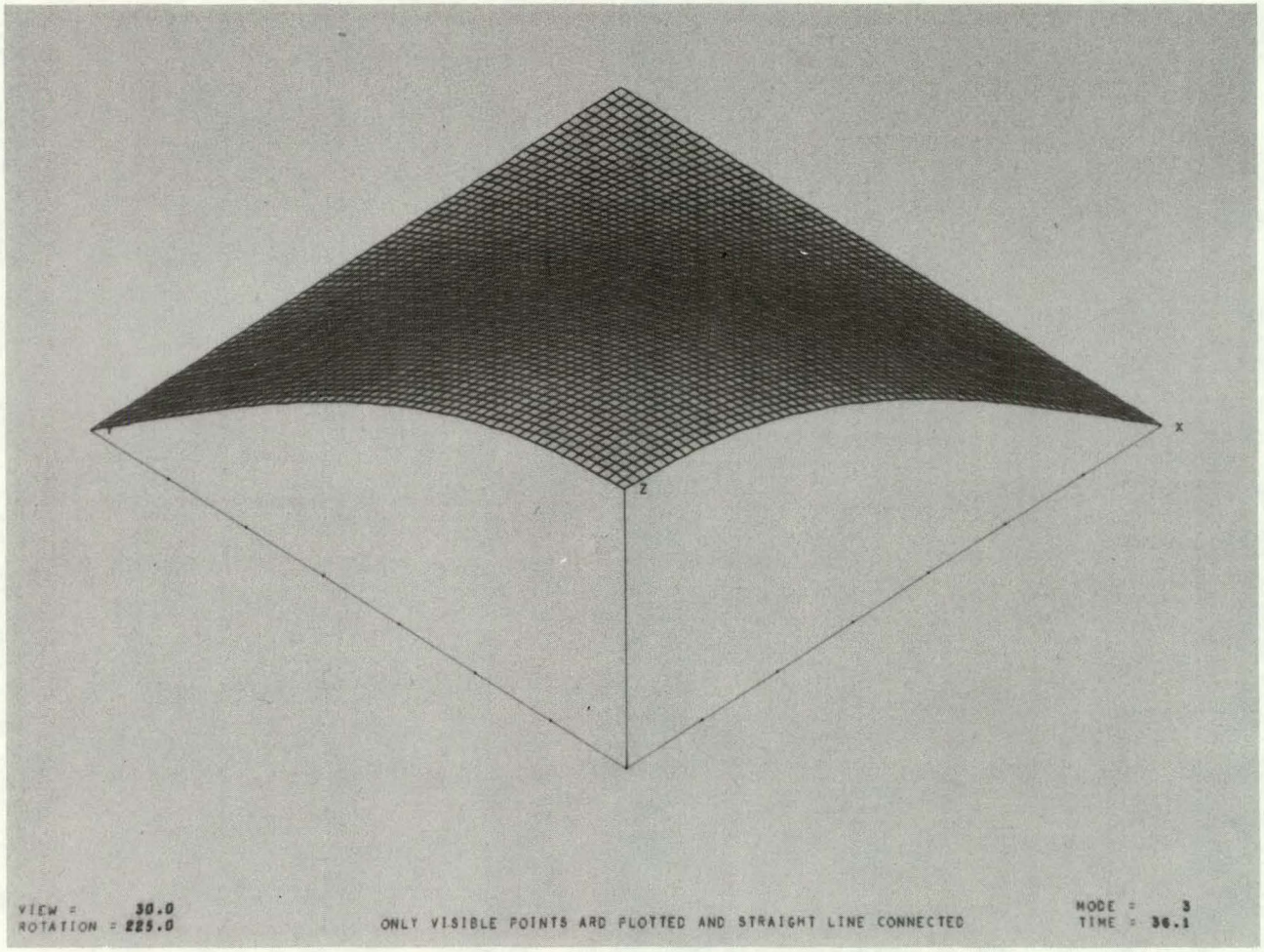

Fig. 6.5. Thermal Neutron Fluxes: Example 6.3
(a) t = 0.0

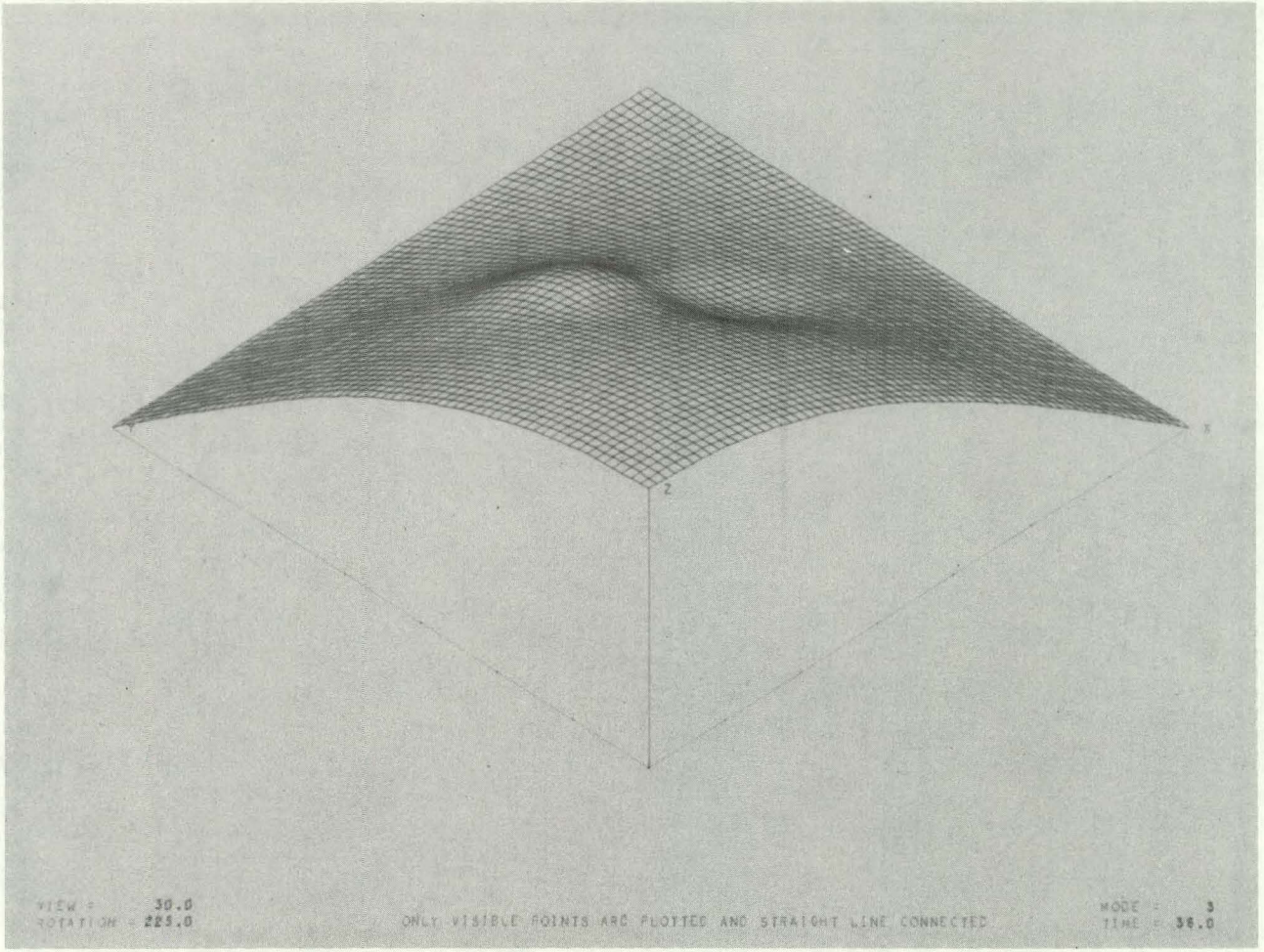
VIEW = 30.0
ROTATION = 225.0
ONLY VISIBLE POINTS ARE PLOTTED AND STRAIGHT LINE CONNECTED
MODE = 3
TIME = 36.0

Fig. 6.5(b) t = T/4

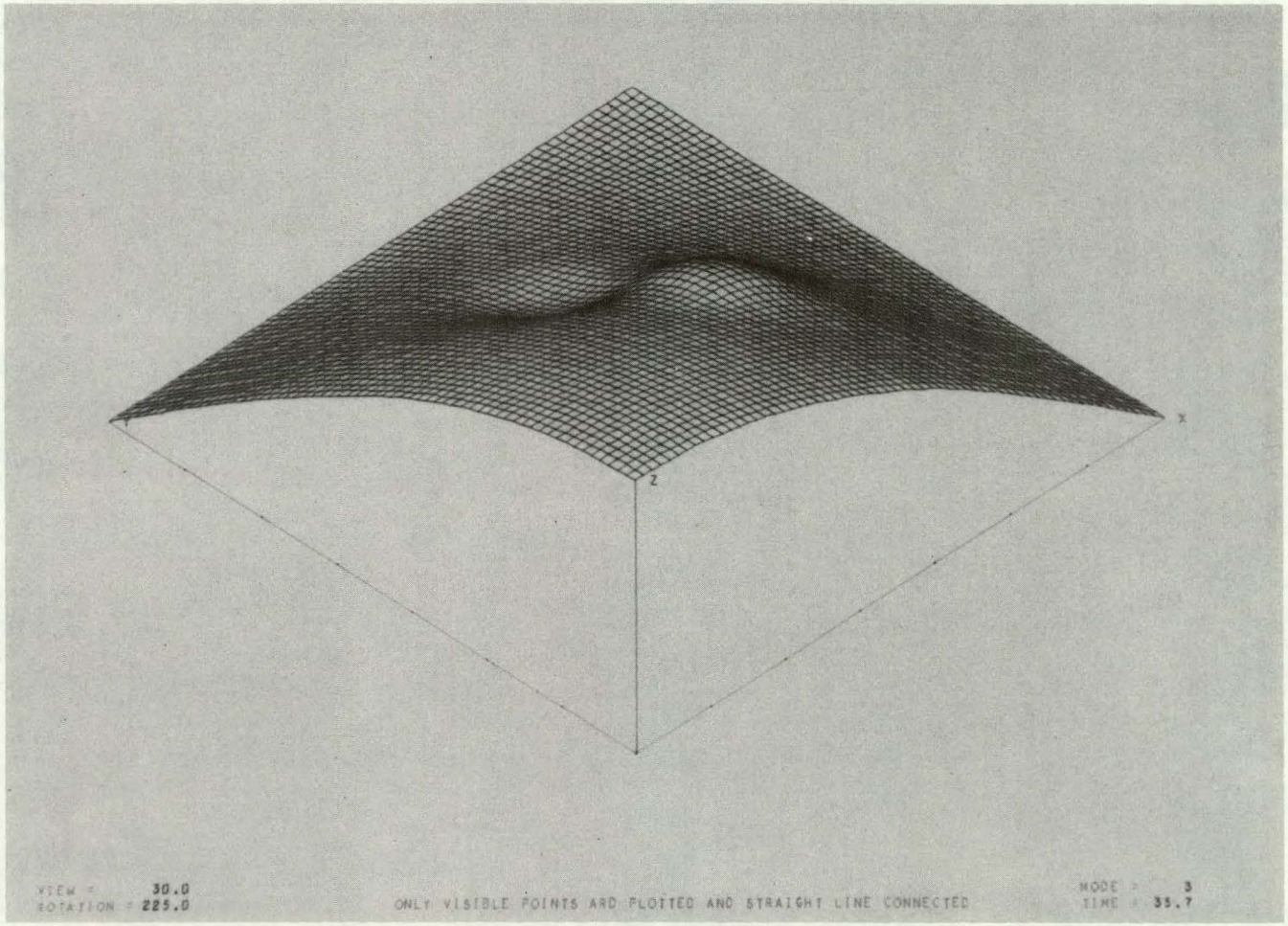
Y
Z
X
VIEW = 30.0
ROTATION = 225.0
ONLY VISIBLE POINTS ARE PLOTTED AND STRAIGHT LINE CONNECTED
MODE = 3
TIME = 35.7

Fig. 6.5(c) t = 3T/4

Chapter VII

CONCLUSIONS AND RECOMMENDATIONS

In this thesis, we have developed the finite element method for the neutron diffusion problems using piecewise polynomials in space, energy and time variables. The advantages of using piecewise polynomials are discussed in Chapter I. In addition, this method possesses the following properties:

(i) The finite element method allows direct approximations to the diffusion problem and requires no assumption on the separability of solutions with respect to independent variables.

(ii) This method yields high-order approximations with the order of accuracy depending upon the degree of the polynomials used.

(iii) This method treats problems in a continuum and it permits high accuracy for problems with variables coefficients. The approximate solution is a continuous function and it is possible to find function values at any point.

(iv) In view of properties (ii) and (iii), the method allows one to use coarse meshes or large mesh elements in space, energy and time variables compared to the finite difference scheme.

The finite element method using low degree polynomials are shown to lead to various types of conventional numerical methods. However, the method developed in this thesis generalizes the existing methods in the sense that it retains high accuracy for problems with variable

coefficients. Furthermore, the method suggests means for numerical approximations for higher accuracies. Table 7.1 summarizes the orders of accuracies of the finite element method when applied to the neutron diffusion problems in energy, space and time variables. Also, in the table, the finite element methods are compared with the existing numerical methods. For example, the finite element method using piecewise constant functions in energy variable reduces the energy-dependent diffusion equations to the conventional multigroup equations (cf., Chaps. III, IV, VI). It is also shown that the 3-point finite difference formula for the differential operator d^2/dx^2 can be obtained by the finite element method using piecewise linear functions in space variable (cf., Chap.IV). Furthermore, the Hermite method applied to the first-order ordinary differential equations gives the Padé formulae for e^{At} when A is constant (cf., Chap. V).

The orders of convergence of the finite element methods are checked in numerical examples in Chapters IV, V and VI. For example, these are numerically checked for multigroup diffusion problems with piecewise constant cross sections in one- and two-dimensional spaces and for kinetics problems with variable coefficients. Thus far, the method has been limited to applications in linear problems. We have considered only regular partitions which are generated by orthogonal coordinate surfaces. Numerical calculations which are not presented in this thesis and remain for further study are as follows:

(i) Neutron spectrum calculations using piecewise linear or cubic polynomials.

Table 7.1

The Finite Element Method Applied to Neutron Diffusion Problems

H_m	Energy (E)	Space (r) †	Time (t)
m = 1/2 (const.)	$O(\Delta E^1)$ Multigroup method	$O(\Delta r^1)$	$O(\Delta t^1)$
m = 1 (linear)	$O(\Delta E^2)$	$O(\Delta r^2)$* 3-pt. formula for d^2/dx^2	$O(\Delta t^2)$* Crank-Nicolson Padé (1, 1)
m = 2 (cubic)	$O(\Delta E^4)$	$O(\Delta r^4)$*	$O(\Delta t^4)$* Padé (2, 2)
Remarks	Chaps. III, IV, VI	Chaps. IV, VI *Numerical examples available †No singularity	Chaps. V, VI Order of conv. for Padé formulae applies only for constant coefficients. *Numerical examples

(ii) Few group calculations for multidimensional problems using piecewise polynomial basis functions in space and energy as discussed in Example 2.2, Chapter II.

(iii) Neutron diffusion problems with variable cross sections. One can use basis functions defined in Example 2.3, Chapter II. The calculation using coarse meshes will be very useful in studying the fuel depletion in multidimensional reactors.

(iv) Calculations for two- or three-dimensional problems in spherical or cylindrical geometries.

The finite element methods developed in this thesis can further be extended to the following problems:

(i) Transport equations:

$$\Omega \cdot \nabla\phi(\underline{r}, \Omega) + \Sigma_T \phi(\underline{r}, \Omega) = \int \Sigma(\underline{r}, \Omega', \Omega)\phi(\underline{r}, \Omega')\, d\Omega' + q(\underline{r}, \Omega)$$

Expand the approximate solution as

$$\hat{\phi}(\underline{r}, \Omega) = \sum_{i=1}^{I} \sum_{j=1}^{J} a_{ij}\, u_i(\underline{r})\, u_j(\Omega)$$

where $u_i(r)$ and $u_j(\Omega)$ are polynomial basis functions defined in Chapter II. The expansion coefficients a_{ij} are then determined by the Galerkin scheme.

(ii) Coarse mesh calculations which account for the geometric and energetic fine structures.

(iii) Applications to nonlinear problems.

The areas which require further investigations are:

(i) Finite element methods which use other types of partitions such as triangular elements or combinations of these elements.

(ii) Development of efficient numerical techniques for the inversion of large-order matrices which are obtained by the finite element method.

(iii) Investigation of the condition number of the stiffness matrices for the neutron diffusion problems resulting in the application of finite element methods.

(iv) High-order approximation schemes which incorporate the singular functions in numerical processes.

BIBLIOGRAPHY

1. S. Kaplan, O.J. Marlowe and J. Bewick, "Application of Synthesis Techniques to Problems Involving Time Dependence," Nucl. Sci. Eng. 18, 163 (1964).

2. S. Kaplan, "Synthesis Methods in Reactor Analysis," in Advances in Nuclear Science and Technology, Vol. III, P.R. Greebler, Ed., Academic Press, New York (1966).

3. W.M. Stacey, Jr., Modal Approximations: Theory and an Application to Reactor Physics, M.I.T. Press, Cambridge, Massachusetts (1967).

4. R. Avery, "Theory of Coupled Reactors," Proc. Intern. Conf. Peaceful Uses At. Energy, 2nd, Geneva 12, 182 (1958).

5. D.L. Delp, "FLARE-A Three-Dimensional Boiling Water Reactor Simulator," GEAP-5498, General Electric Co. (1964).

6. J.W. Riese, "VARI-QUIR: A Two-Dimensional Time-Dependent Multigroup Diffusion Code," USAEC Report WANL-TNR-133, Westinghouse Astronuclear Laboratory (1963).

7. K.F. Hansen and S.R. Johnson, "An Approximate Method for Multidimensional Diffusion Theory Problem," USAEC Report GA-7544, General Atomic (1967).

8. G. Fix and G. Strang, "Fourier Analysis of the Finite Element Method in Ritz-Galerkin Theory," Studies in Applied Math. 48, 265-273 (1969).

9. G. Strang, "The Finite Element Method and Approximation Theory," Numerical Solution of Partial Differential Equations-II, SYNSPADE 1970, Ed. B. Hubbard, pp. 547-583, Academic Press, New York (1971).

10. M. Zlamal, "On the Finite Element Method," Numer. Math. 12, 394-409 (1968).

11. I. Babuska, "The Finite Element Method for Elliptic Differential Equations," Numerical Solution of Partial Differential Equations-II, SYNSPADE 1970, Ed. B. Hubbard, pp. 69-106, Academic Press, New York (1971).

12. R. Courant, "Variational Methods for the Solution of Problems of Equilibrium and Vibrations," Bull. Amer. Math. Soc. 49, 1-23 (1943).

13. M. Rose, "Finite Difference Schemes for Differential Equations," Math. of Comp. 18, 179-195 (1964).

14. R.S. Varga, "Hermite Interpolation-Type Ritz Methods for Two-Point Boundary Value Problems," Numerical Solution of Partial Differential Equations, Ed. J.H. Bramble, pp. 365-373, Academic Press, New York (1966).

15. G. Birkhoff, C. de Boor, B. Swartz and B. Wendroff, "Rayleigh-Ritz Approximation by Piecewise Cubic Polynomials," SIAM J. Numer. Anal. 3, 188-203 (1966).

16. P.G. Ciarlet, M.H. Schultz, and R.S. Varga, "Numerical Methods of High-Order Accuracy for Nonlinear Boundary Value Problems I, One Dimensional Problem," Numer. Math. 9, 394-430 (1967); also see III, Numer. Math. 12, 120-133 (1968), V, Numer. Math. 13, 51-77 (1969).

17. G. Birkhoff, M.H. Schultz and R.S. Varga, "Piecewise Hermite Interpolation in One and Two Variables with Applications to Partial Differential Equations," Num. Math. 11, 232-256 (1968).

18. G. Fix, "Higher Order Rayleigh-Ritz Approximation," J. Math. Mech. 18, 645-658 (1969). Also, Ph.D. Thesis, Harvard University (1968).

19. M.H. Schultz, "Multivariate Spline Functions and Elliptic Problems," Approximation with Special Emphasis on Spline Functions, Ed., I.J. Schoenberg, pp. 279-347, Academic Press, New York (1969).

20. I. Babuska, "Approximation by Hill Functions," Technical Note BN-648, Institute for Fluid Dynamics and Applied Mathematics, University of Maryland (1970).

21. G.I. Wakoff, "Piecewise Polynomial Spaces and Their Use with Rayleigh-Ritz-Galerkin Method," Ph.D. Thesis, Harvard University (1970).

22. B. Davison, Neutron Transport Theory, Oxford University Press (Clarendon), London (1958).

23. S. Glasstone and M.C. Edlund, Nuclear Reactor Theory, Van Nostrand, Princeton, N.J. (1952).

24. A.M. Weinberg and E.P. Wigner, The Physical Theory of Neutron Chain Reactors, University of Chicago Press, Chicago (1958).

25. L. Collatz, Functional Analysis and Numerical Mathematics, Academic Press, New York (1966).

26. G. Birkhoff, "Angular Singularities of Piecewise Helmholtz Equations," N.S.F. Regional Research Conf. on Num. Sol. of Elliptic Diff. Eqs. at Rolla, Mo., Sept. 8-12, 1969.

27. R.B. Kellog, "Singularities in Interface Problems," Numerical Solution of Partial Differential Equations - II, SYNSPADE 1970, Ed., B. Hubbard, pp. 351-400, Academic Press, New York (1971).

28. O.C. Zienkiewicz, The Finite Element Method in Structural and Continuum Mechanics, McGraw-Hill, London (1967).

29. C.A. Felippa and R.W. Clough, "The Finite Element Method in Solid Mechanics," Numerical Solution of Field Problems in Continuum Physics, Ed., G. Birkhoff, pp. 74-94, Am. Math. Soc., Providence (1970).

30. B. Swartz and B. Wendroff, "Generalized Finite-Difference Schemes," Math. of Comp. 23, 37-50 (1969).

31. H.S. Price, R.S. Varga, "Error Bounds for Semidiscrete Galerkin Approximations of Parabolic Problems with Applications to Petroleum Reservoir Mechanics," Numerical Solution of Field Problems in Continuum Physics, Ed., G. Birkhoff, pp. 74-94, Am. Math. Soc., Providence (1970).

32. G. Fix and N. Nassif, "On Finite Element Approximations to Time-Dependent Problems," To appear in Numer. Math.

33. L.V. Kantrovich and V.I. Krylov, Approximate Methods of Higher Analysis, Interscience Publishers, New York (1964).

34. S.G. Mikhlin, Variational Methods in Mathematical Physics, MacMillan, New York (1964).

35. G. Forsythe and C.B. Moler, Computer Solution of Linear Algebraic Systems, Prentice-Hall, Englewood Cliffs, N.J. (1967).

36. I.J. Schoenberg, "Contribution to the Problem of Approximation of Equidistant Data by Analytic Functions, Parts A and B," Quart. Appl. Math. 4, 45-99, 112-141 (1946).

37. P.J. Davis, Interpolation and Approximation, Blaisdell Publ. Co., New York (1963).

38. G. Strang and G. Fix, An Analysis of the Finite Element Method, Prentice-Hall. To appear.

39. J.H. Wilkinson, The Algebraic Eigenvalue Problem, Oxford University Press, London (1965).

40. R.S. Varga, Matrix Iterative Analysis, Prentice-Hall, Englewood Cliffs, N.J. (1962).

41. K. Yosida, Functional Analysis, Springer, Berlin (1968).

42. S. Agmon, Lectures on Elliptic Boundary Value Problems, Van Nostrand, Princeton, N.J. (1965).

43. M. Clark and K.F. Hansen, Numerical Methods of Reactor Analysis, Academic Press, New York (1964).

44. E.L. Wachspress, Iterative Solution of Elliptic Systems, Prentice-Hall, Englewood Cliffs, N.J. (1966).

45. G. Bilodeau and L. Hageman, "A Survey of Numerical Methods in the Solution of Diffusion Problems," WAPD-TM-64, July, 1957.

46. H.S. Wall, Analytic Theory of Continued Fractions, Van Nostrand, Princeton, N.J. (1948).

47. R.O. Brittan, "Some Problems in the Safety of Fast Reactors," ANL-5577 (1955).

48. J.J. Kaganove, "Numerical Solution of the One-Group, Space Independent Reactor Kinetics Equations for Neutron Density Given the Excess Reactivity," ANL-6132 (1960).

49. F.R. Loscalzo, "An Introduction to the Application of Spline Functions to Initial Value Problems," Theory and Application of Spline Functions, Ed., T.N.E. Greville, pp. 37-64, Academic Press, New York (1969).

50. R.S. Varga, "Error Bounds for Spline Interpolation," Approximations with Special Emphasis on Spline Functions, Ed., I.J. Schoenberg, Academic Press, New York (1969).

51. N. Nassif, "Finite Element Approximation to Parabolic Partial Differential Equations," Ph.D. Thesis, Harvard University. To be presented.

52. A.F. Henry, Naval Reactor Physics Handbook, Ed., A. Radkowsky, Vol. I, Sec. 5.2, TID-7030, USAEC, Washington, D.C. (1964).

53. E.P. Gyftopoulos, "General Reactor Dynamics," The Technology of Nuclear Reactor Safety, Ed., T.J. Thompson and J.G. Beckerly, Vol. I, Chap. 3, M.I.T. Press, Cambridge, Massachusetts (1964).

54. J. Descloux, "Stability Properties of Finite Elements," To appear in Numer. Math.

Appendix A

PROOF OF THEOREMS

A.1 Preliminaries

In the previous chapters, we defined the inner products in the energy domain $\mathcal{E}$ and the space domain Ω as

$$(u, v)_{\mathcal{E}} = \int_{\mathcal{E}} uv \, dE ,$$

$$(u, v)_{\Omega} = \int_{\Omega} uv \, dV ,$$

$$(u, v) = \int_{\mathcal{E}} \int_{\Omega} uv \, dV \, dE ,$$

and the corresponding L^2-norms

$$\| u \|_{L^2(\mathcal{E})} = (u, v)_{\mathcal{E}}^{\frac{1}{2}} ,$$

$$\| u \|_{L^2(\Omega \times \mathcal{E})} = (u, v)^{\frac{1}{2}} .$$

In addition, the L^∞-norm is defined by

$$\| u \|_{L^\infty(\Omega)} = \max_{\Omega} | u(x) | .$$

We also denote the vector and matrix norms by $[\,]$ $[\,]$. In particular, the maximum norm for a vector $x = \mathrm{col}\{ x_1, x_2, \ldots, x_N \}$ and a matrix $A = \{ a_{ij} \}$ are defined by

$$[\underline{x}]_\infty = \max_{1 \le i \le N} | x_i | ,$$

$$[A]_\infty = \max_{1 \le i \le N} \sum_{j=1}^{N} | a_{ij} | .$$

We shall frequently need the following inequalities [25] in our proofs:

Triangle inequality,

$$\|u+v\| \leq \|u\| + \|v\| ,$$

Schwarz inequality,

$$|(u, v)| \leq \|u\| \ \|v\| .$$

A.2 Theorem 2.3

Assume that $f(\underline{r}) \in C^{t}(\pi_{\ell})$. Let $s(\underline{r})$ be a multivariate polynomial of degree 2m-1 satisfying Eq. (2.19). Then, $s(\underline{r})$ is uniquely determined and satisfies

$$\left\| \frac{\partial^{q}}{\partial \underline{r}^{q}} (f(\underline{r})-s(\underline{r})) \right\|_{L^{\infty}(\pi_{\ell})} \leq K_1 \Delta r_1^{\mu_1 - q_1} + \ldots + K_n \Delta r_n^{\mu_n - q_n} ,$$

$$0 \leq q \leq m-1 ,$$

where

$$q = (q_1, q_2, \ldots, q_n) ,$$

$$\mu_j = \min(2m_j, t_j) ,$$

$$\Delta r_j = r_{j, i_j+1} - r_{j, i_j} .$$

Proof. The multivariate Hermite interpolate in the element π_{ℓ} can be constructed by repeated applications of univariate Hermite interpolations for each independent variable as shall be demonstrated in the proof of this theorem. Theorem A states the uniqueness of the univariate interpolations and thus the resulting interpolation in multivariables is also unique.

The proof of the error estimation is by induction.

(i) Suppose $n=1$. Let $\tilde{f}(r_1)$ be the Hermite interpolate to $f(r_1)$ in the space $H_{m_1}(\pi_1)$. Then, from Theorem A,

$$\left\| \frac{d^{q_1}}{dr^{q_1}} (f(r_1) - \tilde{f}(r_1)) \right\|_{L^\infty(\pi_1)} \leq K \Delta r_1^{\mu_1 - q_1} . \tag{A.2.1}$$

(ii) Suppose $n=n'$ for arbitrary n'. Let $\tilde{f}(\underline{r}')$ be the Hermite interpolate to $f(\underline{r}')$ in $H_{m'}(\pi_{n'})$ where $\underline{r}' = (r_1, r_2, \ldots, r_{n'})$ and $m' = (m_1, m_2, \ldots, m_{n'})$. Assume that

$$\left\| \frac{d^{q'}}{d\underline{r}^{q'}} (f(\underline{r}') - \tilde{f}(\underline{r}')) \right\|_{L^\infty(\pi)} \leq K_1 \Delta r_1^{\mu_1 - q_1} + \ldots + K_{n'} \Delta r_{n'}^{\mu_{n'} - q_{n'}} . \tag{A.2.2}$$

(iii) Suppose $n=n'+1$. Let $\tilde{f}(\underline{r})$ be the Hermite interpolate to $f(\underline{r})$ in $H_n(\pi_n)$ where $\underline{r} = (r_1, r_2, \ldots, r_n) = (\underline{r}', r_n)$ and $m = (m_1, m_2, \ldots, m_n)$. We also introduce the univariate Hermite interpolate $\tilde{\tilde{f}}(r_n; \underline{r}')$ to $f(\underline{r})$ in $H_{m_n}(\pi_n)$ such that

$$\begin{aligned} \tilde{\tilde{f}}^{(q)}(r_{n, i_n}; \underline{r}') &= f^{(q)}(\underline{r}', r_{n, i_n}) , \\ \tilde{\tilde{f}}^{(q)}(r_{n, i_n+1}; \underline{r}') &= f^{(q)}(\underline{r}', r_{n, i_n+1}) , \quad 0 \leq q \leq m-1 . \end{aligned} \tag{A.2.3}$$

Theorem A implies that $\tilde{\tilde{f}}(r_n; \underline{r}')$ satisfies

$$\left\| \frac{d^q}{dr_n^q} (f(\underline{r}) - \tilde{\tilde{f}}(r_n; \underline{r}')) \right\|_{L^\infty(\pi)} \leq K \Delta r_n^{\mu_n - q_n} . \tag{A.2.4}$$

Furthermore, from the assumptions (A.2.2) and Eq. (A.2.3),

$$\max\left\{\left\|\frac{d^q}{d\underline{r}^q}\left(\tilde{f}(\underline{r})-\tilde{\tilde{f}}(r_n;\underline{r}')\right)\Big|_{r_n,\,i_n}\right\|_{L^\infty(\pi)},\ \left\|\frac{d^q}{d\underline{r}^q}\left(\tilde{f}(\underline{r})-\tilde{\tilde{f}}(r_n;\underline{r}')\right)\Big|_{r_n,\,i_n+1}\right\|_{L^\infty(\pi)}\right\}$$

$$\leq K_1\Delta r_1^{\mu_1-q_1}+\ldots+K_{n'}\Delta r_{n'}^{\mu_{n'}-q_{n'}}.$$

Since $\frac{d^{q'}}{d\underline{r}^{q'}}\left(\tilde{f}(\underline{r})-\tilde{\tilde{f}}(r_n;\underline{r}')\right)$ is a polynomial of degree $2m_n-1$ in r_n, this can be represented by

$$\frac{d^{q'}}{d\underline{r}^{q'}}\left(\tilde{f}(\underline{r})-\tilde{\tilde{f}}(r_n;\underline{r}')\right)=\sum_{p=0}^{m-1}\left\{a_{i_n}^p u_{i_n}^{p+}(r_n)+a_{i_n+1}^p u_{i_n+1}^{p-}(r_n)\right\}$$

$$\leq\sum_{p=0}^{m-1}\left\{K_1\Delta r_1^{\mu_1-q_1}+\ldots+K_{n'}\Delta r_{n'}^{\mu_{n'}-q_{n'}}\right\}\Delta r_n^{2m_n-p}\left[u_{i_n}^{p+}(r_n)-u_{i_n+1}^{p-}(r_n)\right]$$

where the factors Δr_n^{2m-p} are introduced as normalization factors to $u_{i_n}^{p+}(r_n)$ and $u_{i_n+1}^{p-}(r_n)$ in order that the error bounds on the right-hand side have correct dimensions. Note that

$$\left|u_{i_n}^{p\pm}(r_n)\right|\leq K_p\Delta r_n^p$$

and so

$$\left|\frac{d^q}{dr^q}u_{i_n}^{p\pm}(r_n)\right|\leq K_p\Delta r_n^{p-q}.$$

Thus,

$$\left\|\frac{d^q}{d\underline{r}^q}\left(\tilde{f}-\tilde{\tilde{f}}\right)\right\|_{L^\infty(\pi)}\leq\sum_{p=0}^{m-1}\left\{K_1\Delta r_1^{\mu_1-q_1}+\ldots+K_{n'}\Delta r_{n'}^{\mu_{n'}-q_{n'}}\right\}\Delta r_n^{2m-p+p-q_n}$$

$$=\sum_{p=0}^{m-1}\left\{K_1\Delta r_1^{\mu_1-q_1}+\ldots+K_{n'}\Delta r_{n'}^{\mu_{n'}-q_{n'}}\right\}\Delta r_n^{2m-q_n}.$$

(A.2.5)

Therefore, applying the triangle inequality and using the inequalities (A.2.4) and (A.2.5), we obtain

$$\left\| \frac{d^q}{dr^q} (f-\tilde{f}) \right\|_{L^\infty(\pi)} \leq \left\| \frac{d^q}{dr^q} (f-\tilde{\tilde{f}}) \right\|_{L^\infty(\pi)} + \left\| \frac{d^q}{dr^q} (\tilde{\tilde{f}}-\tilde{f}) \right\|_{L^\infty(\pi)}$$

$$\leq K_1 \Delta r_1^{\mu_1 - q_1} + \ldots + K_n \Delta r_n^{\mu_n - q_n} . \qquad \text{(A.2.6)}$$

We have shown that for $n = n' + 1$ the error bound (A.2.6) holds. Thus, as a consequence of the steps (i), (ii) and (iii), we conclude that (A.2.6) holds for any n. This completes the proof.

A.3 Theorem 3.1

Assume that the inequality (3.4) holds. Let $\phi(E)$ be the solution to Eq. (3.3) and $\phi(E) \in C^t(\mathcal{E})$. If $\hat{\phi}(E)$ is the solution to Eq. (3.7) in the space $H_m(\pi(\mathcal{E}))$, then $\hat{\phi}(E)$ satisfies

$$\| \phi - \hat{\phi} \|_{L^\infty(\mathcal{E})} \leq K \overline{\Delta E}^{\mu}$$

where $\mu = \min(2m, t)$, $\overline{\Delta E} = \max_i |E_{i+1} - E_i|$ and K is a constant independent of $\overline{\Delta E}$.

Proof. ϕ and $\hat{\phi}$ satisfy

$$(T\phi, v)_{\mathcal{E}} = (Q, v)_{\mathcal{E}} ,$$

$$(T\hat{\phi}, v)_{\mathcal{E}} = (Q, v)_{\mathcal{E}} ,$$

for all $v = u_g(E)$, $1 \leq g \leq G$. The difference of the two equations is given by

$$(T(\phi - \hat{\phi}), v)_{\mathcal{E}} = 0 . \qquad \text{(A.3.1)}$$

Let $\tilde{\phi}$ be the Hermite interpolate of ϕ in the space of $H_m(\pi(\mathcal{E}))$ (cf., Sec. 2.1, Chap. II). Then Eq. (A.3.1) can be represented as

$$(T(\hat{\phi}-\tilde{\phi}), v)_{\mathcal{E}} = (T(\phi-\tilde{\phi}), v)_{\mathcal{E}} . \tag{A.3.2}$$

Theorem 2.1 implies that

$$\| \phi - \tilde{\phi} \|_{L^\infty} = K\overline{\Delta E}^{\mu} . \tag{A.3.3}$$

Then we can show easily that

$$(T(\phi - \tilde{\phi}), u_g)_{\mathcal{E}} \leq (T(K\overline{\Delta E}^{\mu}), u_g)_{\mathcal{E}}$$

$$\leq K_g \overline{\Delta E}^{\mu} , \qquad 1 \leq g \leq G ,$$

where $K_g = (TK, u_g)_{\mathcal{E}}$.

Let $e(E) = \hat{\phi}(E) - \tilde{\phi}(E)$. Since $\hat{\phi} - \tilde{\phi}$ is a polynomial of degree $2m_E-1$, we may represent $e(E)$ as

$$e(E) = \sum_{g=1}^{G} e_g u_g(E) .$$

Then Eq. (A.3.2) becomes

$$B\,\underline{e} \leq \underline{K}\overline{\Delta E}^{\mu}$$

where

$$B = L - S - \frac{1}{\lambda} F ,$$

$$\underline{K} = \mathrm{col}\{K_1, K_2, \ldots, K_G\} ,$$

$$\underline{e} = \mathrm{col}\{e_1, e_2, \ldots, e_G\} .$$

Other matrices are defined in Eq. (3.8) in Chapter III. Then,

$$\underline{e} \leq B^{-1}\underline{K}\overline{\Delta E}^{\mu}$$

and thus

$$\|\underline{e}\|_\infty \leq \|B^{-1}\|_\infty \|\underline{K}\|_\infty \overline{\Delta E}^{\mu} .$$

$\|K\|_\infty$ is a constant and thus it remains to prove that $\|B^{-1}\|_\infty$ is bounded. Descloux [54] considered bounds of the stiffness matrix and its inverse for a wide class of problems in the finite element methods. We appeal to the work of Descloux to assert that there is a constant γ such that

$$\|B^{-1}\|_\infty \leq \gamma.$$

Hence,

$$\begin{aligned} \|\tilde{\phi} - \hat{\phi}\|_{L^\infty} &\leq \max_{\mathcal{E}} |e(E)| \leq K\|\underline{e}\|_\infty \\ &\leq K\overline{\Delta E}^{\mu} . \end{aligned} \tag{A.3.4}$$

Therefore, applying the triangle inequality and the inequalities (A.3.3) and (A.3.4), we obtain

$$\begin{aligned} \|\phi - \hat{\phi}\|_{L^\infty} &\leq \|\phi - \tilde{\phi}\|_{L^2} + \|\tilde{\phi} - \hat{\phi}\|_{L^2} \\ &\leq K\overline{\Delta E}^{\mu} . \end{aligned}$$

This completes the proof.

A.4 Theorem 4.1

Assume that the inequality (4.3a) holds. Let $\phi(\underline{r}, E)$ be the solution of Eq. (4.2) and $\phi \in C_p^t(\pi_{\mathcal{E}} \times \pi_\Omega)$ where $t = (t_r, t_E)$ and $m = (m_r, m_E)$. If $\hat{\phi}(\underline{r}, E)$ is the solution of Eq. (4.5) in the space $H_m(\pi_{\mathcal{E}} \times \pi_\Omega)$, then $\hat{\phi}(\underline{r}, E)$ satisfies

$$\|\phi - \hat{\phi}\|_{L^\infty} \leq K_1 \overline{\Delta r}^{\mu_r} + K_2 \overline{\Delta E}^{\mu_E}$$

where $\mu_r = \min(2m_r, t_r)$, $\mu_E = \min(2m_E, t_E)$, $\overline{\Delta r} = \max_{\pi_\Omega} \Delta r$, $\overline{\Delta E} = \max_{\pi_\mathcal{E}} \Delta E$ and K_1 and K_2 are constants independent of $\overline{\Delta r}$ and $\overline{\Delta E}$, respectively.

Proof. ϕ and $\hat{\phi}$ satisfy

$$a(\phi, v) = (Q, v) ,$$

$$a(\hat{\phi}, v) = (Q, v) ,$$

for all $v = u_i(\underline{r}, D)\, u_g(E)$, $1 \leq i \leq N$, $1 \leq g \leq G$. The difference of the two equations is given by

$$a(\phi - \hat{\phi}, v) = 0 . \tag{A.4.1}$$

Let $\tilde{\phi}$ be a Hermite-interpolate of ϕ in the space $H_m(\pi_\Omega \times \pi_\mathcal{E})$ (cf., Sec. 2.2, Chap. II). Then Eq. (A.4.1) can be written as

$$a(\hat{\phi} - \tilde{\phi}, v) = a(\phi - \tilde{\phi}, v) . \tag{A.4.2}$$

Also, Theorem 2.4 implies that

$$\| \phi - \tilde{\phi} \|_{L^\infty} \leq K_1 \overline{\Delta r}^{\mu_r} + K_2 \overline{\Delta E}^{\mu_E} .$$

We now establish that

$$a(\phi - \tilde{\phi}, v) \leq K_1 \overline{\Delta r}^{\mu_r} + K_2 \overline{\Delta E}^{\mu_E} . \tag{A.4.3}$$

for all $v = u_g(E)\, u_i(\underline{r}, D)$, $1 \leq g \leq G$, $1 \leq i \leq N$.

Strang and Fix [38] have shown that the interpolate $\tilde{f}(\underline{r})$ of $f(\underline{r})$ in the smooth Hermite space of degree $2m_r$ satisfies

$$(\underline{\nabla}(f(\underline{r}) - \tilde{f}(\underline{r})), \underline{\nabla} u_i(\underline{r}))_\Omega \leq K \overline{\Delta r}^{2m_r} \tag{A.4.4}$$

where $\{u_i(\underline{r})\}$ is a basis of the Hermite space. In the space $H_m(\pi(\Omega))$, however, the above relation holds locally in each mesh element only

if $f(r) \in C_p^t(\pi)$. We can then show that the inequality (A.4.4) holds in the entire region by a procedure similar to those in the proofs of Theorems 2.1 and 2.4. Furthermore, when $\phi(\underline{r}, E)$ is dependent on both $\underline{r}$ and E, it is conjectured from the result of Strang and Fix that

$$(\underline{\nabla}(\phi-\tilde{\phi}), \underline{\nabla}v) \leq K' \overline{\Delta r}^{\mu_r} + K'' \overline{\Delta E}^{\mu_E}$$

for all $v = u_g(E)\, u_i(\underline{r}, D)$, $1 \leq g \leq G$, $1 \leq i \leq N$. We now show that

$$\begin{aligned}(\phi-\tilde{\phi}, v) &\leq (K' \overline{\Delta r}^{\mu_r} + K'' \overline{\Delta E}^{\mu_E}, v) \\ &\leq K' \overline{\Delta r}^{\mu_r} + K'' \overline{\Delta E}^{\mu_E},\end{aligned}$$

$$\begin{aligned}\Big(\int_{\mathcal{E}} \Sigma(r, E' \to E)\, [\phi(r, E') - \tilde{\phi}(r, E')]\, dE', v \Big) &\\ \leq K \Big(\int_{\mathcal{E}} (\phi-\tilde{\phi})\, dE', v \Big) &\\ \leq K \Big(\int_{\mathcal{E}} \Big(K_1 \overline{\Delta r}^{\mu_r} + K_2 \overline{\Delta E}^{\mu_E} \Big)\, dE', v \Big) &\\ \leq K_1' \overline{\Delta r}^{\mu_r} + K_2' \overline{\Delta E}^{\mu_E}, &\end{aligned}$$

where $u_i(r)$, $u_g(E)$ are normalized such that $\int_\Omega u_i\, dV = \int_{\mathcal{E}} u_g\, dE = 1$. Combining the above results, we obtain the inequality (A.4.3) which was to be established. Let $e(\underline{r}, E) = \hat{\phi}(\underline{r}, E) - \tilde{\phi}(\underline{r}, E)$. Since $\hat{\phi} - \tilde{\phi}$ is a polynomial of degree $2m_1 - 1$ and $2m_E - 1$ in $\underline{r}$ and E, respectively, $e(\underline{r}, E)$ can be represented by

$$e(\underline{r}, E) = \sum_{g=1}^{G} \sum_{i=1}^{N} e_{ig}\, u_g(E)\, u_i(\underline{r}, D).$$

Then, it can be shown easily that Eq. (A.4.3) becomes

$$B\underline{e} \leq \underline{K}_1 \overline{\Delta r}^{\mu_r} + \underline{K}_2 \overline{\Delta E}^{\mu_E}$$

where

$$B = L - S - \frac{1}{\lambda} F ,$$

$$\underline{e} = \text{col}\{e_{11}, e_{12}, \ldots, e_{21}, e_{22}, \ldots, e_{GN}\} ,$$

$$\underline{K}_j = \text{col}\{K_{j11}, K_{j12}, \ldots, K_{j21}, K_{j22}, \ldots, K_{jGN}\} , \quad j = 1, 2 .$$

K_{jgi}, $1 \leq g \leq G$, $1 \leq i \leq N$ are constants. Other matrices are defined in Section 4.2.2, Chapter IV. Then,

$$\underline{e} \leq B^{-1}\underline{K}_1 \overline{\Delta r}^{\mu_r} + B^{-1}\underline{K}_2 \overline{\Delta E}^{\mu_E}$$

so that

$$\|\underline{e}\|_\infty \leq \|B^{-1}\|_\infty \|\underline{K}_1\|_\infty \overline{\Delta r}^{\mu_r} + \|B^{-1}\|_\infty \|\underline{K}_2\|_\infty \overline{\Delta E}^{\mu_E} .$$

$\|\underline{K}_1\|_\infty$ and $\|\underline{K}_2\|_\infty$ are constant. We claim that there exists a constant γ such that

$$\|B^{-1}\|_\infty < \gamma .$$

As in proofs in Sections (A.3) and (A.6), we appeal to the work of Descloux [54] to assert the above statement. Then,

$$\begin{aligned} \|\tilde{\phi} - \hat{\phi}\|_{L^\infty} &\leq \max_{\Omega \times \mathcal{E}} |e(\underline{r}, E)| \leq K \|\underline{e}\|_\infty \\ &\leq K_1 \overline{\Delta r}^{\mu_r} + K_2 \overline{\Delta E}^{\mu_E} . \end{aligned} \tag{A.4.5}$$

Finally, applying the triangle inequality and using the inequalities (A.4.3) and (A.4.5), we obtain

$$\|\phi - \hat{\phi}\|_{L^\infty} \leq K_1 \overline{\Delta r}^{\mu_r} + K_2 \overline{\Delta E}^{\mu_E} .$$

This completes the proof.

A.5 Theorem 5.1

Let $\underline{\phi}(t)$ be the solution to Eq. (5.1) where A(t) is Lipschitz continuous, i.e., there exists a positive constant σ such that

$$\| A(t)\,(\underline{f}(t) - \underline{g}(t)) \|_\infty \leq \sigma \| \underline{f}(t) - \underline{g}(t) \|_\infty .$$

Let $\hat{\underline{\phi}}(t)$ be the solution of Eq. (5.6) in the space $H_m(\pi_t)$. Assume that there exists a constant τ such that

$$\Big\| \sum_{p=0}^{m=1} \mathcal{A}_{i+1}^{p-} A_{i+1}^{p} \Big\|_\infty \leq 1$$

if $|t_{i+1} - t_i| < \tau$ for $1 \leq i \leq N_t - 1$. If $\underline{\phi} \in C_p^t(\pi_t)$ and $\Delta t = \max_{1 \leq i \leq N_t} |t_{i+1} - t_i| < \tau$, then $\hat{\underline{\phi}}$ satisfies

$$\max_{[0,T]} \left\| \frac{d^q}{dt^q} (\underline{\phi}(t) - \hat{\underline{\phi}}(t)) \right\|_\infty \leq K \Delta t^{\mu - q}$$

where $\mu = \min(2m, t)$ and K is a constant independent of Δt.

Proof. Let $\tilde{\underline{\phi}}(t)$ be the Hermite interpolate of $\underline{\phi}(t)$ of degree 2m-1 in the interval $[t_{i+1}, t_i]$ (cf., Sec. 2.1, Chap. II). Then Theorem A implies that

$$\max_{[t_{i+1}, t_i]} \left\| \frac{d^q}{dt^q} (\underline{\phi}(t) - \tilde{\underline{\phi}}(t)) \right\|_\infty \leq K \Delta t_i^{\mu - q} \qquad \text{(A.5.1)}$$

where $\Delta t_i = |t_{i+1} - t_i|$ and K is a constant independent of Δt_i.

Note that $\underline{\phi}(t)$ and $\hat{\underline{\phi}}(t)$ satisfy

$$\underline{\phi}_{i+1} - \underline{\phi}_i = \int_{t_i}^{t_{i+1}} A(t)\, \underline{\phi}(t)\, dt ,$$

$$\hat{\underline{\phi}}_{i+1} - \hat{\underline{\phi}}_i = \int_{t_i}^{t_{i+1}} A(t)\, \hat{\underline{\phi}}(t)\, dt .$$

The difference of the two equations can be expressed by

$$\hat{\underline{\phi}}_{i+1} - \tilde{\underline{\phi}}_{i+1} = \hat{\underline{\phi}}_i - \tilde{\underline{\phi}}_i + \int_{t_i}^{t_{i+1}} \{A(\underline{\phi}-\tilde{\underline{\phi}}) + A(\tilde{\underline{\phi}}-\hat{\underline{\phi}})\}\, dt \,. \qquad (A.5.2)$$

Let $\underline{e}_i(t) = \tilde{\underline{\phi}}(t) - \hat{\underline{\phi}}(t)$. Since $\underline{e}(t)$ is a vector whose elements consist of polynomials of degree 2m-1, $\underline{e}_i(t)$ may be expanded in terms of the element functions $u_i^{(p\pm)}(t)$ such that

$$\underline{e}_i(t) = \sum_{p=0}^{m-1} \left\{ \underline{e}_i^p\, u_i^{(p+)}(t) + \underline{e}_{i+1}^p\, u_{i+1}^{(p-)} \right\} .$$

By applying the Hermite method developed in Chapter V, Eq. (A.5.2) becomes

$$C_{i+1}\underline{e}_{i+1} = C_i\underline{e}_i + \int_{t_i}^{t_{i+1}} A(\underline{\phi}-\tilde{\underline{\phi}})\, dt \qquad (A.5.3)$$

where

$$\underline{e}_i = \underline{e}_i(t_i) \,,$$

$$\underline{e}_{i+1} = \underline{e}_i(t_{i+1}) \,,$$

$$C_{i+1} = \left\{ I - \sum_{p=0}^{m-1} \mathcal{A}_{i+1}^{(p-)} A_{i+1}^{\{p\}} \right\} ,$$

$$C_i = \left\{ I + \sum_{p=0}^{m-1} \mathcal{A}_i^{(p+)} A_i^{\{p\}} \right\} .$$

Other matrices are defined in Section 5.1, Chapter V. Hence,

$$\| \underline{e}_{i+1} \| \leq \| C_{i+1}^{-1} C_i \|_\infty \| \underline{e}_i \|_\infty + \| C_{i+1}^{-1} \|_\infty \int_{t_i}^{t_{i+1}} \| A(\underline{\phi}-\tilde{\underline{\phi}}) \|_\infty \, dt$$

$$\leq \| C_{i+1}^{-1} C_i \|_\infty \| \underline{e}_i \|_\infty + \| C_{i+1}^{-1} \|_\infty K \Delta t^\mu \,. \qquad (A.5.4)$$

Define

$$P_i = \sum_{p=0}^{m-1} \mathcal{A}_i^{(p+)} A_i^{\{p\}} ,$$

$$P_{i+1} \sum_{p=0}^{m-1} \mathcal{A}_{i+1}^{(p-)} A_{i+1}^{\{p\}} .$$

$A_i^{\{p\}}$ and $A_{i+1}^{\{p\}}$ are independent of Δt, and $\int |u_i^{p\pm}(t)| \, dt = O(\Delta t_i^{p+1})$ (cf., Sec. 2.1, Chap. II) and thus

$$P_i \leq \sum_{p=0}^{m-1} K_{i,p} \, \Delta t_i^{p+1} ,$$

$$P_{i+1} \leq \sum_{p=0}^{m-1} K_{i+1,p} \, \Delta t_i^{p+1} ,$$

where $K_{i,p}$ and $K_{i+1,p}$ are constant matrices independent of Δt_i. From the assumption, $\| P_{i+1} \|_\infty < 1$ for $|t_{i+1} - t_i| < \tau$ and thus we can express

$$[I - P_{i+1}]^{-1} = [I + P_{i+1} + P_{i+1}^2 + \ldots] = I + O(\Delta t_i) ,$$

$$[I - P_{i+1}]^{-1} [I + P_i] = [I + P_{i+1} + P_{i+1}^2 + \ldots] [I + P_i]$$

$$= I + O(\Delta t_i) .$$

Hence, the inequality (A.5.4) becomes

$$\| \underline{e}_{i+1} \|_\infty \leq \{ 1 + O(\Delta t_i) \} \, \| \underline{e}_i \|_\infty + K \Delta t_i^\mu .$$

Since $\| \underline{e}_1^p \|_\infty = 0$ for $0 \leq p \leq m-1$, it can be shown easily that

$$\| \underline{e}_{i+1} \|_\infty \leq K \Delta t_i^\mu , \qquad i \geq 1 .$$

Furthermore, since $\underline{e}_i^p = A_i^{\{p\}} \underline{e}_i$,

$$\| \underline{e}_{i+1}^p \|_\infty \leq K_p \Delta t_i^\mu , \qquad i \geq 1 .$$

Then,

$$\max_{[t_i, t_{i+1}]} \left\| \frac{d^q}{dt^q} \underline{e}_i(t) \right\|_\infty \leq \sum_{p=0}^{m-1} \left\{ \| \underline{e}_i^p \|_\infty \left| \frac{d^q}{dt^q} u_i^{p+}(t) \right| + \| \underline{e}_{i+1}^p \|_\infty \left| \frac{d^q}{dt^q} u_{i+1}^{p-}(t) \right| \right\}$$

$$\leq \sum_{p=0}^{m-1} K_p' (\Delta t_i^\mu)(\Delta t_i^{p-q})$$

$$= \sum_{p=0}^{m-1} K_p' \Delta t_i^{\mu+p-q} \qquad \text{(A.5.5)}$$

where $\left| \frac{d^q}{dt^q} u_i^{p+}(t) \right| = \left| \frac{d^q}{dt^q} u_{i+1}^{p-}(t) \right| = O(\Delta t^{p-q})$ are used. Therefore, applying the triangle inequality and using the inequalities (A.4.1) and (A.5.5), we obtain

$$\max_{[0,T]} \left\| \frac{d^q}{dt^q} (\underline{\phi}(t) - \hat{\underline{\phi}}(t) \right\|_\infty \leq \max_{[0,T]} \left\| \frac{d^q}{dt^q} (\underline{\phi} - \tilde{\underline{\phi}}) \right\| + \max_{[0,T]} \left\| \frac{d^q}{dt^q} (\tilde{\underline{\phi}} - \hat{\underline{\phi}}) \right\|_\infty$$

$$\leq \max_{[0,T]} \left\| \frac{d^q}{dt^q} (\underline{\phi} - \tilde{\underline{\phi}}) \right\|_\infty + \max_{1 \leq i \leq N_t - 1} \left\| \frac{d^q}{dt^q} \underline{e}_i(t) \right\|_\infty$$

$$\leq K \Delta t^{\mu - q} .$$

This completes the proof.

A.6 Theorem 6.1

Assume that the inequality (6.2) holds. Let $\phi(\underline{r}, E, t)$ be the solution of Eq. (6.3) and $\phi(\underline{r}, E, t) \in C_p^t(\pi_\Omega \times \pi_\mathcal{E})$ where $t = (t_r, t_E)$. If $\hat{\phi}(\underline{r}, E, t)$ is the solution to the semidiscrete equation (6.6) in the space $H_m(\pi_\Omega \times \pi_\mathcal{E})$, then

$$\| \phi(\underline{r}, E, t) - \hat{\phi}(\underline{r}, E, t) \|_{L^\infty(\pi_\Omega \times \pi_{\mathcal{E}})} \leq K_1 \overline{\Delta r}^{\mu_r} + K_2 \overline{\Delta E}^{\mu_E}$$

where $\mu_r = \min(2m_r, t_r)$, $\mu_E = \min(2m_E, t_E)$, $\overline{\Delta r} = \max_{\pi_\Omega} \Delta r$, and $\overline{\Delta E} = \max_{\pi_{\mathcal{E}}} \Delta E$ and K_1 and K_2 are positive constants independent of $\overline{\Delta r}$ and $\overline{\Delta E}$, respectively.

Proof. ϕ and $\hat{\phi}$ satisfy

$$\left(\frac{1}{\mathscr{V}} \frac{\partial}{\partial t} \phi, v\right) + a(\phi, v) = (Q, v) ,$$

$$\left(\frac{1}{\mathscr{V}} \frac{\partial}{\partial t} \hat{\phi}, v\right) + a(\hat{\phi}, v) = (Q, v),$$

for all $v = u_i(\underline{r}, D)\, u_g(E)$, $1 \leq i \leq N$, $1 \leq g \leq G$. The difference of the two equations is given by

$$\left(\frac{1}{\mathscr{V}} \frac{\partial}{\partial t} (\phi - \hat{\phi}), v\right) + a(\phi - \hat{\phi}, v) = 0 . \qquad \text{(A.6.1)}$$

Let $\tilde{\phi}$ be the Hermite-interpolate of ϕ in $H_m(\pi_\Omega \times \pi_{\mathcal{E}})$. Then, Theorem 2.4 implies that

$$\| \phi - \tilde{\phi} \|_{L^\infty} \leq K_1 \overline{\Delta r}^{\mu_r} + K_2 \overline{\Delta E}^{\mu_E} . \qquad \text{(A.6.2)}$$

Then, we can write

$$\left(\frac{1}{\mathscr{V}} \frac{\partial}{\partial t} (\hat{\phi} - \tilde{\phi}), v\right) + a(\hat{\phi} - \tilde{\phi}, v) = \left(\frac{1}{\mathscr{V}} \frac{\partial}{\partial t} (\phi - \tilde{\phi}), v\right) + a(\phi - \tilde{\phi}, v) .$$

In the proof of Theorem 4.1, it was established that

$$a(\phi - \tilde{\phi}, v) \leq K_1 \overline{\Delta r}^{2m_r} + K_2 \overline{\Delta E}^{2m_E} .$$

By a procedure similar to that in the above proof, we also have

$$\left(\frac{1}{\mathscr{V}} \frac{\partial}{\partial t} (\phi - \tilde{\phi}), v\right) \leq \frac{1}{\mathscr{V}_{\min}} \left(\frac{\partial}{\partial t} (\phi - \tilde{\phi}), v\right) \leq K' \overline{\Delta r}^{\mu_r} + K'' \overline{\Delta E}^{\mu_E} .$$

Hence,

$$\left(\frac{1}{\mathscr{V}}\frac{\partial}{\partial t}(\hat{\phi}-\tilde{\phi}), v\right) + a(\hat{\phi}-\tilde{\phi}, v) \leq K_1\overline{\Delta r}^{\mu_r} + K_2\overline{\Delta E}^{\mu_E}. \qquad (A.6.3)$$

Define $e(\underline{r}, E, t) = \hat{\phi} - \tilde{\phi}$. Since $\hat{\phi}(t) - \tilde{\phi}(t)$ is a polynomial of degree $2m_r-1$ and $2m_E-1$ in $\underline{r}$ and E, respectively, $e(t)$ can be represented by

$$e(\underline{r}, E, t) \equiv \hat{\phi} - \tilde{\phi} = \sum_{g=1}^{G}\sum_{i=1}^{N} e_{ig}(t)\, v_{ig}(\underline{r}, E).$$

Then the inequality (A.6.3) becomes

$$V\frac{\partial}{\partial t}\underline{e} + A\,\underline{e} \leq \underline{K}_1\overline{\Delta r}^{\mu_r} + \underline{K}_2\overline{\Delta E}^{\mu_E}$$

where

$$A = L - S - (1-\beta)F,$$

$$\underline{e} = \mathrm{col}\{e_{11}, e_{12}, \ldots, e_{21}, e_{22}, \ldots, e_{GN}\},$$

$$\underline{K}_j = \mathrm{col}\{K_{j11}, K_{j12}, \ldots, K_{j21}, K_{j22}, \ldots, K_{jGN}\},$$

$$K_{jig} = \int_{\mathscr{E}}\int_{\Omega} K_j v_{ig}\, dV\, dE \qquad \text{for } j = 1, 2.$$

Other matrices are defined by Eq. (6.11). Solving the differential inequality, we obtain

$$\underline{e}(t) \leq \exp\left[-\int_0^t V^{-1}A\, ds\right]\underline{e}_o + \int_0^t \exp\left[-\int_s^t V^{-1}A\, d\tau\right]V^{-1}\left[\underline{K}_1\overline{\Delta r}^{\mu_r} + \underline{K}_2\overline{\Delta E}^{\mu_E}\right]ds. \qquad (A.6.4)$$

We claim that there exists constants γ_1, γ_2 and γ_3 such that

$$\gamma_1 < \|V^{-1}\|_\infty < \gamma_2 \quad \text{and} \quad \|A\|_\infty < \gamma_3.$$

As in proofs in Sections A.3 and A.4, we appeal to the work by Descloux [54] to assert the above statement. Consequently,

$$[]\underline{e}(t)[]_\infty \leq K\,[]\underline{e}_o[]_\infty + K_1\overline{\Delta r}^{\mu_r} + K_2\overline{\Delta E}^{\mu_E}.$$

Since $[]\underline{e}_o[]_\infty = O\left(\overline{\Delta r}^{\mu_r} + \overline{\Delta E}^{\mu_E}\right)$,

$$[]\underline{e}(t)[]_\infty \leq K_1'\overline{\Delta r}^{\mu_r} + K_2'\overline{\Delta E}^{\mu_E}.$$

Hence,

$$\|\hat{\phi} - \tilde{\phi}\|_{L^\infty(\Omega\times\mathcal{E})} = \max_{[0,T]} |e(t)| \leq K[]\underline{e}(t)[]_\infty \leq K_1''\overline{\Delta r}^{\mu_r} + K_2''\overline{\Delta E}^{\mu_E}. \quad \text{(A.6.5)}$$

Finally, applying the triangle inequality and using the inequalities (A.6.2) and (A.6.5), we obtain

$$\|\phi - \hat{\phi}\|_{L^\infty(\Omega\times\mathcal{E})} \leq K_1\overline{\Delta r}^{\mu_r} + K_2\overline{\Delta E}^{\mu_E}.$$

This completes the proof.

Appendix B

INNER PRODUCTS FOR ELEMENT FUNCTIONS

Nonvanishing inner products for the univariate element functions $\{u_i^{p\pm}(s);\ 0 \leq p \leq m-1\}$ for $m = 1, 2$ (cf., Sec. 2.1, Chap. II) are listed below: Let $h_- = x_i - x_{i-1}$ and $h_+ = x_{i+1} - x_i$.

(i) $m = 1$

$$\left(u_i^{0-}, u_{i-1}^{0+}\right) = \frac{h_-}{6} \qquad \left(u_i^{0-}, u_i^{0-}\right) = \frac{h_-}{3}$$

$$\left(u_i^{0+}, u_i^{0+}\right) = \frac{h_+}{3} \qquad \left(u_i^{0+}, u_{i+1}^{0-}\right) = \frac{h_+}{6}$$

$$\left(\frac{d}{dx} u_i^{0-}, \frac{d}{dx} u_{i-1}^{0+}\right) = -\frac{1}{h_-} \qquad \left(\frac{d}{dx} u_i^{0-}, \frac{d}{dx} u_i^{0-}\right) = \frac{1}{h_-}$$

$$\left(\frac{d}{dx} u_i^{0+}, \frac{d}{dx} u_i^{0+}\right) = \frac{1}{h_+} \qquad \left(\frac{d}{dx} u_i^{0+}, \frac{d}{dx} u_i^{0-}\right) = -\frac{1}{h_+}$$

(ii) $m = 2$

$$\left(u_i^{0-}, u_{i-1}^{0+}\right) = \frac{9}{70} h_- \qquad \left(u_i^{0-}, u_{i-1}^{1+}\right) = \frac{13}{420} h_-^2$$

$$\left(u_i^{0-}, u_i^{0-}\right) = \frac{13}{35} h_- \qquad \left(u_i^{0-}, u_i^{1-}\right) = -\frac{11}{210} h_-^2$$

$$\left(u_i^{0+}, u_i^{0+}\right) = \frac{13}{35} h_+ \qquad \left(u_i^{0+}, u_i^{1+}\right) = \frac{11}{210} h_+^2$$

$$\left(u_i^{0+}, u_{i+1}^{0-}\right) = \frac{9}{70} h_+ \qquad \left(u_i^{0+}, u_{i+1}^{1-}\right) = -\frac{13}{420} h_+^2$$

$$\left(u_i^{1-}, u_{i-1}^{0+}\right) = -\frac{13}{420} h_-^2 \qquad \left(u_i^{1-}, u_{i-1}^{1+}\right) = -\frac{1}{140} h_-^3$$

$$\left(u_i^{1-}, u_i^{0-}\right) = -\frac{11}{210} h_-^2 \qquad \left(u_i^{1-}, u_i^{1-}\right) = \frac{1}{105} h_-^3$$

$$\left(u_i^{1+}, u_i^{0+}\right) = \frac{11}{210} h_+^2 \qquad \left(u_i^{1+}, u_i^{1+}\right) = \frac{1}{105} h_+^3$$

$$\left(u_i^{1+}, u_{i+1}^{0-}\right) = \frac{13}{420} h_+^2 \qquad \left(u_i^{1+}, u_{i+1}^{1-}\right) = -\frac{1}{140} h_+^3$$

$$\left(\frac{d}{dx} u_i^{0-}, \frac{d}{dx} u_{i-1}^{0+}\right) = -\frac{6}{5}\frac{1}{h_-} \qquad \left(\frac{d}{dx} u_i^{0-}, \frac{d}{dx} u_{i-1}^{1+}\right) = -\frac{1}{10}$$

$$\left(\frac{d}{dx} u_i^{0-}, \frac{d}{dx} u_i^{0-}\right) = \frac{6}{5}\frac{1}{h_-} \qquad \left(\frac{d}{dx} u_i^{0-}, \frac{d}{dx} u_i^{1-}\right) = -\frac{1}{10}$$

$$\left(\frac{d}{dx} u_i^{0+}, \frac{d}{dx} u_i^{0+}\right) = \frac{6}{5}\frac{1}{h_+} \qquad \left(\frac{d}{dx} u_i^{0+}, \frac{d}{dx} u_i^{1+}\right) = \frac{1}{10}$$

$$\left(\frac{d}{dx} u_i^{0+}, \frac{d}{dx} u_{i+1}^{0-}\right) = -\frac{6}{5}\frac{1}{h_+} \qquad \left(\frac{d}{dx} u_i^{0+}, \frac{d}{dx} u_{i+1}^{1-}\right) = \frac{1}{10}$$

$$\left(\frac{d}{dx} u_i^{1-}, \frac{d}{dx} u_{i-1}^{0+}\right) = \frac{1}{10} \qquad \left(\frac{d}{dx} u_i^{1-}, \frac{d}{dx} u_{i-1}^{1+}\right) = -\frac{1}{30} h_-$$

$$\left(\frac{d}{dx} u_i^{1-}, \frac{d}{dx} u_i^{0-}\right) = -\frac{1}{10} \qquad \left(\frac{d}{dx} u_i^{1-}, \frac{d}{dx} u_i^{1-}\right) = \frac{2}{15} h_-$$

$$\left(\frac{d}{dx} u_i^{1+}, \frac{d}{dx} u_i^{0+}\right) = \frac{1}{10} \qquad \left(\frac{d}{dx} u_i^{1+}, \frac{d}{dx} u_i^{1+}\right) = \frac{2}{15} h_+$$

$$\left(\frac{d}{dx} u_i^{1+}, \frac{d}{dx} u_{i+1}^{0-}\right) = -\frac{1}{10} \qquad \left(\frac{d}{dx} u_i^{1+}, \frac{d}{dx} u_i^{1-}\right) = -\frac{1}{30} h_+$$

The inner products for multivariate element functions can be determined using the univariate inner products. Consider an n-dimensional space and let multivariate element functions be defined by

$$v_{i_1 i_2 \ldots i_n}(\underline{r}) = u_{i_1}(r_1)\, u_{i_2}(r_2) \ldots u_{i_n}(r_n).$$

Then, the multivariate inner products can be represented by

$$(v_i, v_{i'}) = \prod_{j=1}^{n} (u_{i_j}, u_{i'_j}),$$

$$(\underline{\nabla} v_i, \underline{\nabla} v_{i'}) = \sum_{j=1}^{n} (v_i, v_{i'}) \frac{\left(\frac{d}{dr_j} u_{i_j}, \frac{d}{dr_j} u_{i'_j}\right)}{(u_{i_j}, u_{i'_j})} .$$

For example, for $n = 2$, the bivariate inner products are given by

$$(v_i, v_{i'}) = (u_{i_1}, u_{i'_1}) (u_{i_2}, u_{i'_2}) ,$$

$$(\underline{\nabla} v_i, \underline{\nabla} v_{i'}) = \left(\frac{d}{dr_1} u_{i_1}, \frac{d}{dr_1} u_{i'_1}\right) \left(u_{i_2}, u_{i'_2}\right) ,$$

$$+ \left(u_{i_1}, u_{i'_1}\right) \left(\frac{d}{dr_2} u_{i_2}, \frac{d}{dr_2} u_{i'_2}\right) .$$

Appendix C

NUCLEAR DATA

Table C.1. Delayed Neutron Constants

Group	β_i	λ_i
1	0.285×10^{-3}	0.127×10^{-1}
2	0.15975×10^{-2}	0.317×10^{-1}
3	0.141×10^{-2}	0.115
4	0.30525×10^{-2}	0.311
5	0.96×10^{-3}	0.14×10^{1}
6	0.195×10^{-3}	0.387×10^{1}

$\beta = \Sigma \beta_i = 0.0075$

Table C.2. Multigroup Nuclear Constants

(a) Thermal Group

	Fuel	Reflector
D_2	0.4	0.15
Σ_{T_2}	0.2	0.02
$\nu\Sigma_f$	(0.218)	0.0

$\mathcal{V}_2 = 2.2 \times 10^5$ cm/sec.

(b) Fast Group

	Fuel	Reflector
D_1	1.5	1.2
Σ_{T_1}	0.0623	0.101
$\Sigma_{1\to 2}$	0.06	0.1
$\nu\Sigma_{f_1}$	0.0	0.0

$\mathcal{V}_1 = 1.0 \times 10^8$ cm/sec.

Appendix D

COMPUTER PROGRAMS

The computer program HERMITE-0D for the numerical solution of the point kinetics equations is described in Section D.1. The two-dimensional reactor kinetics program HERMITE-2D is described in Section D.2. These programs are written in FORTRAN IV for the IBM 360/65 computer system. The source listings of the programs are presented in Appendix E.

D.1 The Point Kinetics Program HERMITE-0D

In this section, the general features of the program HERMITE-0D are discussed. Section D.1.1 discusses the preparation of input data cards and Section D.1.2 presents a list of sample input data cards.

HERMITE-0D is written for the purpose of testing piecewise polynomial methods for the point kinetics equations. The general numerical methods are developed in Chapter V. The present program permits approximations using piecewise polynomials of degree up to 3. The reactivity change is limited to ramp variation in time.

HERMITE-0D provides four methods for the solution of the point kinetics equations:

(i) Crank-Nicolson scheme,

$$\left\{I - \frac{\Delta t}{2} A_i\right\} \hat{\phi}_{i+1} = \left\{I + \frac{\Delta t}{2} A_i\right\} \hat{\phi}_i \,, \qquad \text{Eq. (5.6b)}$$

(ii) Hermite method, m=1,

$$\{I - \frac{\Delta t}{2} A_i - \frac{\Delta t^2}{3} A_\Delta\} \hat{\phi}_{i+1} = \{I + \frac{\Delta t}{2} A_{i+1} - \frac{\Delta t^2}{3} A_\Delta\} \hat{\phi}_i , \qquad \text{Eq. (5.10b)}$$

(iii) Hermite method, m=2,

$$\{I - \frac{\Delta t}{2} A_i - \frac{7}{20} \Delta t^2 A_\Delta + [\frac{\Delta t^2}{12} A_i + \frac{\Delta t^3}{20} A_\Delta] A_{i+1}\} \hat{\phi}_{i+1}$$

$$= \{I + \frac{\Delta t}{2} A_{i+1} - \frac{7}{20} \Delta t^2 A_\Delta + [\frac{\Delta t^2}{12} A_{i+1} - \frac{\Delta t^3}{20} A_\Delta] A_i\} \hat{\phi}_i ,$$

Eq. (5.10c)

(iv) Hermite method applied to the time-integrated point kinetics equation, m=1,

$$B_{i+1} \hat{n}_{i+1} = B_i \hat{n}_i + \sum_{j=1}^{J} \left(e^{-\lambda_j t_i} - e^{-\lambda_j t_{i+1}} \right) S_{ji} \qquad \text{Eq. (5.14)}$$

where B_{i+1}, B_i and S_{ji} are defined in Eq. (5.14).

In the program, the solutions of the methods (i), (ii) and (iii) are determined by using the Jacobi iteration scheme. However, the unknown in the method (iv) is a scalar and is determined simply by dividing the right-hand side by the coefficient of the unknown.

D.1.1 Input Preparation for HERMITE-0D

Card 1. FORMAT (20A4)

Alphanumeric title with 1 in column 1 for page control.

Card 2 FORMAT (16I5)

This card provides the general information which specifies the problem. IC1>1 allows calculations of the same problem with different time steps.

IC1 = Number of different Δt's (see Card 6).

IC2 = Maximum number of iterations: Methods (i), (ii) and (iii) only.

IC3 = Number of delayed precursor groups.

IC4 = Number of time zones ≤ 2.

IC5 = Numerical method options:

= 0 Method (i),

= 1 Method (ii), (cf., Sec. D.1)

= 2 Method (iii),

= 3 Method (iv).

Card 3 FORMAT (8D10.5)

ρ_o = Reactivity $\rho(t)$ in dollars at t = 0.

ϵ = Convergence criterion.

$\rho_{\Delta,1}$ = Linear coefficient of $\rho(t)$ in dollars in the first time zone.

T_1 = Time at the end of the first time zone.

$\rho_{\Delta,2}$ = Linear coefficient of $\rho(t)$ in dollars in the second time zone.

T_2 = Time at the end of the second time zone.

Card 4 FORMAT (8D10.5)

Λ = Generation time.

$(\lambda(I), I=1, J)$ = Decay constant of group I.

Card 5 FORMAT (8D10.5)

$(\beta(I), I=1, J)$ = Fraction of delayed neutrons of group I.

Card 6 FORMAT (8D10.5)

ΔT = Time step size.

Repeat Card 6 as many as IC1 times for different Δt's.

For another problem, a set of Cards 1 to 6 may be placed immediately after Card 6.

D.1.2 Input for Sample Problem

On the next page, a list of input cards is presented for a calculation using the cubic Hermite method (m=2) and Δt=0.5 sec in Example 5.1, Chapter V. For computation using other methods, it is necessary to change IC5 in Card 2 as directed in the input preparation. As the computer output, the neutron density and the precursor densities will be printed at every time step.

D.2 The Two-Dimensional Reactor Kinetics Program HERMITE-2D

The general features of the two-dimensional kinetics program HERMITE-2D are described in Section D.2.1. Section D.2.2 discusses the preparation of input data cards and Section D.2.3 presents a list of sample input data cards.

D.2.1 Description of HERMITE-2D

The program HERMITE-2D is written for the purpose of testing the finite element method for two-dimensional reactor kinetics problems. The program solves the time-dependent neutron diffusion equation, Eq. (6.1), using bicubic polynomial basis functions in space and piecewise linear functions in time. The selection of polynomial basis functions is discussed in Chapter II and the finite element methods in space and time domains are developed in Chapters IV, V and VI. The program also permits steady state calculations involving the determination of eigenvalues and the search for critical fission cross sections.

```
1  SAMPLE INPUT FOR FXAMPLE 5.1,CHAP.V --HERMITE-OD                                  INPT0001
     1    50     6     1     2                                                       INPT0002
      0.0D0    1.0D- 9      0.5D0      2.0D0                                        INPT0003
     5.0D-4  0.127D-1  0.317D-1  0.115D 0  0.311D 0   0.14D 1  0.387D 1            INPT0004
  0.285D-30.15975D-2  0.141D-20.30525D-2   0.96D-3  0.195D-3                       INPT0005
     5.0D-1                                                                        INPT0006
```

HERMITE-2D is not intended to be general and its applications are rather limited to specific problems. Limitations to the present program are:

(i) Rectangular geometry with the quarter core symmetry; rectangular partition.

(ii) Two-group computations only.

(iii) Regionwise constant cross sections; fissions only at thermal group with $\chi_1=1.0$; linear or sinusoidal time variations in thermal absorption cross sections.

Numerical results for steady state problems presented in Chapter IV are obtained by using a modified version of HERMITE-2D which is mainly written for eigenvalue calculations in one- and two-group problems. The modified program allows the use of a larger number of mesh points compared to HERMITE-2D.

The reactor configurations $[0, a] \times [0, b]$ and the time interval $[0, T]$ are partitioned such that

$$0 = x_1 = x_2 < \ldots < x_{N_x} = a,$$

$$0 = y_1 = y_2 < \ldots < y_{N_y} = b,$$

$$0 = t_1 = t_2 < \ldots < t_{N_t} = T.$$

It is assumed that material properties in each mesh element are continuous.

Bicubic basis functions are imposed on the spatial partition (c.f., Example 2.1 - 2.3, Chap. II). In order to facilitate the representation of the bicubic basis functions in linear indices, the basis functions are arranged alphabetically as follows (see figures):

At regular points,

Type	Equation	Expansion Coefficient
a	(2.28b)	$\frac{d\phi}{dx}$
b	(2.28d)	$\frac{d^2\phi}{dxdy}$
c	(2.28c)	$\frac{d\phi}{dy}$
d	(2.28a)	ϕ

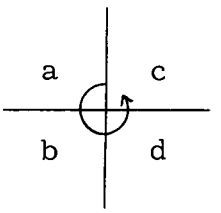

and at singular points,

Type	Equation	Expansion Coefficient
A	(2.30b)	$\frac{d\phi}{dx}\Big\|_-$
B	(2.30c)	$\frac{d\phi}{dx}\Big\|_+$
C	(2.30f)	$\frac{d^2\phi}{dxdy}$
D	(2.30d)	$\frac{d\phi}{dy}\Big\|_-$
E	(2.30e)	$\frac{d\phi}{dy}\Big\|_+$
F	(2.30a)	ϕ

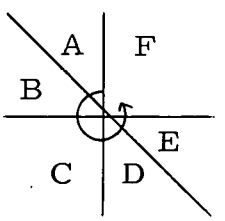

The group dependent normalization factors θ_g for the bicubic functions are assumed to be equal to the average of diffusion constant over the entire material regions. Expansion coefficients of the bicubic basis functions correspond to function values and their derivatives at mesh points and these are indicated in the right columns.

Figure D.1 illustrates how the cubic basis functions are linearly indexed in the program. The region is partitioned into four elements

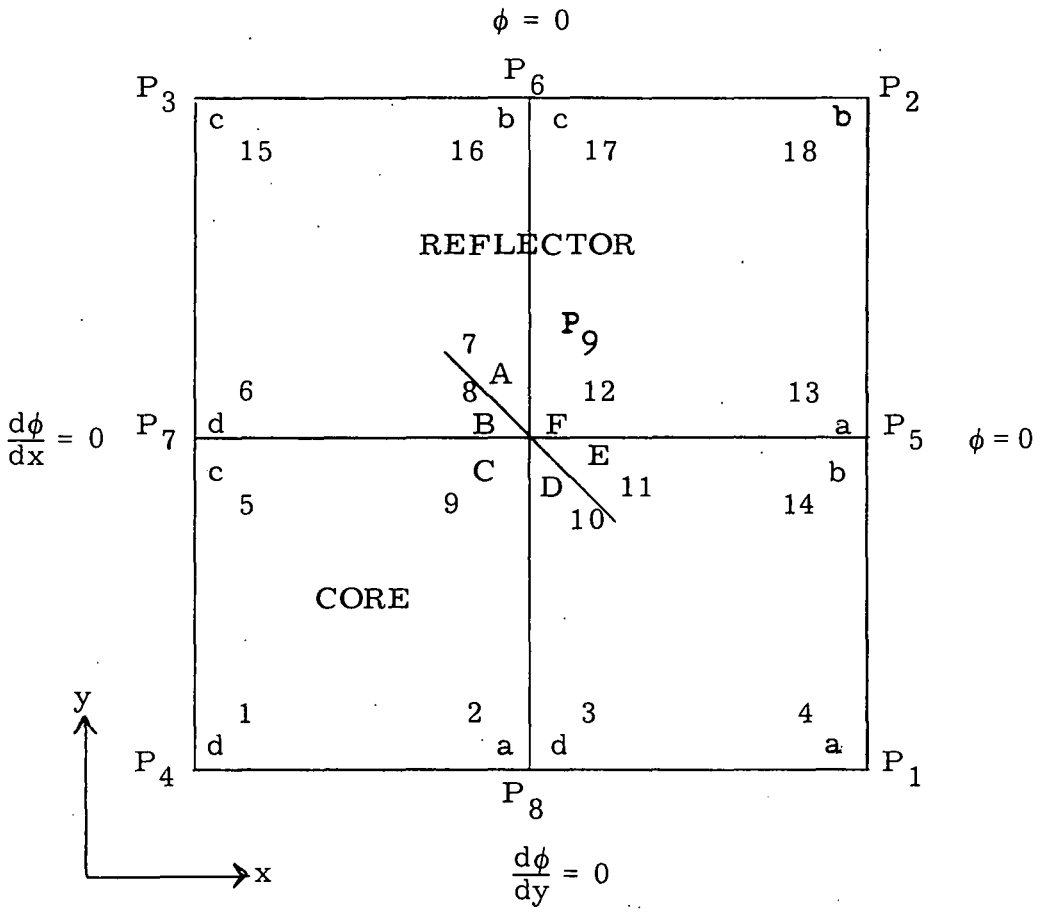

Fig. D.1. Linear Representation of Bicubic Basis Functions on a Rectangular Partition

and the point P_9 is a singular point. It can be shown easily that the bicubic basis functions at boundary points, which satisfy the quarter core symmetry boundary conditions, consist of the regular basis functions whose regions of definition in the above convention lie within the reactor geometry. For example, basis functions at corner points P_1, P_2, P_3 and P_4 consist of functions of types a, b, c and d, respectively. Basis functions at boundary points P_5, P_6, P_7 and P_8 consist of sets of functions (a, b), (b, c), (c, d) and (a, d), respectively. The singular point P_9 possesses functions of types A to F. If P_9 is a regular point, then it contains functions of types a to d.

The bicubic functions are numbered in a linear fashion sweeping in the x-direction and at each mesh point basis functions are ordered alphabetically: x sweep begins at P_4 and moves up to the increasing y-direction. The linear indices of basis functions are shown in Fig. D.1. In this example, the total number of basis functions is 18. If P_9 is a regular point, then it becomes 16.

Let $\{v_i(\underline{r})\}_{i=1}^{N}$ and $\{u_k^{0\pm}(t)\}_{k=1}^{N_t}$ be the linearly indexed basis functions, bicubic in $\underline{r}$ and linear in t, respectively. Then the approximate solution for the g-th group and $t_k \leq t \leq t_{k+1}$ is represented by

$$\phi(\underline{r}, t) = \sum_{i=1}^{N} \{a_{gik} u_k^{0+}(t) + a_{gi,k+1} u_{k+1}^{0-}(t)\} v_i(\underline{r}) .$$

Applying the Galerkin scheme to the time-dependent neutron diffusion equation, Eq. (6.1), leads to a system of linear equations, Eq. (6.14), for the expansion coefficients.

In HERMITE-2D, the elements of the stiffness matrices in Eq. (6.14) are determined by using inner products of bicubic functions as defined in Appendix B. The resulting matrix equation is then solved by the source iterative scheme incorporated with the Cholesky procedure which is discussed in Section 4.3, Chapter IV. The equation for the (K+1)th iterative solution is set in the following form:

$$\left\{ V_g + \frac{\Delta t}{2} L_{gk} + \mathcal{L}_{g,k+1} \right\} \underline{a}^{K+1}_{g,k+1}$$

$$= \sum_{g'=1}^{G} \left\{ V_g \delta_{gg'} + \frac{\Delta t_k}{2} [-\delta_{gg'} L_{gk} + S_{gg'} + (1-\beta) F_{gg'}] \right.$$

$$\left. + \sum_{j=1}^{J} \alpha_{kj} \lambda_j \beta_j F_{dgg'} + \delta_{gg'} \mathcal{L}_{gk} \right\} \underline{a}^{K}_{g'k} \qquad \text{(D.1)}$$

$$+ \sum_{g'=1}^{G} \left\{ \frac{\Delta t}{2} [S_{gg'} + (1-\beta) F_{gg'}] + \sum_{j=1}^{J} \gamma_{kj} \lambda_j \beta_j F_{dgg'} \right\} \underline{a}^{K}_{g', k+1}$$

$$+ \sum_{j=1}^{J} [e^{-\lambda_j t_k} - e^{-\lambda_j t_{k+1}}] \underline{\mathcal{L}}_{jkg}$$

where

$$\underline{a}_{gk} = \text{col}\{a_{g1k}, a_{g2k}, \ldots, a_{gNk}\}.$$

Matrices in the above equation are defined in Eq. (6.14). The coefficient matrix of the vector $\underline{a}^{K+1}_{g,k+1}$ is symmetric and positive definite and thus the Cholesky scheme can be used in inverting the matrix.

The matrices defined in Eq. (D.1) have band structures whose half width is given by

$$\text{Half-band width} = 4NX + 2NRX + 5$$

where NX is the number of x mesh points and NRX is the number of x regions. In the program, only the band part of the coefficient matrices is stored in order to reduce the computer storage requirements. Furthermore, the variable dimensioning features of FORTRAN IV are used for coefficient matrices and the matrices are stored in a vector called A(NDIM) with a length NDIM. The length of the vector A can be estimated from the formula,

$$NDIM = N\{4G + J + NWD(1+4G)\} + NT$$

where N = number of basis functions in each group, G = number of groups, J = number of precursor groups, NT = number of time steps and NWD = total band width which is equal to 2(half-band width) + 1.

Figure D.2 describes iteration procedures for the steady state calculation in HERMITE-2D. The general numerical methods are discussed in Section 4.3, Chapter IV. In Box 1, the initial coefficient vector is read in or generated in the program as simple hill-shaped functions. The (J+1)th iterate for the coefficient vector is determined by solving Eq. (4.14) in Box 2. The eigenvalue is computed after every INNMAX iteration according to equations in Box 3. If IC4 $\neq$ 2 and the eigenvalue satisfies the condition in Box 4, the computation of eigenvalue is completed. However, if IC4 = 2, the eigenvalue is required to be equal to 1.0 with some tolerance as indicated in Box 5. In this case, the fission cross section is adjusted according to the equation in Box 6 and computations of the eigenvalue are repeated until the condition in Box 5 is satisfied. The final cross section corresponds to the critical fission cross section.

The general procedures for the kinetics calculation in HERMITE-2D are illustrated in Fig. D.3. In Box 1, the initial flux is either read in or computed in the steady state part of the program. The new time-dependent coefficient matrices for the time step k+1 are defined in Box 2. Then the coefficient vector at the step k+1 is computed from Eq. (D.1) and extrapolated as shown in Box 3. The convergence of the coefficient vector is then checked in Boxes 4 and 5. If they are not satisfied, the process returns to Box 3 and the same routine is repeated. If the solution vector

is converged satisfying the conditions in Boxes 4 and 5, the computation in the time step k+1 is completed. The process then returns to Box 2 for the next time step. These stepwise computations are continued until the maximum time limit is reached. The program also provides for running multiple jobs by specifying ISTOP $\neq$ 0.

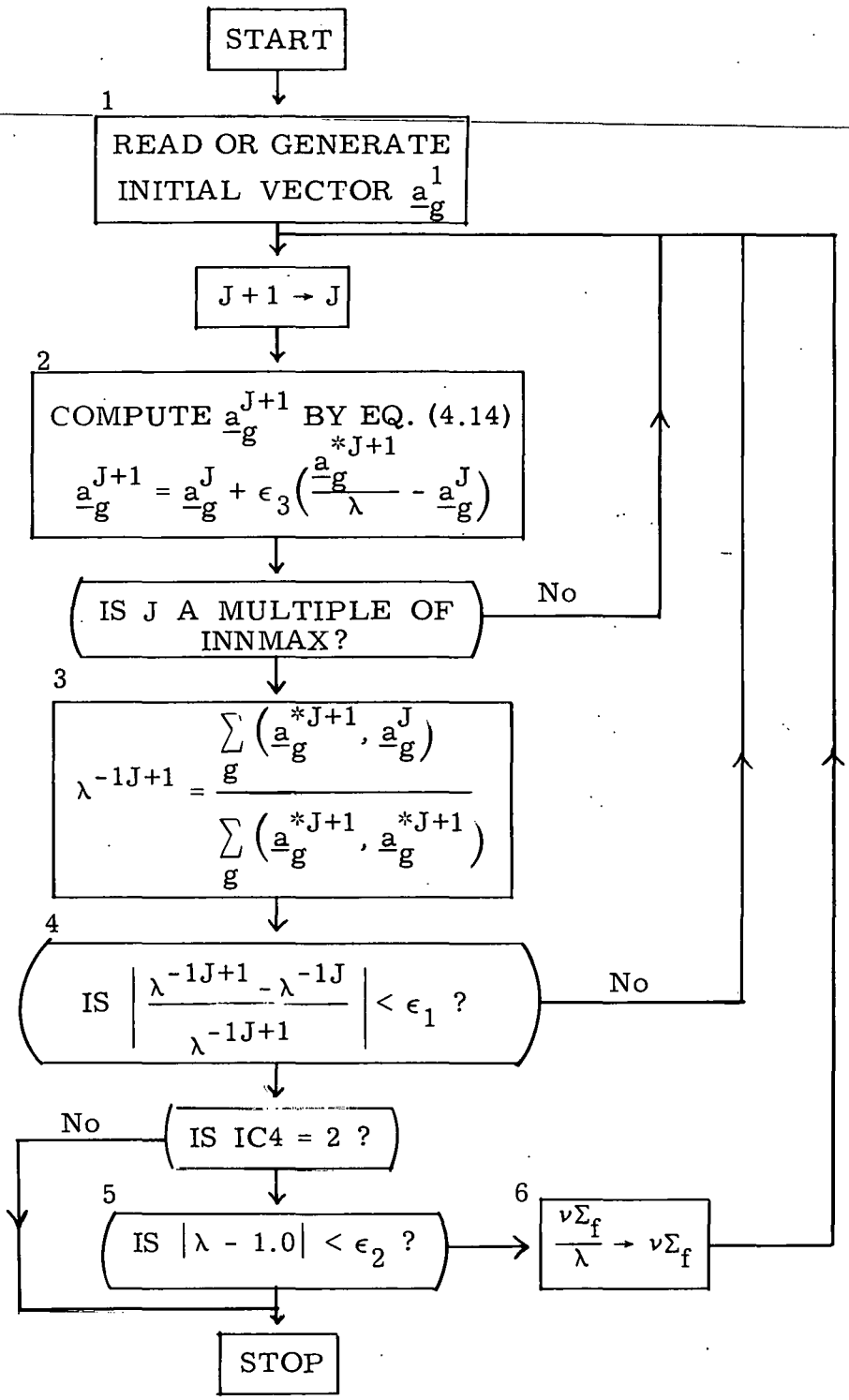

Fig. D.2. Logic for Steady State Calculation

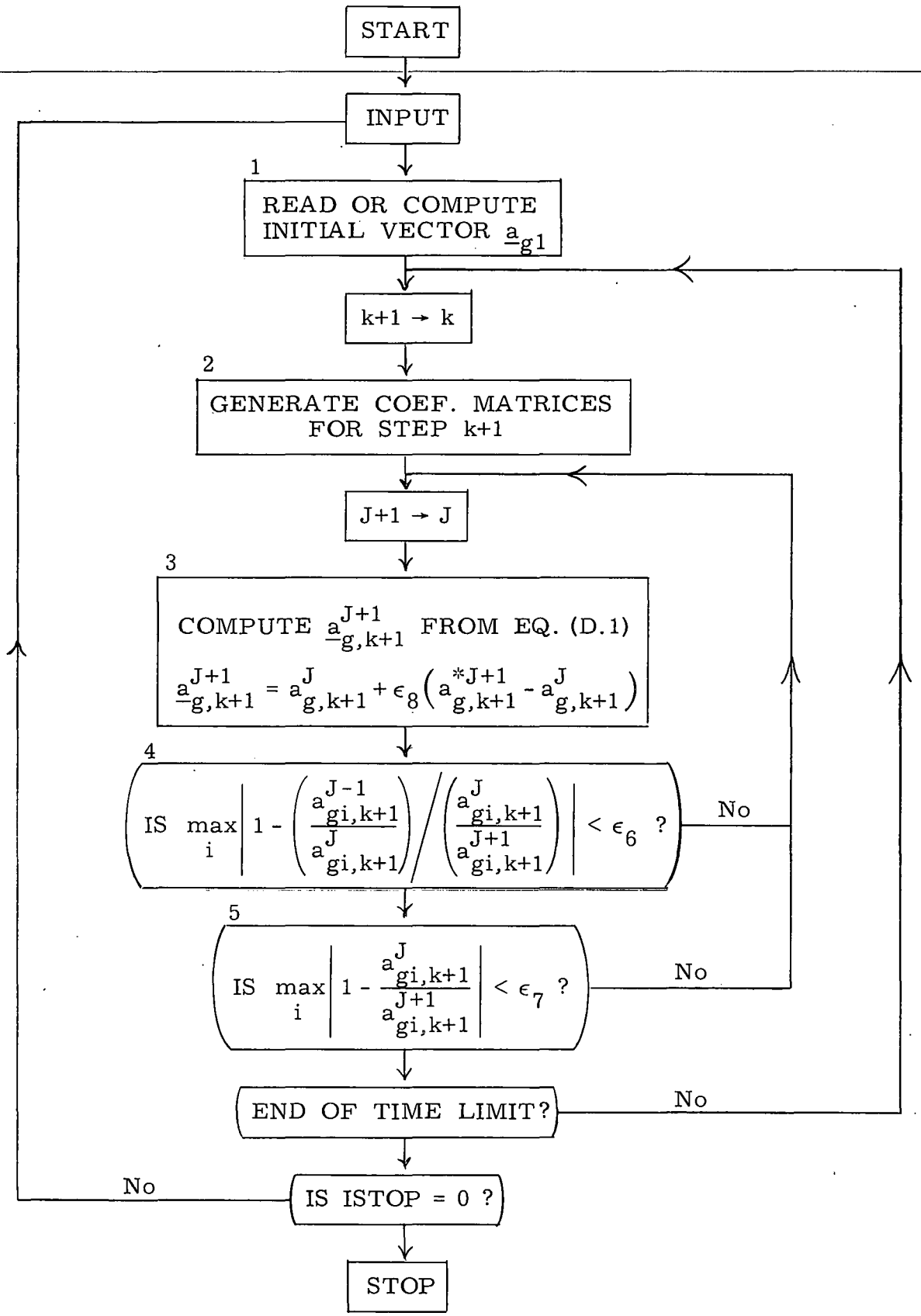

Fig. D.3. Logic for Time-Dependent Calculation

D.2.2 Input Preparation for HERMITE-2D

Card 1 FORMAT (20A4)

Alphanumeric title with 1 in column 1 for page control.

Card 2 FORMAT (16I5)

NG = Number of energy groups = 2.

NX = Number of x mesh points.

NY = Number of y mesh points.

NRX = Number of x regions.

NRY = Number of y regions.

NZ = Number of time zones $\leq$ 2.

NPREC = Number of delayed neutron groups.

(LF(1,JR),JR=1,NRX) = Mesh point number on the right region boundary; mesh point number on the left boundary of the first region is 1.

(LF(2,KR),KR=1,NRY) = Mesh point number on the top region boundary; mesh point number on the bottom boundary of the first region is 1.

Card 3 FORMAT(16I5)

This card contains control variables which specifies the problem.

IC1 = Type of perturbation in thermal absorption cross section:

= 0 ramp,

= 1 sine function.

IC2 = Frequency of flux print-outs: fluxes are printed every IC2 time steps.

IC3 = Maximum number of outer iterations.

IC4 = A variable which controls steady state calculation:

= 0 no; initial fluxes are read in,

= 1 eigenvalue calculation,

= 2 search for critical thermal fission cross sections or calculation of initial equilibrium fluxes.

IC5 = A variable which controls the kinetics calculation:

= 0 no,

= 1 yes.

IC6 = Maximum number of inner iterations.

IC7 = Number of iterations per inner iteration.

IC8 = A variable which controls initial fluxes:

= 0 generate,

≠ 0 read in.

IC9 = A variable which controls the termination of computations:

= 0 last problem,

≠ 0 next problem to follow.

IC10 = A variable which controls flux punch in every IC2 time step including the initial flux:

= 0 no,

= 1 yes.

Card 4 FORMAT (D10.4)

EPS1 = Convergence criterion for the eigenvalue:

$$\left| \frac{\lambda^{-1J+1} - \lambda^{-1J}}{\lambda^{-1J+1}} \right| < \text{EPS1}.$$

EPS2 = Convergence criterion for the eigenvalue:

$$|\lambda - 1.0| < \text{EPS2}.$$

EPS3 = Extrapolation parameter for the eigenvector:

$$\underline{a}^{J+1} = \underline{a}^{J} + EPS3^{*}(\underline{a}^{*J+1} - \underline{a}^{J}).$$

EPS4 = Not used.

EPS5 = Frequency of the sine function (see Card 7).

EPS6 = Convergence criterion for the flux vector in the kinetics calculation:

$$\max_i \left| 1 - \left(\frac{a_i^{J-1}}{a_i^{J}}\right) \Big/ \left(\frac{a_i^{J}}{a_i^{J+1}}\right) \right| < EPS6 .$$

EPS7 = Convergence criterion for the flux vector in the kinetics calculation:

$$\max_i \left| 1 - \frac{a_i^{J}}{a_i^{J+1}} \right| < EPS7 .$$

EPS8 = Extrapolation parameter for the flux vector in the kinetics calculation:

$$\underline{a}_{k+1}^{K+1} = \underline{a}_{k+1}^{K} + EPS8^{*}\left(\underline{a}_{k+1}^{*K+1} - \underline{a}_{k+1}^{K}\right).$$

Card 5 FORMAT (8D10.4)

(H(1, JR), JR=1, NRX) = mesh size in the JR-th x region.

(H(2, KR), KR=1, NRY) = mesh size in the KR-th y region.

Card 6 FORMAT (16I5)

NMAT = Number of different materials.

NDATA = Number of material specification cards (Card 8).

Card 7 FORMAT (5D10.4)

Card 7 provides two-group cross sections for different materials. A group of Card 7 is read in the following order:

DO I=1, NG,

DO M=1, NMAT.

D(I, M) = Diffusion coefficient.

Σ_T(I, M) = Total removal cross section.

$\tau(I, M)$ = Cross section for neutron transfer;

$= \Sigma_{s1\to 2}$ if I = 1,

$= \nu\Sigma_{f2}$ if I = 2.

$\delta\Sigma_1(I, M)$ = Coefficient of the ramp or sine function in thermal absorption cross section in time zone 1: I = 2 only.

$\delta\Sigma_2(I, M)$ = Coefficient of the ramp or sine function in thermal absorption cross section in time zone 2: I = 2 only.

The time-dependent thermal absorption cross sections have the form $\Sigma_{a2}(t) = \Sigma_{a2}(0) + \delta\Sigma f(t)$ where f(t) = t or sin(EPS5·t).

Card 8 FORMAT (16I5)

This card specifies material types in each material region of a reactor.

NXL = x region number on the left boundary.

NXR = x region number on the right boundary.

NYB = y region number on the bottom boundary.

NYT = y region number on the top boundary.

NM = Material type $\leqslant$ NMAT.

Repeat Card 8 NDATA times.

Card 9 FORMAT (8D10.4)

Δt = time step size.

(TZ(IZ), IZ-1, NZ) = time at the end of time zone IZ.

Card 10 FORMAT (8D10.4)

(VEL(I), I=1, NG) = Neutron speed of group I.

Card 11 FORMAT (8D10.4)

(λ(I), I=1, NPREC) = Decay constant of I-th precursor group.

Card 12 FORMAT (8D10.4)

(β(I), I=1, NPREC) = Fraction of delayed neutrons of group I.

Card 13 FORMAT (5D16.8)

If IC8 $\neq$ 0, the initial flux coefficient vector is read in the following order:

DO I=1, NG

(U(I, J), J=1, N) = J-th flux expansion coefficient of group I.

If IC9 $\neq$ 0, a set of Cards 1 to 13 is to be placed immediately after Card 13.

D.2.3 Input for Sample Problem:

In the following page, a list of input cards is presented for a calculation using $\Delta t = T/4$ in Example 6.2, Chapter VI. The initial flux coefficient vector, which was computed in a steady state calculation in HERMITE-2D, is also includes as part of the input data. As the computer output, the neutron flux vector will be printed and produced in the form of punched cards at every time step.

```
1  SAMPLE INPUT FOR EXAMPLE 6.2,CHAP.VI -- HERMITE-2D                                                    INPT0001
    2    4    4    3    3    1    0    2    3    4    2    3    4                                        INPT0002
    1    1   50    0    1   20    5    1    0    1                                                      INPT0003
   1.0D-7    1.0D-7     1.8D0     0.0D06283.1853     1.0D-6    1.0D-6     1.8D0                        INPT0004
   1.0D 1     5.0D0    1.0D 1    1.0D 1     5.0D0    1.0D 1                                            INPT0005
    2    2                                                                                             INPT0006
    1.5D0  0.0623D0   0.C6D 0     0.0D0     0.0D0                                                      INPT0007
    1.5D0  0.0623D0   0.C6D 0     0.0D0     0.0D0                                                      INPT0008
    0.4D0     0.2D00.25104796     0.0D0     0.0D0                                                      INPT0009
    0.4D0     0.2D00.25104786    0.04D0     0.0D0                                                      INPT0010
    1    3    1    3    1                                                                             INPT0011
    2    2    2    2    2                                                                             INPT0012
   2.5D-4    1.0D-3                                                                                   INPT0013
   1.0D 8    2.2D 5                                                                                   INPT0014
    0.0D0                                                                                             INPT0015
    0.0D0                                                                                             INPT0016
 0.338597130 01 -0.125376590 C0  0.273903630 01 -0.172047500 C0  0.198998190 01                       INPT0017
-0.212866840 00 -0.125376590 C0  0.273903630 01 -0.101630900 00 -0.101014090 00                       INPT0018
 0.464266310-02 -0.101630900 00 -0.101014090 00  0.221531050 01 -0.139259910 00                       INPT0019
-0.139061510 00  0.637243580-C2 -0.738011430-01 -0.734719620-01  0.160958130 01                       INPT0020
-0.172159460 00  0.788316210-C2 -0.172047500 C0  0.198998190 01 -0.738011430-01                       INPT0021
-0.734719620-01  0.637243580-C2 -0.139259910 00 -0.139061510 00  0.160958130 01                       INPT0022
-0.101162000 00 -0.101053840 C0  0.874231230-02 -0.101162000 00 -0.101053840 00                       INPT0023
 0.116945270 01 -0.125086370 00  0.108165310-01 -0.212866840 00  0.788316210-02                       INPT0024
-0.172159460 00  0.108165310-01 -0.125086370 00  0.133828250-01                                       INPT0025
 0.100000000 01 -0.370282500-C1  0.808936660 00 -0.508118600-01  0.587713740 00                       INPT0026
-0.628672900-01 -0.370282500-01  0.808936660 00 -0.300152870-01 -0.298331200-01                       INPT0027
 0.137114660-02 -0.300152870-C1 -0.298331200-01  0.654261470 C0 -0.411284970-01                       INPT0028
-0.410699030-01  0.188201120-02 -C.217961510-C1 -0.216989330-01  C.475367690 00                       INPT0029
-0.508449260-01  0.232318340-02 -0.508118600-01  0.587713740 C0 -0.217961510-01                       INPT0030
-0.216989330-01  0.188201120-02 -0.411284970-C1 -0.410699030-01  0.475367690 00                       INPT0031
-0.298768C50-01 -0.298448600-01  0.258192160-02 -0.298768C50-01 -0.298448600-01                       INPT0032
 0.345381760 00 -0.369425370-01  0.319451340-02 -0.628672900-01  0.232818340-02                       INPT0033
-0.508449260-01  0.319451340-C2 -C.369425370-01  0.395243310-02                                       INPT0034
```

Appendix E

SOURCE LISTINGS OF COMPUTER PROGRAMS

(Only in M. I. T. Library copies)